Adipocyte mTORC1 Signaling Separately Regulates Metabolic Homeostasis and Adipose Tissue Mass, Independent of RagGTPase Activity

A Dissertation Presented

By

Peter Lin Lee

Submitted to the Faculty of the

University of Massachusetts Graduate School of Biomedical Sciences, Worcester

in partial fulfillment of the requirements for the degree of

DOCTOR OF PHILOSOPHY

July 5, 2018

MD/PHD PROGRAM

Adipocyte mTORC1 Signaling Separately Regulates Metabolic Homeostasis and Adipose Tissue Mass, Independent of RagGTPase Activity

A Dissertation Presented By Peter Lin Lee

The signatures of the Dissertation Defense Committee signifies completion and approval as to the style and content of the Dissertation

_____

David Guertin, Ph.D., Thesis Advisor

_____

Roger Davis, Ph.D., Member of Committee

_____

Amy Walker, Ph.D., Member of Committee

_____

Ingolf Bach, Ph.D., Member of Committee

_____

Stephen Farmer, Ph.D., Member of Committee

The signature of the Chair of the Committee signifies that the written dissertation meets the requirements of the Dissertation Committee

_____

Michael Czech, Ph.D., Chair of Committee

The signature of the Dean of the Graduate School of Biomedical Sciences signifies that the student has met all graduation requirements of the school.

_____

Mary Ellen Lane, Ph.D.
Dean of the Graduate School of Biomedical Sciences

MD/PhD Program July 5, 2018

Acknowledgements:

First and foremost I would like to thank Dr. David Guertin for welcoming me into his lab and providing me with exemplary guidance and mentorship as I developed as a student. His support and drive have been key in helping me overcome inevitable obstacles and difficulties encountered in research. Dr. Guertin's enthusiasm and passion for scientific inquiry resonates throughout all members of the lab and I am excited to see what the future holds for him and his lab. I am fortunate to have had this experience and look forward to the opportunity continuing to work with Dr. Guertin for years to come.

I would also like to thank the members of my dissertation committee for their guidance, insight, and commitment over the last 4 years as my research project evolved. Thank you Dr. Amy Walker, Dr. Roger Davis, and Dr. Michael Czech for your scientific input, advice, and support. Special thanks to Dr. Michael Czech for serving as my committee chair throughout my time here. Additionally, thank you to Dr. Steve Farmer for taking the time to serve as my external examiner.

I could not have been successful without the support from all members, past and present, of the Guertin Lab. Thank you Dr. Juan Sanchez-Gurmaches and Dr. Chien-Min Hung for welcoming me into the lab with open arms and mentoring me at the benchside throughout my graduate career. Thank you Dr. Yuefeng Tang for invaluable scientific discussions and input into my projects over the years. Thanks to Dr. Camila Martinez Calejman, Dr. Amelia Luciano, Dr.

SuMyung Jung, and Wen-Yu Hsaio for both your scientific contributions and camaraderie in the lab. I am grateful for the support of the MD/PhD program here at UMass, along with the outstanding MD/PhD whom I am proud to call friends. Thank you Jan Czerminski, Patrick Lowe, Zachary Milstone, Eric Schmidt, and all others who are on this path.

Last, and most importantly, I must thank my family for the sacrifices they've made to provide for me and support me in my life pursuits. My parents Dr. Yefu Li and Dr. Lin Xu, undoubtedly the greatest role models that I have. I look up to you every day, and it is from your hard work, enthusiasm, and positivity that allow me to pursue and achieve my goals in life.

Abstract (250 word limit):

Metabolic disorders are commonly associated with obesity, a condition where excess caloric intake leads to massive adipose tissue (AT) expansion and eventual dysfunction. When adipose tissue loses its ability to store excess energy properly, lipids accumulate in non-adipose tissues such as liver, and muscle. This ectopic lipid deposition is a significant risk factor in the development of a collection of disorders described as metabolic syndrome. While metabolic syndrome is typically linked with obesity, patients who have an inability to develop adipose tissue depots (lipodystrophy) develop similar clinical outcomes. There is evidence that aberrant mTORC1 signaling may occur in both settings, and may be a factor that contributes to adipose dysfunction.

I find that adipocyte specific loss of *Raptor*, a key mTORC1 subunit, leads to progressive lipoatrophy, and associated metabolic dysfunction including AT inflammation, hepatosteatosis, and insulin resistance. Interestingly, inhibition of autophagy, a pathway upregulated during *Raptor* deletion, prevents lipoatrophy but does not protect from ectopic lipid deposition and AT inflammation. These results suggest that outputs of mTORC1 in adipocytes individually regulate adipocyte storage capacity, and AT health. Furthermore, ablation of the amino acid sensing RagGTPases, thought to be necessary for mTORC1 activity, does not phenocopy Raptor KO, suggesting RagGTPase independent functions of mTORC1 in adipocytes. RagA/B deletion, however, did consistently increase

Ucp1 expression in WAT, indicating a possible noncanonical role of the Rags in regulating Ucp1.

Overall, these studies advance our understanding of regulation of adipose tissue metabolism, and shed light on previously unstudied nutrient specific signaling pathways in adipocytes.

TABLE OF CONTENTS

Title……i

Signature Page……ii

Acknowledgements……iii

Abstract……v

Table of Contents……vii

List of Figures……xii

List of Copyrighted Materials Produced by the Author……xv

List of Abbreviations……xvi

CHAPTER I: Introduction……1

Obesity in the USA……2

Adipose Tissue Mass vs Health……2

Adipose Tissue Depots……4

Brown Adipose Tissue……5

Beige Adipose Tissue……6

Metabolic Signaling……9

mTOR Complex1……10

mTOR in the Clinic……13

Adipose Tissue mTORC1……16

mTORC1 Effectors in Adipose Tissue……17

Adipose mTORC1 and Lipodystrophy……18

mTORC1 in BAT……19

mTORC1 in Browning/Beiging……..……...20

Summary……..21

CHAPTER II: Raptor/mTORC1 Loss in Adipocytes Causes Progressive Lipodystrophy and Fatty Liver Disease……26

ABSTRACT……27

1. INTRODUCTION……..……28

2. MATERIALS & METHODS……..29

3. RESULTS AND DISCUSSION……34

3.1. Adipocyte Raptor KO mice have normal WAT mass early in life……..……34

3.2. Adipocyte Raptor KO mice progressively develop lipodystrophy associated with hepatic steatosis and insulin intolerance……38

3.3. Altered lipid metabolic pathways in adipocyte Raptor KO mice……..……...41

3.4. Raptor KO mice are resistant to diet-induced obesity but develop severe hepatic steatosis……45

3.5. Adipocyte Raptor KO mice have normal energy expenditure and a lipid absorption defect……48

3.6. Decreased C/EBPa activity in Raptor-deficient WAT……52

3.7. Comparison to human lipodystrophy……...53

4. FUTURE DIRECTIONS AND CONCLUSIONS……54

Supplementary Data……..……57

CHAPTER III: Adipose mTORC1 Regulates Adipose Tissue Health Independent of Autophagy-mediated Lipoatrophy ……60

INTRODUCTION……61

MATERIALS & METHODS……...62

RESULTS……67

Adipose Raptor KO mice do not regain metabolic homeostasis…67

Inducing Raptor deletion in healthy adult mice causes a similar progressive lipodystrophy……70

Adipocyte differentiation is preserved in acute Raptor deletion, while chronic deletion leads to adipocyte death……73

Raptor loss in vivo impairs autophagy inhibition, while also associating with a decrease in mitochondrial mass. Paradoxically, mitochondria are significantly larger in KO tissues……...76

Acute response to Raptor deletion in vitro induces mitochondrial growth, increased autophagic flux, and resistance to classical apoptotic cell death……79

Lipoatrophy is rescued by inhibiting autophagy in the setting of Raptor KO mice, however AT inflammation and hepatosteatosis persist……82

DISCUSSION……..85

CHAPTER IV: RagGTPases are dispensable for mTORC1 in adipose tissue. RagA and RagB have an mTORC1 independent role in regulating Ucp1 activity in WAT……..90

INTRODUCTION……91

MATERIALS AND METHODS……....93

RESULTS……...96

Adipose specific RagA KO mice are phenotypically normal, with evidence of increased Ucp1 expression in WAT……...96

RagA KO mice are not resistant to HFD induced obesity……...98

Increased Ucp1 expression persists at thermoneutrality, but does not alter energy balance……...100

Adiponectin-Cre RagA RagB KO mice do not phenocopy Adiponectin-Cre Raptor KO mice. Adipose deletion of RagGTPases is dispensable for overall metabolic health in mice……102

DISCUSSION……..105

CONCLUSION……..107

CHAPTER V: DISCUSSION AND FUTURE DIRECTIONS……109

Adipose mTORC1……..110

Adiponectin-Cre Raptor Caveats……111

Dissecting WAT vs BAT roles in Whole Body Metabolism……..113

Further Work for Adipose ATG7/Raptor dKO.....114

Can Adipocyte mTORC1 Localize to Lysosome Absent RagGTPases?.....117

Adipocyte Mitochondrial Dynamics in Relationship With mTORC1.....119

mTORC1, Adipose Tissue Health, and Tumor Environments.....120

Conclusion.....122

REFERENCES.....124

List of Figures:

Figure 1.1: Anatomic diagram of adipose tissue depots, and adipocyte dynamics in mice……8

Figure 1.2: Schematic representation of mTORC1 and its regulatory pathways……..……11

Figure 1.3: Table and description of common downstream mTORC1 targets…13

Figure 1.4: Description of past and current mTOR targeted therapeutics……15

Figure 2.1: Adipocyte Raptor KO mice exhibit normal WAT mass and mild BAT defects early in life…….37

Figure 2.2: Adipocyte Raptor KO mice develop lipodystrophy with age……..40

Figure 2.3: The progressive lipodystrophy of adipocyte Raptor KO mice associates with hepatic steatosis and insulin intolerance……43

Figure 2.4: Altered lipid metabolic pathways in the adipose tissues of adipocyte Raptor KO mice……..44

Figure 2.5: Adipocyte Raptor KO mice are resistant to HFD obesity but suffer from more severe hepatic steatosis…….47

Figure 2.6: Energy utilization and adipocyte transcriptional regulation……51

Figure 2.7. S1) Ucp1-Cre driven *Raptor* KO reveal similar BAT phenotype as Adipoq-Cre driven mice…….57

Figure 2.8: Supplementary Table 1 – Raw Energy Expenditure data……...58

Figure 2.9: Supplementary Table 2- A comparison between the *Raptor Adipo*$^{q\text{-}Cre}$ mice described in this study and previously described *Raptor*$^{aP2\text{-}Cre}$ mice……58

Figure 3.1: Adipose Raptor KO adipocytes are universally targeted, and KO mice are unable to metabolically adapt as they age…….69

Figure 3.2: In vivo, metabolic consequences arise weeks after inducing Raptor deletion…….72

Figure 3.3: Evidence of chronic cell death in Raptor KO adipose tissue depots…..…….75

Figure 3.4: mTORC1 exhibits control over mitochondrial size and maintenance in adipose tissue…….78

Figure 3.5: Contrasting changes in mitochondria in response to acute Raptor inhibition in vitro……..81

Figure 3.6: Inhibition of autophagy in Raptor KO rescues adipose tissue mass, but not hepatic steatosis of AT inflammation…….84

Figure 4.1: Adipose specific RagA KO mice are phenotypically normal, with evidence of increased Ucp1 expression in WAT……..97

Figure 4.2: RagA KO mice are not resistant to HFD induced obesity……..99

Figure 4.3: Increased Ucp1 expression persists at thermoneutrality, but does not alter energy balance……101

Figure 4.4: Adipose tissue RagGTPase deletion does not phenocopy Raptor KO mice. Adipocyte RagGTPases appear to be dispensable for overall metabolic stability……...104

Figure 5.1: Diagram of known carriers for amino acid sensing. Speculative pathways highlighted in red……119

Figure 5.2: Model of mTORC1 pathways and their influence on adipose tissue metabolism in wildtype (A), adipose Raptor KO (B), and adipose ATG7/Raptor KO (C) mice……..123

List of Copyrighted Materials Produced by the Author:

Lee, P. L.[1], Jung, S. M.[1]., Guertin, D. A. (2017). "The Complex Roles of Mechanistic Target of Rapamycin in Adipocytes and Beyond." Trends Endocrinol Metab **28**(5): 319-339.

Lee, P. L., Tang Y., Li H., Guertin D.A., (2016). "Raptor/mTORC1 loss in adipocytes causes progressive lipodystrophy and fatty liver disease." Mol Metab **5**(6): 422-432.

List of Abbreviations:

ACC ─ Acetyl CoA carboxylase
ACLY ─ ATP-citrate lyase
Ad lib - Ad libitum
Adipoq ─ Adiponectin
AGPAT1 ─ 1-acylglycerol-3-phosphate O-acyltransferase 1
AGPAT2 ─ 1-acylglycerol-3-phosphate O-acyltransferase 2
APC – Adipocyte precursor cell
AT - Adipose Tissue
ATGL - Adipose triglyceride lipase
ATGL ─ Adipose Triglyceride Lipase
BAT- Brown adipose tissue
C/EBPα ─ CCAAT-enhancer-binding proteins α
C/EBPβ ─ CCAAT-enhancer-binding proteins β
ChREBPβ ─ Carbohydrate-responsive element-binding protein β
CPT1a ─ Carnitine palmitoyltransferase 1A
CPT1b ─ Carnitine palmitoyltransferase 1B Triacylglyceride biosynthesis
DAPI - 4',6-diamidino-2-phenylindole
DKO - Double knock out
F4/80 - F4/80 antigen
FABP4 ─ Fatty Acid Binding Protein 4
FACS - Fluorescence activated cell sorting
FASN ─ Fatty acid synthase
FFA - Free fatty acid
GFP - Green fluorescent protein
GTT – Glucose Tolerance Test
H&E - Hematoxylin and eosin stain
HFD - High fat diet
HSL ─ Hormone-sensitive lipase
IGF - Insulin-like growth factor
IRD4 ─ Interferon regulatory factor 4
ITT – Insulin Tolerance Test
KO – Knock Out
LPL ─ lipoprotein lipase
NASH – Nonalcoholic Steatohepatitis
PGC1α ─ Peroxisome proliferator-activated receptor gamma coactivator 1-α
PPARα ─ Peroxisome proliferator-activated receptor α
PPARγ1 ─ Peroxisome proliferator-activated receptor γ isoform 1
PPARγ2 ─ Peroxisome proliferator-activated receptor γ isoform 2
PRDM16 ─ PR domain containing 16
qRT-PCR quantitative - Real-Time polymerase chain reaction
RFP – Red fluorescent protein
SCD1 ─ Stearoyl-CoA desaturase 1 Brown enriched and/or thermogenic genes

TNF-α - Tumor necrosis factor-α
UCP1 ─ Uncoupler protein 1
WAT - White adipose tissue
WT – Wildtype

CHAPTER I: Introduction

This chapter contains materials that are reprinted or have been adapted with permission from the *Trends in Endocrinology and Metabolism* article:

Lee, P. L.[1], Jung, S. M.[1]., Guertin, D. A. (2017). "The Complex Roles of Mechanistic Target of Rapamycin in Adipocytes and Beyond." Trends Endocrinol Metab **28**(5): 319-339.

Obesity in the USA

In this day and age, obesity and its associated health consequences are generally well appreciated throughout society. From the 1980s into the early 2000s, the USA experienced rapidly increasing rates of obesity throughout both the adult and youth population, quickly reaching epidemic levels. In recent years, extensive efforts have been made as a society to curb the obesity epidemic, and evidence indicates that the prevalence of obesity has been leveling off [1]. Despite this, obesity numbers in the USA remain staggering, with more than a third of adults classified as obese, as defined by a BMI of greater than 30 [2]. Comorbidities associated with obesity are vast and affect nearly all organs of the body. These include hypertension, diabetes, cardiovascular disease, stroke, gout, osteoarthritis, and more [3]. Given the serious health consequences associated with obesity, tremendous effort has been given in understanding the relationships between adipose tissue and overall human health.

Adipose Tissue Mass vs Health

While there is certainly a war on obesity in modern culture, it is important to note that the functionality of adipose tissue may be just as, or more, important to metabolic health than its gross mass. This idea was reported on as early as in the 1980s, with the identification of metabolically obese normal weight persons (MONW), whereby an individual may have generally a normal proportion of adipose tissue, however still suffer from metabolic consequences commonly

associated with obesity [4, 5]. Furthermore, there has also been interest generated in metabolically healthy obesity (MHO), in which a person's BMI may be well within the obese range, however they do not suffer from metabolic consequences associated with obesity [6, 7, 8, 12]. More recently, it has been identified that the development of metabolic diseases and its relationship with adiposity may be significantly different among different cultures. In fact, recommendations have been made to adjust BMI standards for certain populations, for example, lowering the threshold of "overweight" for certain Asian populations [9]. To better understand the underlying reasons for these clinical outputs, we must investigate the biology of adipose tissue and adipocytes.

The ability to store excess energy in the form of lipids is a trait well conserved throughout evolution. From single-celled organisms storing lipids in the form of lipid droplets, to mammals with a complex heterogenous collection adipocytes, the storage of energy is critical for organism survival during times of nutrient starvation [10]. In addition to providing energy during times of need, it is thought that sequestration of lipids within adipocytes importantly protect other organs from "lipotoxicity" [11, 12]. This theory suggests that while other organs such as liver and muscle are capable themselves of transient energy stores, these tissues quickly become overwhelmed by excess lipids and will suffer metabolically when stressed [11, 12]. Indeed, high circulating free-fatty acid levels are tightly correlated with the development of insulin resistance and metabolic disease [13]. It has been shown that reducing circulating FFA, by

preventing the release of lipids from adipose tissue, may help improve insulin sensitivity and whole body metabolic function [14]. While metabolic dysfunction can still occur in cases of normal FFA levels, it is clear that proper adipose tissue function is critical in relieving peripheral organs of energy stress. This is well documented in the case of human lipodystrophy, a disease in which patients have a near complete inability to develop adipose stores, and thus suffer from severe insulin resistance and other metabolic diseases often seen in obesity [15]. In the case of obesity, MONW, and MHO persons, it is still unclear why, at different points, the adipocytes begin to lose their ability to safely and effectively store lipids.

Adipose Tissue Depots

In humans, adipocytes organize themselves into generally contained depots throughout the whole body, collectively making up the adipose organ. Historically, adipose tissue was generally thought to be a passive yet critical energy sink, storing lipids during times of nutrient excess, and providing energy sources during times of nutrient deprivation [10, 16]. On a more detailed level, adipose tissue is often classified as either white adipose tissue (WAT) or brown adipose tissue (BAT), although this is yet still an oversimplification as mounting evidence indicates different depots, and even individual adipocytes within depots, are heterogeneous with respect to development and function [17-19]. For

simplicity's sake, however, I will touch on the significant differences between BAT and WAT.

Both WAT and BAT depots are found in several anatomically defined locations in nearly all mammals. In mice, common depots used in the study of adipose tissue include interscapular BAT, anterior subcutaneous WAT, and perigonadal WAT [Figure 1.1A]. WAT persists in the body in distinct locations, and are commonly differentiated between visceral WAT (vWAT) and subcutaneous WAT (sWAT). Research has shown that vWAT, located internally and typically surrounding organs such as the gut and the heart, is highly associated with metabolic disorders [20]. sWAT, on the other hand, is found at the periphery, underneath the skin, and has been suggested that it may in fact provide metabolic benefits [15]. As a whole, WAT is unique in its incredible growth potential and energy storing capacity, which can be subsequently released when dietary nutrients are unavailable. WAT can expand tremendously during periods of chronic nutrient excess, which can be appreciated both under normal conditions, such as bears as they prepare for hibernation, or under diseased conditions such as human obesity.

Brown Adipose Tissue

While WAT is the most abundant type of adipose tissue present in humans, there is great interest in understanding the biology of BAT. Unlike white adipocytes, brown adipocytes are a highly active cell, consisting of many small

lipid droplets and packed with mitochondria (giving the “brown” appearance). Unlike WAT, BAT is actually a net energy consumer, and acts as a nutrient sink. The primary function of BAT is to generate heat (thermogenesis), which is an energy expending process mediated by uncoupling protein 1 (UCP1) [21, 22]. By consuming lipid species, the mitochondria in BAT generate tremendous amounts of heat while consuming intracellular energy stores. In humans, BAT is most abundant in infants, and is believed to play an important in role in maintaining body temperature at young ages. As humans age, they develop greater ability to generate heat through muscle contraction (shivering), and rely on manmade environments to help maintain temperature control, thus losing their dependence on BAT. Despite this, there has been intensified interest in understanding brown adipocyte biology in parallel with the idea that stimulating BAT activity therapeutically may be a way to combat obesity or hyperglycemia and hyperlipidemia [23]. Overall, it is clear that adipose tissue is an extremely complicated organ, and while its basic role is in storing lipids, there are a plethora of outputs and connections that cement it as a critical metabolic organ. Beyond controlling its overall growth in mass, regulating adipose tissue’s role as an endocrine organ, or its role in energy expenditure, may provide significant benefits in battling metabolic disorders.

Beige Adipose Tissue

Interestingly, it has been shown that adipocytes that arise in traditionally WAT depots do have the ability to develop a brown-like characteristic, a process called “browning” or “beiging” [24]. Under certain stimulatory conditions, these white adipocytes can become energetically active with high numbers of mitochondria, and multiple small lipid droplets, becoming somewhat of an intermediary type of cell often referred to as a “beige” adipocyte [24]. These cells express high amounts of Ucp1, like brown adipocytes, and behave similarly in that they will consume nutrients to expend energy in the form of heat. The most common way to stimulate this “beiging” process is cold exposure. In mice, housing animals in cold conditions (most commonly around 4°C-6°C), induces a thermal stress that significantly activates and produces many beige cells within WAT depots [25]. More specifically, white adipocytes found in subcutaneous depots appear to have a greater propensity for beiging, while vWAT adipocytes undergo minimal transitions even during times of chronic cold stimulation [26]. This activity and ability to beige in scWAT is one mechanism proposed to explain the observations that scWAT may be a “healthier” type of WAT depot when compared to vWAT. On the other-side of the spectrum, when stimulatory factors are minimalized, such as at warm, “thermoneutral” conditions, brown adipocytes can take on a white-like morphology in greatly expanding the size of their lipid droplets [27]. It is clear that adipose tissue and adipocytes are dynamic in nature, and feature the ability to regulate their metabolic programs in response to

environmental cues and stresses. Examples of these dynamics shifts are shown in Figure 1.1.

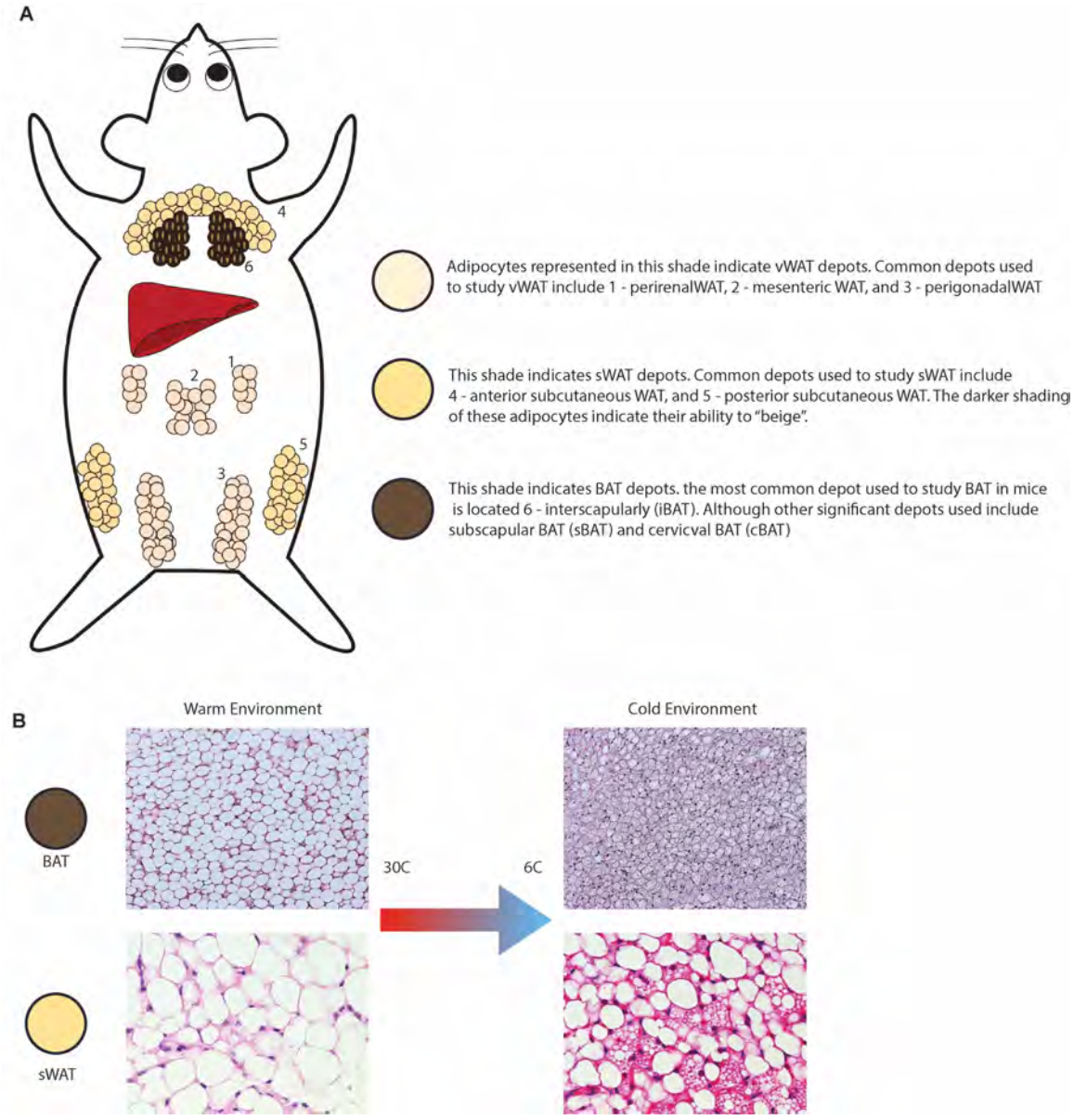

Figure 1.1: Diagram representing anatomic location of commonly studied WAT and BAT depots in mice. Histological images show the dynamic response of adipose tissue morphology to environmental cues.

Metabolic Signaling

As appreciation for the diversity of adipose tissue grows, so does the interest in understanding how nutrients and signaling molecules regulate adipocyte dynamics. The ability of biological systems to sense and respond appropriately to nutrient availability is crucial for survival. Consequently, animals are layered with multiple nutrient sensing mechanisms at the cell, organ, and organism level. At the cellular level, nutrient signaling biochemistry is best understood in cells where mTOR is the marquee intracellular kinase linking nutrient availability with metabolic control. In many studies utilizing different model cell lines, it's been shown that mTOR deregulation is a hallmark of diabetes and cancer [28]. The functions of mTOR are split between two multi-subunit complexes, called mTOR complex 1 (mTORC1) and mTORC2 [Figure 1.2A]. The best-understood complex is mTORC1, which is a well-known engine of anabolic metabolism that functions downstream of an ancient amino acid sensing network superimposed by growth factor signaling in higher eukaryotes [Figure 1.2C] [28, 29]. Its sibling, mTORC2 is less well-defined biochemically, but is emerging as a central regulator of glucose and lipid metabolism. The intracellular mechanics of mTOR signaling are being extensively defined in cell culture systems [30-33]; less understood are the in vivo organ-specific functions of mTOR and its role in organ-to-organ communication networks. Interest in mTOR is also driven by the fact that mTOR inhibitors are highly desirable pharmacological agents, particularly in oncology and immunology. Thus,

understanding how mTOR's diverse cellular functions are integrated at the organ and organism level is key challenge area.

mTOR Complex 1

The complexity of mTORC1 signaling has been extensively described [28, 34]. To summarize, mTORC1 is mainly activated by combined inputs from amino acid sensing pathways and growth factor signaling such as the insulin and insulin like growth factor 1 (IGF1) pathways [Figure 1.2C]. Many additional inputs ranging from the energy sensing AMP-activated protein kinase (AMPK) signaling pathway to cellular stresses like hypoxia fine-tune mTORC1 activity essentially to optimize (or restrict) anabolic growth in coordination with the cell's nutrient and energy availability. Recent breakthroughs in understanding the amino acid sensing mTORC1 inputs reveal that cytoplasmic levels of leucine and arginine are directly sensed by the Sestrins and Castor proteins respectively, which promote the GTP loading of a small GTPase called RagA/B. The mechanistic link between Senstrins/Castor and RagA/B activation is poorly understood but involves two large protein complexes, the Gator2 (Mios, Seh1L, WDR24, WDR59, Sec13) and Gator1 (DEPDC5, Nprl2, Nprl3) complexes. Glutaminolysis, the breakdown of glutamine to α-ketoglutarate, might also help facilitate leucine-dependent RagB loading [35]. RagA/B GTP loading promotes mTORC1 localization to lysosomes where it encounters its activator, the Rheb-GTPase. By mechanisms less clear, amino acids can also signal to mTORC1 from within the

lysosomes through Slc38A9 and the v-ATPase [36, 37]. Elucidating the amino acid inputs to mTORC1 is an ongoing and exciting area of research in part because it may be possible to manipulate mTORC1 activity pharmacologically with amino acid analogs.

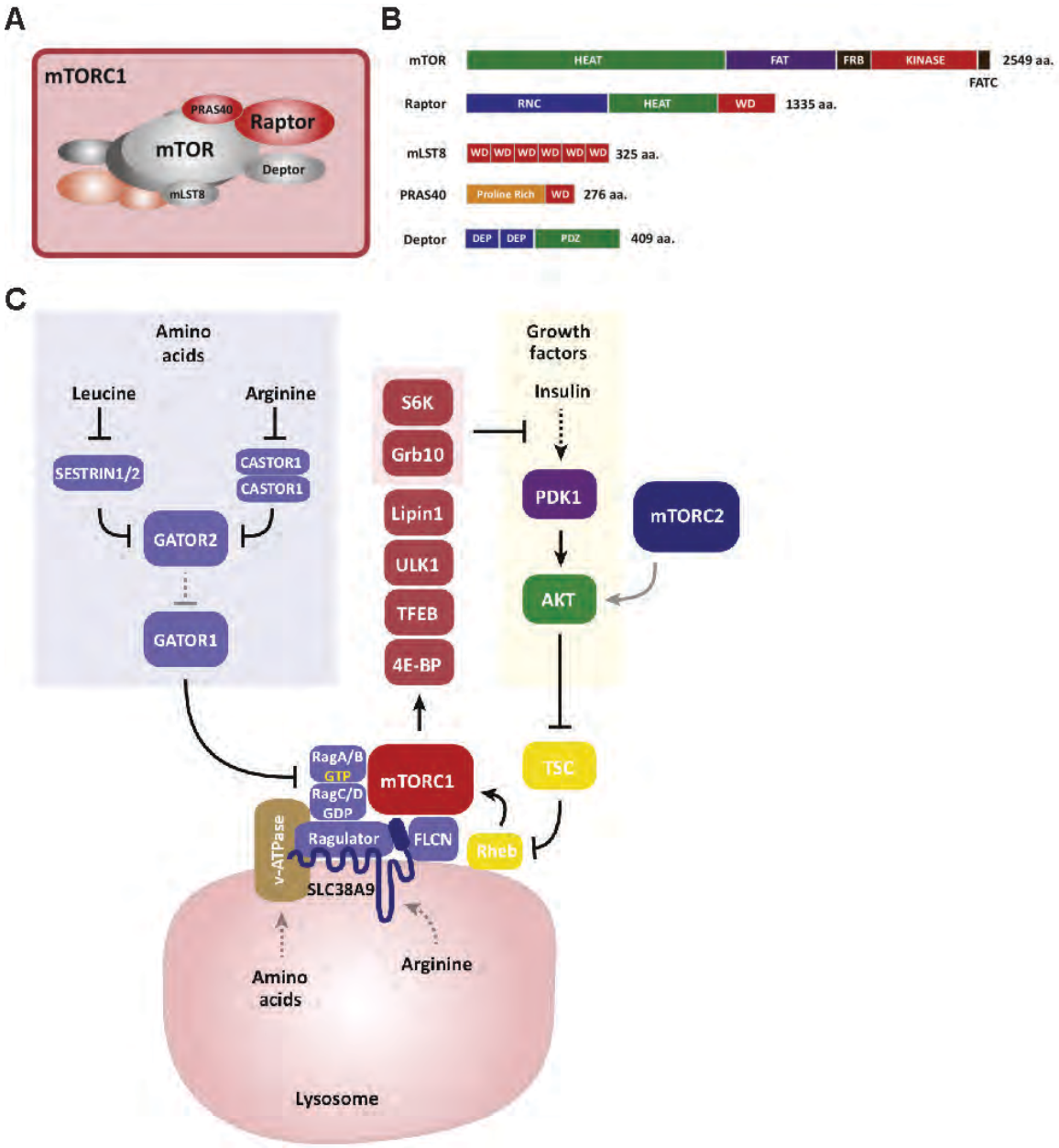

Figure 1.2: A, B) Individual components of mTOR Complex 1 C) Identified upstream and downstream effectors of mTORC1

At the lysosome, Rheb directly activates mTORC1 [38-40]. Rheb activity is controlled by the TSC complex (TSC1, TSC2, TBC1D7), a GAP that is inhibited by insulin/AKT signaling forming the main convergence point between growth factor and amino acid regulation of mTORC1 [41, 42]. There are several known mTORC1 substrates that collectively promote anabolic growth [Table 1] including the classic mTORC1 effectors S6K1 and 4E-BP1, which regulate protein synthesis [28] Other effectors include Ulk1, a kinase involved in autophagy [43], and TFEB, a transcription factor protein also important in autophagy through its role in lysosomal biogenesis [44]. Additional evidence exists for mTORC1 being involved in lipid metabolism through phosphorylation of Lipin1, a phosphatidic acid phosphatase [45, 46], and Grb10, a negative regulator of insulin/IGF receptor signaling that may play a role in regulating lipolysis and thermogenesis in adipose tissue [47, 48]. Some substrates, such as S6K1 and Grb10 can also inhibit insulin signaling forming powerful negative feedback loops allowing for tight control of insulin/IGF signaling [49, 50].

Complex	Substrates	Reported functions
mTORC1	4E-BP1	Translation initiation; Cap-dependent translation
	S6K	AGC family kinase that functions in protein synthesis, cell survival, and suppression of insulin/IGF signaling
	ULK1	Autophagy and cellular starvation response; regulates autophagosome formation
	TFEB	Transcription factor; regulates lysosome biogenesis
	Lipin-1	Triglyceride synthesis; may regulate SREBP-mediated expression of lipid synthesis genes
	GRB10	Negative regulator of receptor tyrosine kinase signaling including insulin and IGF1 receptor signaling

Figure 1.3: Common downstream targets of mTORC1 activity

mTOR in the Clinic

Pharmacological inhibitors of mTOR are highly desired agents in oncology and transplant medicine, thus understanding the mechanistic basis of their side effects could improve efficacy. Rapamycin (Sirolimus, INN/USAN) is a widely used immunosuppressant particularly in kidney transplantation. Mechanistically, rapamycin is an immunophillin that functions as an mTOR inhibitor only when bound to FKBP12. Patients on rapamycin often development new onset diabetes after transplantation (NODAT), which can increase post-transplant morbidity and mortality [3, 51]. The exact mechanisms by which NODAT develops is not understood [51-53]. Could rapamycin cause insulin resistance in part by inhibiting mTOR in adipose tissue? Rapamycin acutely inhibits mTORC1; however, prolonged rapamycin exposure as discussed earlier additionally inhibits mTORC2 [54, 55] by preventing new Rictor-mTOR interactions [54]. Moreover,

very high doses of rapamycin are also capable of binding the FRB domain independently of FKB12 and inhibiting mTORC2 [56]. As genetic studies indicate that selectively losing either mTORC1 or mTORC2 in adipose tissue impairs insulin sensitivity, it is possible that rapamycin can compromise metabolic homeostasis by targeting either complex in the adipose tissue. Rapamycin's ability to inhibit mTORC2 in the liver is likely due to its undesirable side effects in this tissue [55].

Given that many cancers have elevated mTOR signaling, there is also great interest in mTOR inhibitors for use in oncology [57-59]. Rapamycin and its analogs have been developed for this purpose, but in many cases, were met with limited success in part due to incomplete mTOR inhibition and loss of negative feedback inhibition of AKT and cell survival. More recently, major investments have been made towards developing mTOR catalytic inhibitors that target the kinase domain. Several of these compounds, often referred to as 2nd generation mTOR inhibitors, are currently being tested in early clinical trials [Table 2]. While these 2nd generation inhibitors do a better job of complete mTOR inhibition, feedback pathways, drug resistance, and toxicity remain challenges [57]. More recently a novel "3rd generation" mTOR inhibitor (RapaLink) was created by crosslinking rapamycin with an mTOR kinase inhibitor, allowing for the drug to bind at both the FRB and the kinase domain. In preclinical studies, RapaLink has shown promise in overcoming some types of mutation mediated drug resistance [Table 2] [60]. Despite these significant advances, major hurdles still remain in

understanding and overcoming mTOR inhibition related toxicity in normal tissues. Continued elucidation of mTORC1 and mTORC2's mechanisms of action in metabolic tissues like adipose tissue, liver, and skeletal muscle is essential to understanding how to cope with the side effects of mTOR-targeted therapies.

Drug name	Advantage over previous generation	Clinical progress	Challenges
First-generation drugs			
Rapamycin (sirolimus) Everolimus, Temsirolimus		Currently used for immunosuppression in the context of allograft rejection. Chemotherapeutic in some cancers, such as renal cell carcinoma and mantle cell lymphoma.	Enhanced cell survival due to loss of mTORC1-mediated negative feedback on PI3K/AKT signaling. mTOR mutations in tumor cells leading to drug resistance.
Second-generation drugs			
Dual PI3K/mTOR inhibitors Dactolisib GSK2126458 XL765 **mTOR kinase inhibitors** AZD8055 INK128 OSI027	Targeting kinase activity of mTOR, or both PI3K and mTOR, prevents the negative feedback-mediated increase in AKT signaling. This allows for increased efficiency in activation of cell death pathways.	Several candidates in early clinical trials in the setting of various cancers, including solid tumors, which are one group of cancers that were not well targeted by first-generation rapalogs.	Increased toxicity due to targeting of both mTORC1 and mTORC2 pathways. mTOR mutations leading to drug resistance is a challenge.
Third-generation drugs			
RapaLinks	Rapamycin crosslinked with an mTOR kinase inhibitor allows the compound to interact at both the FRB domain of mTOR and the kinase domain at the same time. This allows for potent inhibition of mTORC1 and mTORC2 activity, even in the setting of drug-resistance cell lines.	Currently being studied in a preclinical setting, in cell lines, and mouse xenografts.	Clinical efficacy and toxicity in human patients unclear; may be significantly different than what is found in animal models.

Figure 1.4: Progress of mTOR targeting therapies in clinical development

Adipose Tissue mTORC1

While mTORC1 is a critical regulator of cell growth and anabolic processes in cells, its tissue-specific roles in adipose tissue have not been extensively defined. Because mTOR is the catalytic subunit of both mTORC1 and mTORC2, tissue specific genetic analysis of each complex relies upon the selective deletion of essential regulatory subunits using Cre-Lox technology. For mTORC1, this is achieved by deleting *Raptor* [Figure 1.2A]. A previous genetic study of mTORC1 in adipose tissue utilized the aP2-Cre driver to delete *Raptor* [61]. In summary, this study concluded that deletion of *Raptor* led to mice that had increased energy expenditure and were resistant to high-fat diet induced obesity. This study suggested that mTORC1 inhibition in adipose tissue may overall provide a metabolic benefit. Since that study, however, aP2-Cre has fallen out of favor due to its inefficient targeting of adipocytes and "off-target" expression e.g. in endothelial and brain cells [62-64]. It is generally accepted now that Adiponectin-Cre is more specific and efficient at targeting mature adipocytes (though all Cre drivers should be used with caution). Adiponectin-Cre also targets all mature adipocytes, including both brown and white, therefore it cannot be used to conclusively distinguish the depot independent functions of a specific target. While those results using aP2-Cre were provocative, it will be important to understand a more specific role of mTORC1 in adipocytes utilizing newer genetic tools.

mTORC1 Effectors in Adipose Tissue

Growth factor signaling regulates mTORC1 activity through a pathway different from amino acids, and proteomic studies suggest that the global phosphorylation response to insulin is largely mTOR dependent [47]. It was reported recently that mice lacking the insulin receptor (IR) in mature adipocytes ($IR^{Adipoq\text{-}Cre}$ mice) suffer from lipodystrophy [65], while a fat-specific IR/IGFR double KO model results in a complete loss of adipose tissue and more severe metabolic disease [65]. However, knocking out all adipocyte AKT activity by simultaneously deleting *AKT1* and *AKT2* (i.e. $AKT1;AKT2^{Adipoq\text{-}Cre}$ double KO mice) also causes a severe lipodystrophy [66] indicating other insulin/AKT effectors in addition to mTORC1 are also critical for adipose tissue maintenance. Alternatively, losing mTORC1-dependent feedback inhibition of AKT might preserve some adipose tissue in the absence of *Raptor*. Consistent with the latter possibility, overexpressing the mTORC1/2 complex subunit DEPTOR promotes adipogenesis by dampening mTORC1 activity, which reduces mTORC1-mediated feedback inhibition of insulin signaling, and promotes AKT-PPARy activity [67]. A similar effect was observed in cell culture where a conditional knockdown approach in 3T3-L1 cells that partially inhibits mTOR activity promotes adipogenesis by increasing AKT signaling [68]. One prediction of these observations is that inhibiting both mTORC1 and mTORC2 (because it phosphorylates AKT) might result in more severe loss of adipose tissue.

However, Adipo-Cre mTOR L/L mice are phenotypically similar to Adipo-Cre Raptor L/L mice [69] suggesting that mTORC2-independent AKT signaling may promote the maintenance of some, albeit smaller, fat depots in the Adipo-Cre Raptor L/L mice.

Adipose mTORC1 and Lipodystrophy

At the start of this project, despite many studies in focusing on adipose tissue metabolism, the specific role of mTORC1 activity in mature adipocytes was not completely understood. Given the many downstream mTORC1 targets, there are multiple possibilities that are not necessarily mutually exclusive. Indeed, many mTORC1 effectors have reported roles in adipocytes [70, 71]. Because mTORC1 suppresses autophagy, one possibility is that *Raptor* loss in fat may lead to excessive degradation and loss of adipocytes. In fact, from a human perspective, some types of congenital generalized lipodystrophy (CGL), may occur in part due to mutations that affect autophagic lipid degradation. For example, CGL has been linked to mutations in 1-Acylglycerol-3-Phosphate O-Acyltransferase 2 (AGPAT2) and SEIPIN, also known as Bernardinelli-Seip congenital lipodystrophy type 2 protein (BSCL2), both endoplasmic reticulum membrane proteins involved lipid biosynthesis that may also play a role in lipophagy [72, 73]. Additionally, a recent study found that deleting AGPAT2 in adipose tissue increases autophagic structures. Interestingly, other recent work finds that SEIPIN can interact directly with both AGPAT2 and the mTORC1

substrate Lipin1 in a complex [74]. This potentially directly links human lipodystrophies to the mTORC1 signaling pathway as it has been shown that mTORC1 may regulate lipin1 localization and activity [45, 46], and mice carrying a mutation in the *lipin1* gene exhibit features similar to human lipodystrophy and fat-specific *Raptor* loss [75].

Given the above information, I am presented with conflicting ideas, one based on the results of an aP2-Cre driven deletion of *Raptor* which would suggest that mice may benefit metabolically from mTORC1 inhibition, while several others studies suggest that mTORC1-associated proteins and signaling pathways might be crucial for adipose tissue development and maintenance. Given our knowledge of downfalls of the aP2-Cre system and understanding of the role of mTORC1 in anabolic pathways, I believe that inhibition of *Raptor* in mature adipocytes will lead to metabolic dysfunction in an animal model. This sets the groundwork for a major aim of this project.

mTORC1 in BAT

Previously it was discussed that BAT has emerged as a promising type of adipocyte that may play a role in combating metabolic dysfunction. Recent studies have also begun looking at the role of mTORC1 in BAT. Using Adipo-Cre Raptor L/L mice, one study looked carefully at how losing mTORC1 in all mature adipocytes affects BAT adaptation to cold [76]. In wild type mice, prolonged cold challenge significantly increases mTORC1 activity in BAT through sympathetic signaling and this correlates with increased BAT mass,

mitochondrial biogenesis, and oxidative metabolism. Without *Raptor,* BAT cannot expand or metabolically adapt to cold. Deleting *Raptor* only in BAT with Ucp1-Cre *(Raptor$^{Ucp1\text{-}Cre}$)* also reduces BAT mass and lipid content [77], arguing that this is likely a tissue-autonomous effect. Further studies using BAT specific Cre drivers are needed to confirm the BAT-specific mTORC1 functions.

mTORC1 in Browning/Beiging

When mice are exposed to severe cold for prolonged periods of time, or treated with beta-adrenergic agonists, some depots can metabolically reprogram to become characteristically more similar to brown adipocytes, for example they induce UCP1 expression [78, 79]. This is often referred to as the browning of WAT and may have therapeutic potential in humans by functioning as a glucose and energy sink in the setting of diabetes/obesity [80]. In two independent studies, it was recently found that the mTOR inhibitor rapamycin blocks WAT browning [81, 82]. Interpreting the effect of rapamycin is complex because it is systemically delivered, it only partially inhibits mTORC1 [83, 84] and it can also inhibit mTORC2 following prolonged exposure [54]. To address the specificity of rapamycin's effect in vivo, both studies used Adipo-Cre Raptor L/L mice to show that *Ucp1* cannot be induced by cold [81, 82] or beta-adrenergic agonists [81, 82] without functional mTORC1 in WAT. In agreement, another recent study finds that activating mTORC1 in WAT by deleting its negative regulator TSC1 (Adipo-Cre TSC1 L/L mice) elevates Ucp1, PGC-1α, and PPARα levels [85]. In cultured adipocytes, βAR agonists were also shown to stimulate S6K but not AKT

phosphorylation, suggesting a link between mTORC1 and protein kinase A (PKA) signaling [82]. Indeed, a PKA inhibitor blocked this effect and this was attributed to direct phosphorylation of mTORC1 (on both mTOR and Raptor) by PKA [Figure 1C]. Thus, in addition to its regulation by insulin, a well-known antagonist of PKA signaling, mTORC1 also responds to catecholamines in adipocytes. Concurrently, other studies have shown that adrenergic stimulation may also stimulate mTORC2 and AKT signaling in certain settings suggesting that catecholamine-stimulated mTOR activity may be complex [76, 86].

Summary

While there are many paths to pursue in understanding nutrient signaling, adipose tissue metabolism, and whole body metabolic health, I set out to develop a better understanding of the role of mTORC1 signaling in adipose tissue metabolism. Specifically, I want to understand how mTORC1 in mature adipocytes contributes to the ability of adipose tissue to regulate whole body metabolism. While previous studies have suggested that adipose ablation of mTORC1 activity using the aP2-Cre results in metabolically superior mice, there are substantial data that argue downstream targets of the mTORC1 pathway are crucial for adipose tissue function maintenance [61, 69, 87]. To test the role of mTORC1 in mature adipose tissue, I generated mice that are genetically ablated for *Raptor*, specifically in adipocytes using the Adiponectin-Cre. While it was possible this KO may end up phenocopying the aP2-Cre mice, I found that these mice were in fact extremely different than the previously understood model [77].

Adipose tissue ablation of mTORC1, using Adiponectin-Cre, resulted in metabolically unfit mice who suffered from severe lipodystrophy. Using this Cre with greater specificity and efficacy for mature adipocytes, I found that the loss of mTORC1 signaling resulted in mice that not only were unable to expand their adipose tissue, but they also suffered from a progressive loss of adipose stores as they aged. In addition, they suffered from metabolic disfunction such as hepatic steatosis, insulin resistance, and hepatic tumor growth [77].

From these results, I next wanted to dissect the numerous downstream changes in these *Raptor* KO mice to identify key players that contribute to lipodystrophy and metabolic dysfunction. Of interest was understanding time-dependent consequences of mTORC1 ablation. With the previous tool of Adiponectin-Cre, *Raptor* is consequently deleted immediately after an adipocyte differentiates, resulting in mTORC1 inhibition even before birth. To better mimic adipose tissue dysfunction in the setting of human disease, I generated tools to allow me to genetically ablate mTORC1 signaling in adult mice at any time point desired using both a tamoxifen inducible and a doxycycline inducible Cre system linked with adiponectin-drivers. In summary, I find that aberrant signaling responses occur in an acute setting, however the development of lipodystrophy and metabolic disease do not occur until many weeks after these signaling changes. I observed that the progression of metabolic dysfunction closely associated with the appearance of adipose tissue loss, and adipocyte shrinkage

and death. This led me to believe that the onset of lipodystrophy in adipocyte *Raptor* loss may be due to a chronic and progressive loss of adipocytes.

I hypothesized that by activating the autophagic pathway, through loss of mTORC1 inhibition of ULK1, the adipocytes of these animals experienced faster rates of death, leading to loss of adipose tissue mass. I also hypothesized that the development of metabolic disorders such as hepatic steatosis and insulin resistance were dependent on the loss of adipose tissue mass and adipocyte survival capacity, and that rescuing the lipoatrophy defect would also rescue the metabolic dysfunction. To test this, I generated Adiponectin-Cre driven double KO mice of *Raptor* and *ATG7*, a key protein required for autophagy. I found that these mice do in fact recover their adipose tissue mass, suggesting that the progress lipoatrophy seen in adipose *Raptor* KO mice is dependent on mTORC1's inhibition of autophagy. Surprisingly, however, these mice did not seem to recover metabolically, and continued to suffer from adipose tissue inflammation, and hepatic steatosis. These results suggest that recovery of adipose tissue mass alone is insufficient to restore metabolic homeostasis, and that additional mTORC1 dependent pathways in adipocytes may be critical in regulating whole body metabolism.

Lastly, discussed earlier was the current understanding of mTORC1 signaling and its dependence on the amino acid sensing pathway. While most of the biochemistry has been worked out in in vitro cancer cell models, I wanted to explore the role of this pathway in an animal model, specifically relating to

adipose tissue. Based on aforementioned data, I believed that the amino acid sensing RagGTPases would be critical in adipocytes to maintain both mTORC1 activity, and adipose tissue health. I hypothesized that ablation of the RagGTPases in mature adipocytes would phenocopy mTORC1 ablation, indicating the necessity of proper amino acid sensing and signaling to maintain whole body metabolism. To test this, I generated adipose tissue RagA and RagB double KO mice driven by Adiponectin-Cre. Surprisingly these mice are generally phenotypically normal, absent lipodystrophy or metabolic dysfunction. They also appear to have largely intact downstream mTORC1 signaling suggesting that, in mature adipocytes, the RagGTPases may be dispensable for mTORC1 signaling.

Overall, I have identified mature adipocyte mTORC1 as a key regulator for both adipocyte, and whole-body metabolism. It appears that mTORC1's inhibition of autophagy is necessary for the maintenance and growth of adipose tissue, and that loss of mTORC1 results in severe lipoatrophy, along with development of metabolic diseases such as hepatosteatosis, and insulin resistance. Rescue of adipose tissue mass via inhibition of autophagy, however, is also insufficient to restore metabolic homeostasis, suggesting that other downstream mTORC1 pathways within adipocytes are crucial for energy regulation throughout other tissues in the body. Lastly, it appears that while adipocytes are amino acid sensitive in culture, the specific RagGTPases may be dispensable for mTORC1 signaling in adipose tissue. With this knowledge, there are a plethora of future

projects worth pursing related to nutrient sensing signaling, adipose tissue, metabolism, and cancer.

CHAPTER II: Raptor/mTORC1 Loss in Adipocytes Causes Progressive Lipodystrophy and Fatty Liver Disease

This chapter contains materials that are reprinted or have been adapted with permission from the *Molecular Metabolism* article:

Lee, P. L., Tang Y., Li H., Guertin D.A., (2016). "Raptor/mTORC1 loss in adipocytes causes progressive lipodystrophy and fatty liver disease." Mol Metab **5**(6): 422-432.

Abstract:

Objective: Normal adipose tissue growth and function is critical to maintaining metabolic homeostasis and its excess (e.g. obesity) or absence (e.g. lipodystrophy) is associated with severe metabolic disease. The goal of this study was to understand the mechanisms maintaining healthy adipose tissue growth and function.

Methods: Adipose tissue senses and responds to systemic changes in growth factor and nutrient availability; in cells mTORC1 regulates metabolism in response to growth factors and nutrients. Thus, mTORC1 is poised to be a critical intracellular regulator of adipocyte metabolism. Here, I investigate the role of mTORC1 in mature adipocytes by generating and characterizing mice in which the Adiponectin-Cre driver is used to delete floxed alleles of Raptor, which encodes an essential regulatory subunit of mTORC1.

Results: Raptor Adipoq-cre mice have normal white adipose tissue (WAT) mass for the first few weeks of life, but soon thereafter develop lipodystrophy associated with hepatomegaly, hepatic steatosis, and insulin intolerance. Raptor Adipoq-cre mice are also resistant to becoming obese when consuming a high fat diet (HFD). Resistance to obesity does not appear to be due to increased energy expenditure, but rather from failed adipose tissue expansion resulting in severe hepatomegaly associated with hyperphagia and defective dietary lipid absorption. Deleting Raptor in WAT also decreases C/EBPa expression and the

expression of its downstream target adiponectin, providing one possible mechanism of mTORC1 function in WAT.

Conclusions: mTORC1 activity in mature adipocytes is essential for maintaining normal adipose tissue growth and its selective loss in mature adipocytes leads to a progressive lipodystrophy disorder and systemic metabolic disease that shares many of the hallmarks of human congenital generalized lipodystrophy.

1. INTRODUCTION

White adipose tissue (WAT) functions both as the body's major energy storage site, and as a critical endocrine tissue, and interest in understanding its biology has intensified with the obesity epidemic. Obesity (defined as a BMI > 30) results from energy imbalance and can lead to ectopic lipid deposition in non-adipose tissues (e.g. the liver), type 2 diabetes, cardiovascular disease, and some cancers. Obesity now affects more than 1 in 3 adults in the United States, and between 8% and 25% of adults in countries of the European Union, making this a major international clinical problem of this era. Lack of adipose tissue or lipodystrophy also associates with severe metabolic complications. For example, patients suffering from congenital generalized lipodystrophy (or Berardinelli-Seip Syndrome) also develop insulin resistance, hypertriglyceridemia, and fatty liver disease, which can lead to hepatomegaly and liver failure. Thus, normal adipose tissue growth and function is critical to maintaining metabolic homeostasis and

understanding the mechanisms that promote healthy fat has broad clinical implications.

The mechanistic target of rapamycin complex 1 (mTORC1) integrates multiple upstream signals from nutrient availability to promote anabolic metabolism. For example, mTORC1 detects intracellular amino acid availability through multiple sensors that converge upon the Rag GTPases to control mTORC1 subcellular localization, and circulating glucose levels through the insulin-signaling pathway, which promotes mTORC1 activity through the TSC/Rheb pathway [28] [36] [30] Thus, mTORC1 is poised to be a critical regulator of adipocyte function. To test this, I conditionally deleted the essential mTORC1 regulatory subunit Raptor in mature adipocytes with Adiponectin-Cre, which is reported to have greater efficiency and specificity for mature adipocytes than aP2-Cre [62, 88-91]. I find that Raptor Adipoq-Cre mice have normal WAT mass for the first few weeks of life, but progressively develop a lipodystrophy disorder resembling human congenital generalized lipodystrophy including insulin intolerance and hepatic steatosis. These and several additional characteristics of the Raptor Adipoq-Cre mice differ significantly from those of mice in which Raptor was deleted with aP2-Cre [61]. Our results provide a new framework for understanding how mTORC1 signaling helps maintain healthy adipose tissue and could provide insight into human lipodystrophy disorders.

2. MATERIALS & METHODS

2.1. Mice

Raptor floxed mice are described in [46] and were backcrossed 10 generations to C57BL/6J from Jackson Laboratory, and crossed to C57BL/6J background mice expressing the Adiponectin-Cre driver or the Ucp1-Cre driver (generous gifts of Evan Rosen). Floxed Cre-negative mice were used as controls. Mice were kept on a daily 12 h light/dark cycle and fed a normal chow diet (Prolab Isopro RMH 3000) from Lab Diet ad libitum at 22° C. Male mice were used for experimental studies. All animal experiments were approved by the University of Massachusetts Medical School animal care and use committee.

2.2. Antibodies and reagents

PPARg antibody was from Santa Cruz (sc-7196). UCP1 antibody is from AbCam (ab-10983). All other antibodies were purchased from Cell Signaling Technologies: ACC (3676), ACLY (4332), AKT (9727), P-AKT- S473 (4058), ATGL (2439), FASN (3180), HSL (4107), P-HSL-S660 (4126), ULK1 (8054), P-ULK1-S757 (6888), 4EBP1 (9644), P-4EBP1- S65 (9456), P-4EBP1-T37/46. All other reagents were from Sigma Aldrich.

2.3. Diet & metabolic studies

At 12 weeks of age, male mice were placed on a 60% high fat diet (HFD) (D12492 Harlan Laboratories) for 8 weeks. Body weight was recorded weekly. The analysis of blood metabolites was performed by the Joslin Diabetes Center and MMPC at the University of Cincinnati. For glucose tolerance tests (GTT) mice were fasted overnight (16 h) and then administered 2 g/kg of body weight of

glucose or sodium pyruvate by intraperitoneal (i.p.) injection. For insulin tolerance tests (ITT), mice were fasted for 6 h before i.p. administration of 0.75 unit/kg of body weight of insulin. Blood glucose concentrations from tail vein collection were measured before and after the injection at indicated time points. A GE100 Blood Glucose monitor system was used.

2.4. Tissue harvest and histology

Adipose tissue depots were carefully dissected to avoid contamination from surrounding tissue. Samples for RNA or protein were snap frozen in liquid nitrogen and stored at 80° C until analysis. For histology, tissue pieces were fixed in 10% formalin. Embedding, sectioning, and Hematoxylin & Eosin (HE) staining was done by the UMass Medical School Morphology Core. For Oil Red O staining, liver samples were embedded in Optimal Cutting Temperature compound before sectioning and staining. For cell size measurements a minimum of 10 images were taken used per mouse (n = 3 wild type and 3 conditional knockouts). Image J was used to measure cell size and the distribution of cell size as percentage of total counted cells was analyzed.

2.5. Western blots

Tissue samples or cells were lysed in a buffer containing 50 mM Hepes, pH 7.4, 40 mM NaCl, 2 mM EDTA, 1.5 mM NaVO4, 50 mM NaF, 10 mM sodium pyrophosphate, 10 mM sodium β-glycerophosphate and 1% Triton X-100. Tissues were homogenized using a TissueLyser (Qiagen) in the same lysis buffer supplemented with 0.1% SDS, 1% sodium deoxycholate. Equal amounts

of total protein were loaded into acrylamide/bis-acrylamide gels and transferred to PVDF membranes for detection with the indicated antibodies. Membranes were incubated with primary antibodies in 5% milk/PBST or 5% BSA/PBST overnight. Membranes were then incubated for 1hr with HRP-conjugated secondary antibodies. Western blots were developed by enhanced chemiluminescence (PerkinElmer) and detected by X-ray films.

2.6. Lipolysis

Excised pgWAT tissue was incubated in 12 well cell culture dishes in DMEM with or without isoproterenol at 10 nM for 4 h, respectively, before collecting medium to measure glycerol concentration using a commercial kit (Sigma). The glycerol level was normalized with mass of the excised tissue.

2.7. Fecal lipids extraction

Mice were housed individually for 48 h and 1 g of dried feces was collected from each mouse. Feces were powderized using a tissue grinder, and rehydrated in 5 ml of normal saline. A 2:1 chloroform:methanol solution was used to extract lipids from the suspension. To extract lipids, suspension was centrifuged and liquid phase was extract into a pre-weighed glass tube. Leaving the glass tubes in a fume hood, liquid was let to evaporate, leaving dry lipid content. Glass tubes were reweighed to determined total weight of lipids. A detailed protocol can be found at https://bio-protocol.org/e1375.

2.8. Body composition and metabolic cages

Mice were placed into metabolic cages for 3 days at 25 days into their HFD feeding. Lean mass and whole-body fat mass were measured noninvasively using 1H-MRS (Echo Medical Systems, Houston TX), and a 3-day measurement of physical activity, energy expenditure, respiratory exchange ratio, and food intake were conducted using metabolic cages (TSE Systems, Bad Homburg, Germany) by the UMass Mouse Metabolic Phenotyping Center. Thereafter, mice were kept on HFD in normal housing until dissection.

2.9. Gene expression analysis

Cells or tissues were lysed with Qiazol (Invitrogen) and total RNA was isolated with the RNeasy kit (Invitrogen). Equal amounts of RNA were retro-transcribed to cDNA using a High capacity cDNA reverse transcription kit (#4368813, Applied Biosystems). Quantitative RT- PCR was performed in 10 mL reactions using a StepOnePlus real- time PCR machine from Applied Biosystems using SYBR Green PCR master mix (#4309156, Applied Biosystems) according to manufacturer instructions. Relative mRNA expression was determined by the ΔCt method, and Tbp (TATA sequence binding protein) expression was used as a normalization gene in all conventional RT- PCR experiments. Mouse primers used:

Gene	Forward primer (5'-3')	Reverse primer (5'-3')
Tbp	GAAGCTGCGGTACAATTCCAG	CCCCTTGTACCCTTCACCAAT
Sreb1c	AAGCAAATCACTGAAGGACCTGG	AAAGACAAGCTACTCTGGGAG
Chrebpα	CGACACTCACCCACCTCTTC	TTGTTCAGCCGGATCTTGTC
Chrebpβ	TCTGCAGATCGCGTGGAG	CTTGTCCCGGCATAGCAAC
Acly	CTCACACGGAAGCTCCATAA	ACGCCCTCATAGACACCATC
Acaca	GGAGATGTACGCTGACCGAGAA	ACCCGACGCATGGTTTTCA
Fasn	GCTGCGGAAACTTCAGGAAAT	AGAGACGTGTCACTCCTGGACTT
Scd1	CCCTGCGGATCTTCCTTATC	TGTGTTTCTGAGAACTTGTGGTG
Ppary1	TGAAAGAAGCGGTGAACCACTG	TGGCATCTCGTGTCAACCATG

Ppary2	TGGCATCTCTGTGTCAACCATG	GCATGGTGCCTTCGCTGA
Ucp1	CTGCCAGGACAGTACCCAAG	TCAGCTGTTCAAAGCACACA
Ppargc1a	CCCTGCCATTGTTAAGACC	TGCTGCTGTTCCTGTTTTC
Lpl	GGCCAGATTCATCAACTGGAT	GCTCCAAGGCTGTACCCTAAG
Prdm16	CACCTCTGTATCCGTCAGCA	CACCTCTGTATCCGTCAGCA
Pgc1a	CCCTGCCATTGTTAAGACC	TGCTGCTGTTCCTGTTTTC
Ucp1	CTGCCAGGACAGTACCCAAG	CTGCCAGGACAGTACCCAAG
C/ebpα	CAAGCCCAGCAACGAGTACCG	GTCACTGGTCAACTCCAGCAC
C/ebpβ	TCGGGACTTGATGCAATCC	AAACATCAACAACCCCGC
C/ebpδ	GCTTTGTGGTTGCTGTTGAA	ATCGACTTCAGCGCCTACA
aP2	GATGCCTTTGTGGGAACCT	CTGTCGTCTGCGGTGATTT
Cidea	ATCACAACTGGCCTGGTTACG	TACTACCCGGTGTCCATTTCT
Dpt	CTGCCGCTATAGCAAGAGGT	TGGCTTGGGTACTCTGTTGTC
Srebf2	GGATCCTCCCAAAGAAGGAG	TTCCTCAGAACGCCAGACTT
Tfam	GTCCATAGGCACCGTATTGC	CCCATGCTGGAAAAACACTT
Cpt1b	GGGCACCTCTGGGAGTTTGT	TTGGCTCACCCACACAGTGT

2.10. Statistics

Unless otherwise stated, values given are mean SEM. Two-way ANOVA was performed where indicated. For most experiments, unpaired two-tailed Student's t test was used to determine statistical significance among two groups (*$p < 0.05$; **$p < 0.01$; ***$p < 0.001$).

3. RESULTS AND DISCUSSION:

3.1. Adipocyte Raptor KO mice have normal WAT mass early in life.

To investigate the role of mTORC1 in adipocytes, I generated Adiponectin-Cre;Raptorfl/fl mice (herein Raptor Adipoq-cre mice). Raptor Adipoq-cre mice are born at the expected Mendelian ratio and are grossly indistinguishable from their littermates at birth. At post-natal day 14 (P14), there is no difference in total body weight between Raptor L/L and Raptor L/L Adipoq-cre mice (Figure 2.1A). The major subcutaneous and visceral perigonadal white adipose tissue depots (sWAT and pgWAT) are not significantly different in mass from controls at P14

(Figure 2.1B). The mass of other lean tissues such as the heart, kidney, and skeletal muscle is normal (Figure 2.1C). I confirmed Raptor loss by Western blots using whole sWAT and interscapular brown adipose tissue (iBAT) depots (Figure 2.1D); the residual signal reflects the non-adipocyte population (see Section 3.2). Inactivation of mTORC1 activity was confirmed by decreased phosphorylation of the mTORC1 substrates 4E-BP1 (on phospho-T37/46) and ULK1 (on phospho-S757), and by increased phosphorylation of AKT (on phospho-S473), which is caused by loss of the well-known mTORC1 mediated feedback inhibition of insulin/AKT signaling (Figure 2.1D) [4]. I also noted a slight decrease in total ULK1 protein in the KO tissues (Figure 2.1D).

In post-natal development, the sWAT adipocytes exhibit characteristics of brown adipocytes including the presence of multi-locular lipid droplets and positive UCP1 expression (Figure 2.1D,E) [92, 93]. These adipocytes are called brite or beige adipocytes to distinguish them from classic brown adipocytes [94], and with age, they usually convert to or are replaced by more classic-looking unilocular white adipocytes. Raptor Adipoq-cre mice exhibit no defect in the post-natal formation of brite/beige adipocytes in the sWAT as determined by UCP1 protein expression (Figure 2.1D) and the appearance of multilocular adipocytes (Figure 2.1E). There is also no difference in the histological appearance of the pgWAT adipocytes or the liver at P14 (Figure 2.1E). Thus, Raptor is dispensable in white adipocytes for post-natal adipose tissue growth and normal adipocyte size, and for post-natal formation of brite/beige adipocytes in the sWAT.

In contrast, the interscapular and subscapular brown adipose tissue depots (iBAT and sBAT) of Raptor Adipoq-cre mice are reduced in mass by 37% and 48% respectively at P14 (Figure 2.1B). I also noted an increase in the number of brown adipocytes containing large lipid droplets in the Raptor KO BAT (Figure 2.1F). To test whether this phenotype is tissue autonomous, I deleted Raptor with Ucp1-Cre. This also results in a significant size reduction of the BAT depots (Figure S1A) and the heterogeneous appearance of larger lipid droplets (Figure S1B). Total body mass and individual WAT depot mass was normal in RaptorUcp1-Cre mice (Figure S1C, D). Thus, while adipocyte Raptor is dispensable for post-natal WAT growth, it is required autonomously in brown adipocytes for normal post-natal BAT growth and lipid droplet size.

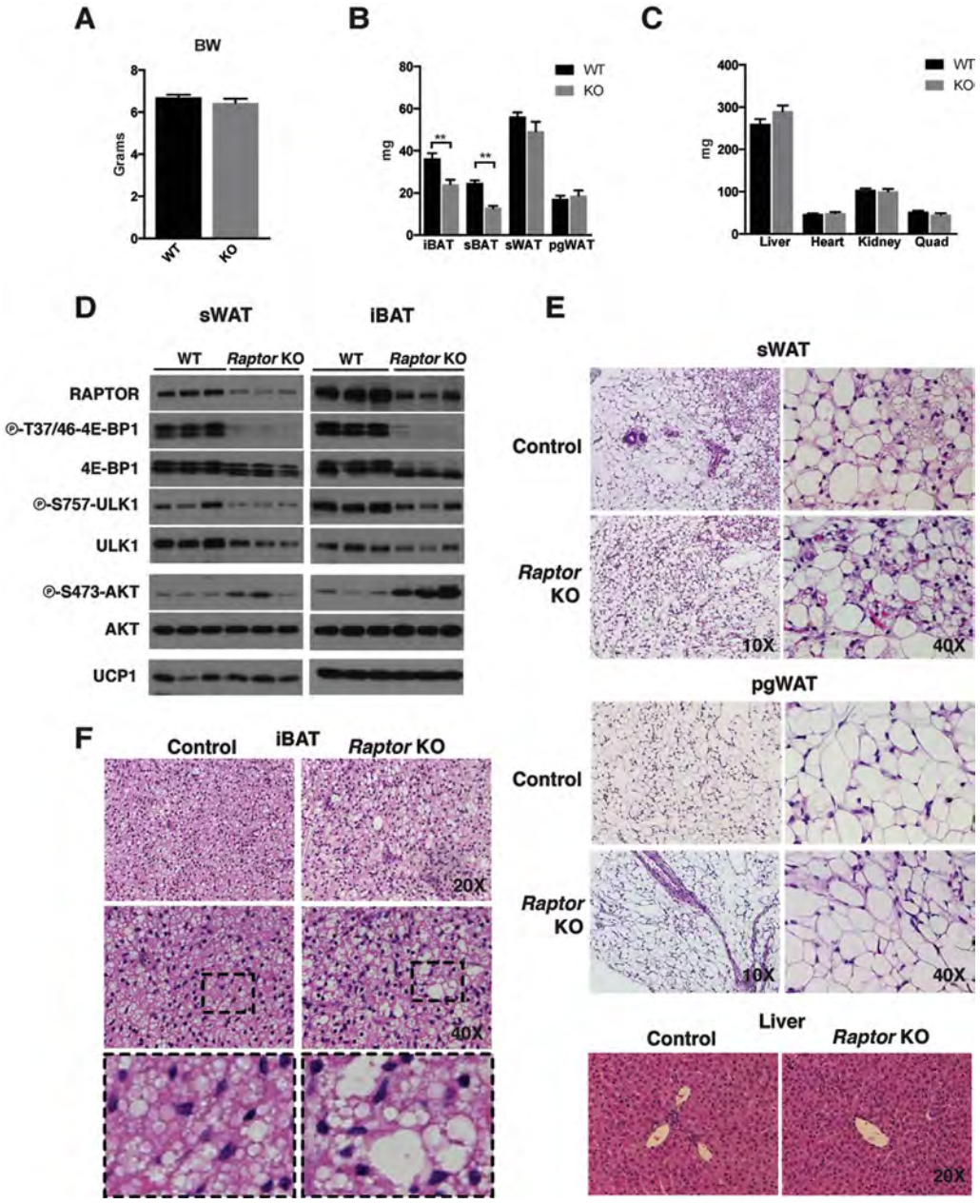

Figure 2.1: 1) Adipocyte Raptor KO mice exhibit normal WAT mass and mild BAT defects early in life. (A) Body weight measurements of KO (n=6) and WT (n=6) mice at 14 days of age. (B) Fat tissue mass of KO and WT mice at 14 days of age. (n=6) (C) Lean tissue mass of KO and WT mice at 14 days of age. (n=6) (D) Western blots of whole tissue lysate from iBAT and sWAT depots for

indicated proteins. (E,F) Representative H&E images of tissues at indicated magnification. (Data were analyzed by Student's t-test. Values expressed as mean ±SEM. *p < 0.05; **p < 0.01; ***p < 0.001).

3.2. Adipocyte Raptor KO mice progressively develop lipodystrophy associated with hepatic steatosis and insulin intolerance.

During the first 4 months of life, Raptor Adipoq-cre mice consuming a normal chow diet (NCD) tend to be slightly heavier than controls although this does not reach statistical significance at least by 12 weeks of age (Figure 2.2A, left). Raptor Adipoq-cre mice also tend to eat slightly more food but again this was not statistically significant (p value = 0.25) (Figure 2.2A, right). However, despite their relatively normal body weight, Raptor Adipoq-cre mice fail to expand their white adipose tissues with age. For example, the KO sWAT, retroperitoneal WAT (rWAT) and pgWAT are 35%, 37%, and 54% smaller respectively in the KOs compared to age matched controls (Figure 2.2B,C); KO BAT tissues also remained small (Figure 2.2B,C). Thus, adipocyte Raptor KO mice progressively develop lipodystrophy with age.

We also confirmed Raptor loss and mTORC1 inactivation in whole sWAT and pgWAT depots from the 12-week old mice (Figure 2.2D). The residual Raptor signal is from stromal vascular fraction (SVF) cells as Raptor is virtually undetectable in purified mature adipocytes (Figure 2.2E). Histological analysis of the white adipocytes from 12-week old Raptor Adipoq-cre mice revealed a

heterogeneous size distribution pattern (Figure 2.2F). For example, pgWAT adipocytes in the Raptor Adipoq- cre mice show a bimodal distribution in which the relative number of small (<100 mM) and large (>200 mM) adipocytes is significantly increased compared to controls (Figure 2.2G). The mutant sWAT also contains two populations of adipocytes: a pool of large unilocular adipocytes and a pool of smaller adipocytes containing multiple lipid droplets (Figure 2.2F). Thus, with age the Raptor Adipoq-cre mice also cannot maintain normal adipocyte morphology.

Strikingly, at 12-weeks of age there is also a 46% increase in liver mass in the Raptor Adipoq-cre mice compared to controls that is associated with a paler color suggesting hepatic steatosis (Figure 2.3A,B). The overgrowth of non-adipose tissues is largely restricted to the liver as the mass of other lean tissues including the heart and skeletal muscles is unchanged (Figure 2.3A). I confirmed hepatic steatosis by Oil Red O staining, which revealed a marked increase in lipid staining in the KO (Figure 2.3C). Consistently, expression of the major de novo lipogenesis (DNL) enzymes ATP-citrate lyase (ACLY), Acetyl-CoA Carboxylase (ACC) and Fatty Acid Synthase (FASN) are also increased in Raptor Adipoq-cre KO livers (Figure 2.3D). Raptor Adipoq-cre KO mice are also insulin intolerant exhibiting a 54% increase in AUC in insulin tolerance tests (Figure 2.3E, top); glucose tolerance is normal (Figure 2.3E, bottom). Serum chemistry analysis indicates normal circulating free fatty acids (FFAs) ($p = 0.77$), circulating triacylglycerides (TAGs) ($p = 0.0851$) and cholesterol.

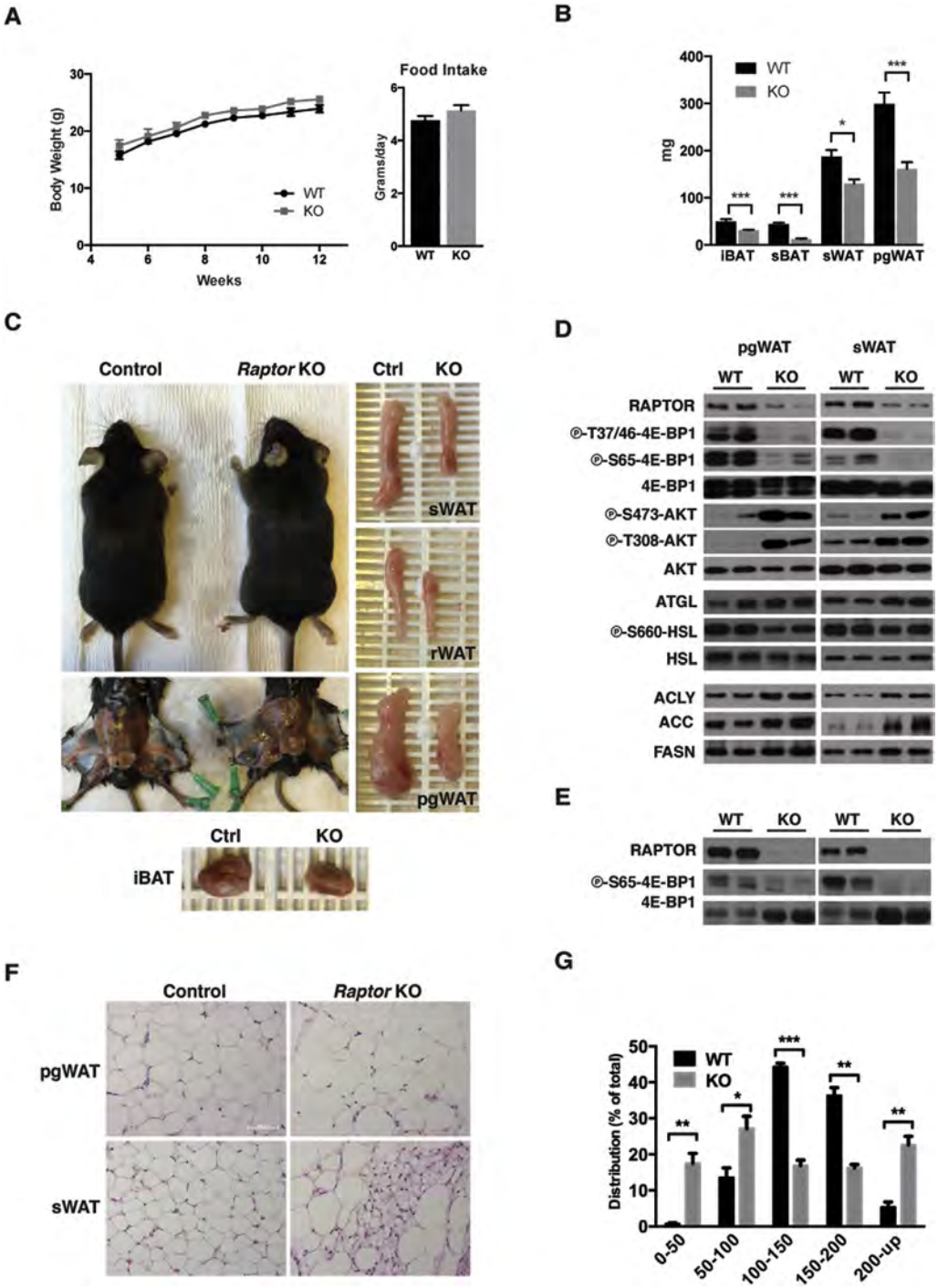

Figure 2.2: 2) Adipocyte Raptor KO mice develop lipodystrophy with age. (A) Body weight growth chart of WT (n = 6) and KO (n = 6) mice up to 12 weeks. Food intake of adult KO and WT mice. (B) Fat tissue mass of KO and WT mice at

12 weeks of age. (n=6) (C) Representative images of adult KO and WT mice, and indicated WAT and BAT depots. (D) Western blots from whole tissue lysate for indicated proteins. (E) Western blots from isolated mature adipocytes for indicated proteins. (F) Representative H&E images of WAT depots from KO and WT mice. (G) Distribution of adipocyte diameter (microns) in pgWAT depots from 12 week old mice on chow diet. (n=6) (Data were analyzed by Student's t-test. Values expressed as mean ±SEM. *p < 0.05; **p < 0.01; ***p < 0.001).

3.3. Altered lipid metabolic pathways in adipocyte Raptor KO mice.

The mTORC1 inhibitor rapamycin can stimulate lipolysis in cultured adipocytes [95, 96]. Therefore, I examined the major regulators of lipolysis in Raptor-deficient adipose tissues. I did not observe a significant increase in hormone sensitive lipase (HSL) phosphorylation between control and KO in pgWAT at 12 weeks of age; in fact it was slightly lower (Figure 2.2D). I also did not detect increased adipose triglyceride lipase (ATGL) protein levels in the sWAT of Raptor Adipoq-cre mice; however, I could detect a slight increase in ATGL in the pgWAT (Figure 2D) that correlated with a modest increase in basal glycerol release from tissue explants (Figure 2.4A). However, *Atgl* mRNA was decreased in both WAT depots (Figure 2.4B). Additionally, I examined regulators of lipogenesis. In the pgWAT of Raptor Adipoq-cre mice I detected significant increases in *Acly* (2.5 fold), *Acc* (2.1 fold), and *Fasn* (2.1 fold) mRNA (Figure 2.4C left) and protein (Figure 2.2D). Similar increases occur in the sWAT

although only the increase in *Acly* mRNA reaches significance even though ACLY, ACC and FASN proteins are all elevated in this depot (Figures 2.2D, 2.4C right). Consistently, expression of *Chrebpb*, which encodes an isoform of ChREBP that potently induces transcription of the DNL genes [19], increases by 124-fold and 48-fold in pgWAT and sWAT respectively (Figure 2.4D). This is interesting because although DNL contributes only a fraction to the total lipid pool of adipocytes, increased *Chrebpb* expression and DNL often correlate with insulin sensitivity [97] indicating this can be uncoupled in the Raptor Adipoq-cre mice. Moreover, while the mTORC1 substrate ULK1 is well known to control autophagy, in mature adipocytes it may have an additional role in lipogenesis downstream of mTORC1 as *in vitro* knockdown of *Ulk1* in differentiated 3T3L1 adipocytes increases Acc and Fasn expression [98]. Thus, *in vivo* Raptor loss in mature adipocytes alters the normal regulation of lipid metabolic pathways, possibly with depot-dependent variances.

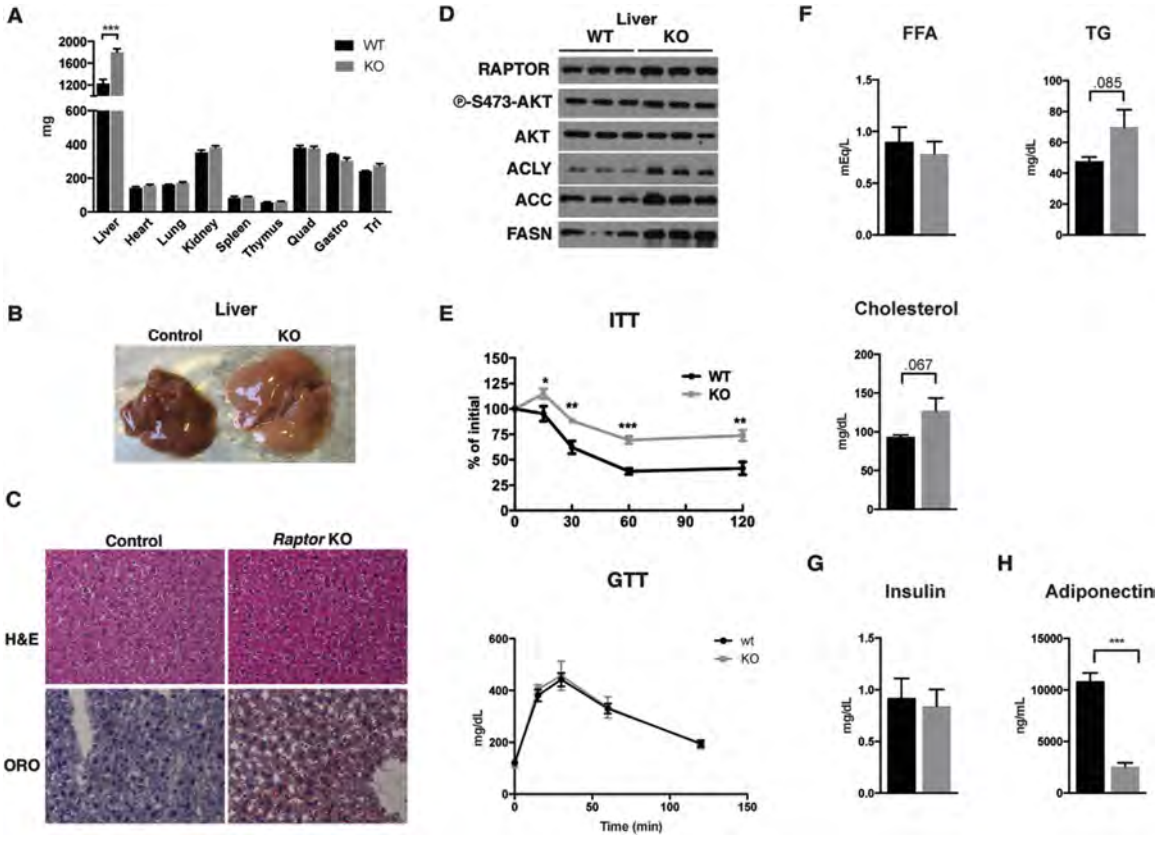

Figure 2.3: 3) The progressive lipodystrophy of adipocyte Raptor KO mice associates with hepatic steatosis and insulin intolerance. (A) Lean tissue mass of KO and WT mice at 12 weeks of age. (n=6) (B) Representative images of liver from KO and WT mice at 12 weeks. (n=6) (C) Representative H&E images of liver from KO and WT mice. (n=6) (D) Western blots of liver lysate for indicated proteins. (E) ITT and GTT of adult KO and WT mice. (n=6) (F) Serum chemistry levels of FFA, TG, and Cholesterol for adult WT and KO mice on chow diet. (n=6) (G) Serum insulin levels for adult WT and KO mice. (H) Serum adiponectin levels for adult WT and KO mice. (n=6) (Data were analyzed by Student's t-test. Values expressed as mean ±SEM. *p < 0.05; **p < 0.01; ***p < 0.001).

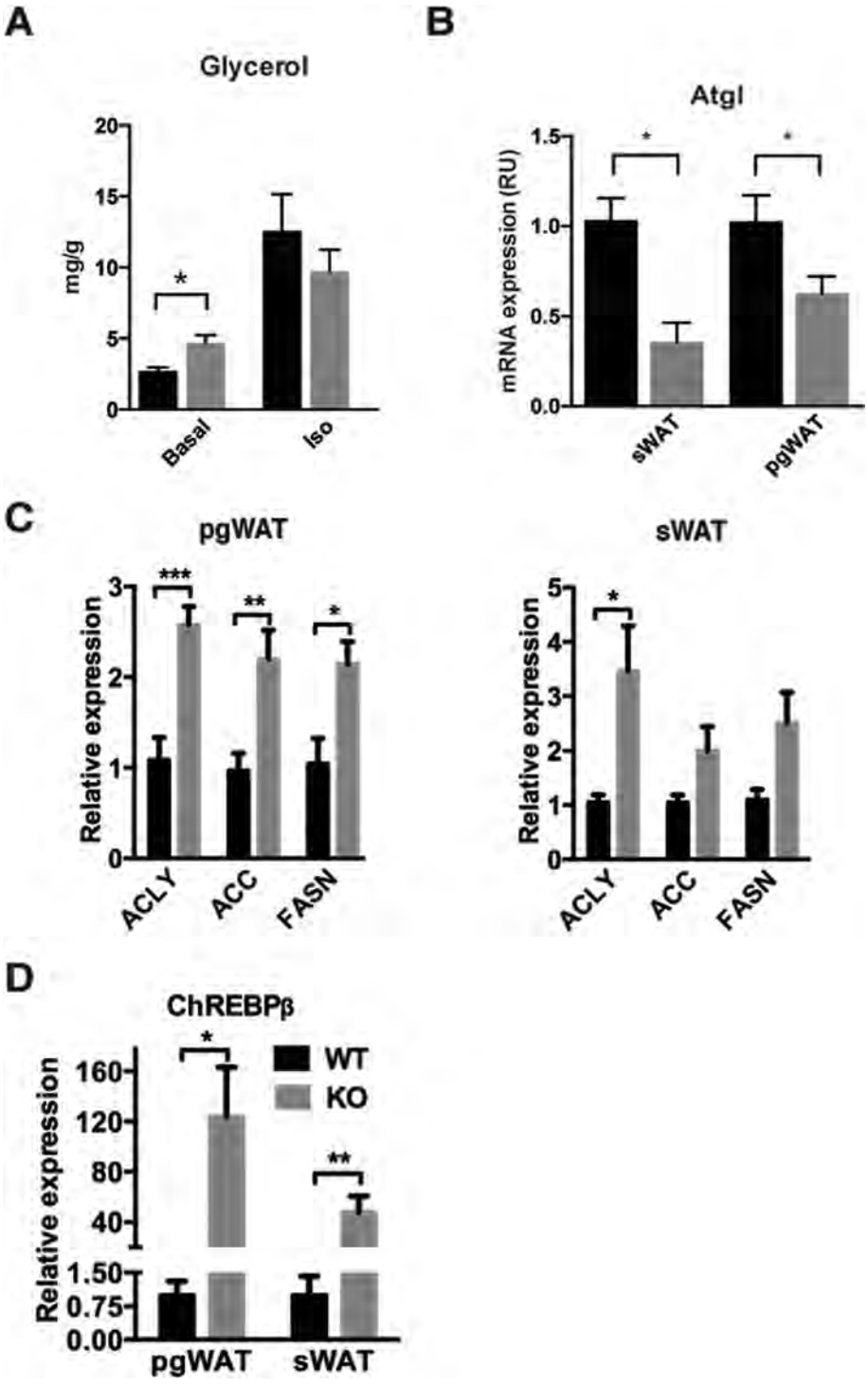
A
Glycerol
mg/g
20
15
10
5
0
*
Basal
Iso
B
Atgl
mRNA expression (RU)
1.5
1.0
0.5
0.0
*
*
sWAT
pgWAT
C
pgWAT
Relative expression
3
2
1
0
***
**
*
ACLY
ACC
FASN
sWAT
Relative expression
5
4
3
2
1
0
*
ACLY
ACC
FASN
D
ChREBPβ
Relative expression
160
120
80
40
1.50
0.75
0.00
*
**
WT
KO
pgWAT
sWAT

Figure 2.4: 4) Altered lipid metabolic pathways in the adipose tissues of adipocyte Raptor KO mice. (A) Concentration of glycerol from media of incubated excised pgWAT depots under specified conditions. (B) ATGL mRNA from whole tissue lysate. (n=6) (C) *Acly*, *Acc*, and *Fasn* mRNA expression in pgWAT and sWAT. (n=6) (D) Chrebpb mRNA expression in pgWAT and sWAT. (n=6) (Data were analyzed by Student's t-test. Values expressed as mean ±SEM. *$p < 0.05$; **$p < 0.01$; ***$p < 0.001$).

3.4. Raptor KO mice are resistant to diet-induced obesity but develop severe hepatic steatosis.

We next asked whether Raptor Adipoq-Cre mice could increase their fat mass if placed on an obesogenic high fat diet (HFD). Beginning at 12-weeks of age, Raptor Adipoq-Cre mice and their age matched controls were switched onto a HFD for 8-weeks. Controls gained on average 9.4 g of body weight while in contrast Raptor Adipoq-Cre mice gained only 2.5 g resulting in a 14% difference in total body mass between the two cohorts after 8 weeks (Figure 2.5A). Body composition analysis indicates the weight difference was due to a 5-fold decrease in fat mass in the mutants, which notably also had slightly higher lean mass (Figure 2.5B). The difference in fat mass is clearly evident upon dissection (Figure 2.5C) and individual tissue mass measurements (Figure 2.5D). Comparing the average mass of individual WAT depots at the start and end of HFD feeding shows that control sWAT increases by 5.9-fold and pgWAT by 6.5-

fold while the mutant sWAT and pgWAT barely grow, increasing by only 1.9-fold and 1.3-fold, respectively (Figure 2.5E). Interestingly, comparing individual adipocyte size at the start and end of HFD feeding indicates that the control and KO adipocytes in both depots increase in size although the size heterogeneity in the KO tissue is still apparent (Figure 2.5F). Thus, despite the inability of whole Raptor KO depots to expand on HFD, Raptor KO adipocytes appear to retain some ability to grow by hypertrophy.

Importantly, at the conclusion of HFD-feeding, the livers of the KO mice are now ~80% larger than controls (as opposed to 46% larger at the start of feeding) resulting in a liver/body weight ratio that is now nearly twice of that of controls (Figure 2.5G,H,I). The livers of the KO mice also exhibit significantly more severe hepatic steatosis (Figure 2.5J). Muscle and heart mass remain unchanged between the cohorts (Figure 2.5G). Thus, the inability of adipose tissues to expand in HFD-fed Raptor Adipoq- Cre mice results in more redistribution of lipids to the liver.

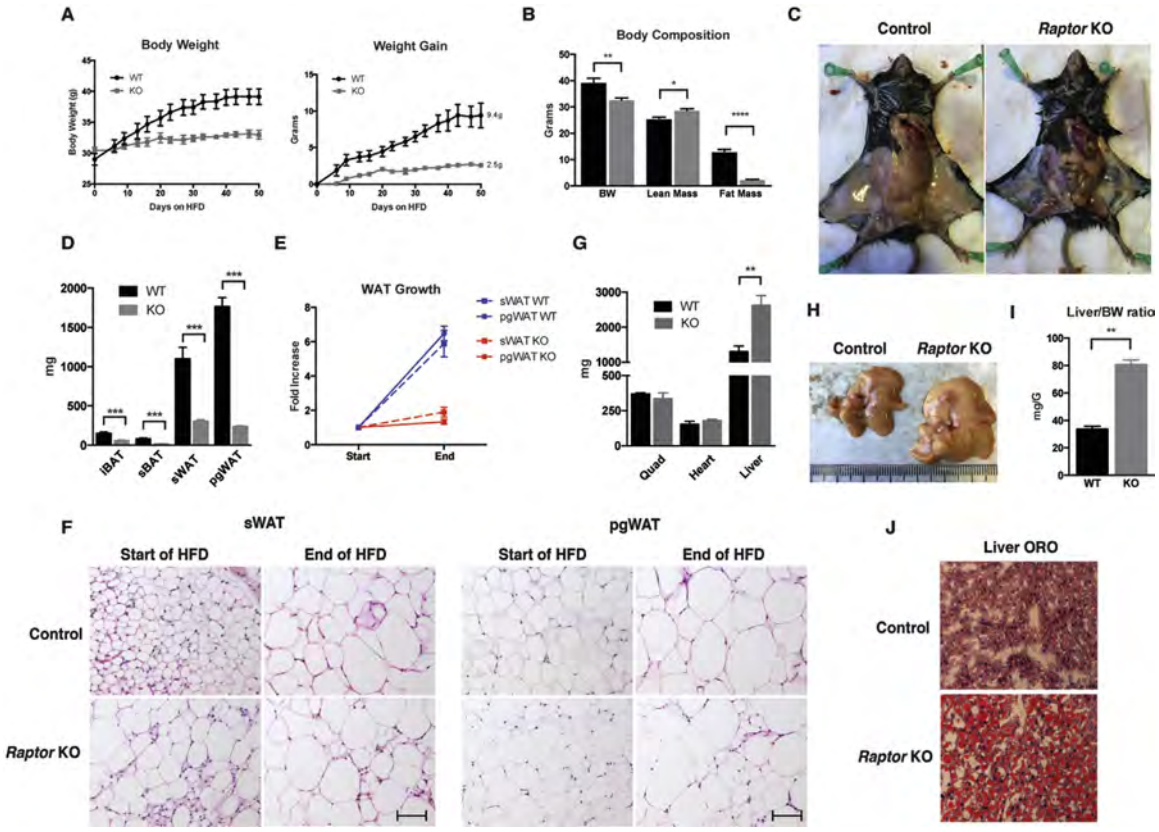

Figure 2.5: 5) Adipocyte Raptor KO mice are resistant to HFD obesity but suffer from more severe hepatic steatosis. (A) Body weight, and weight gain of mice over course of HFD. (n=6) (B) Body weight and body composition after 4 weeks HFD. (C) Representative images of inguinal fat depots after HFD. (n=6) (D) Adipose depot masses at the end of HFD course. (n=6) (E) Fold increase in WAT depot mass after HFD feeding. (n=6) (F) Representative H&E images of specified tissues before and after HFD. (n=6) (G) Lean tissue mass after HFD. (H) Representative images of liver after HFD. (n=6) (I) Liver/BW ratio of mice after HFD. (n=6) (J) Representative ORO staining of liver samples after HFD. (n=6) (Data were analyzed by Student's t-test. Values expressed as mean ±SEM. *p < 0.05; **p < 0.01; ***p < 0.001).

3.5. Adipocyte Raptor KO mice have normal energy expenditure and a lipid absorption defect.

Next I explored possible mechanisms by which deleting Raptor in adipocytes restricts adipose tissue growth. One possibility is that Raptor increases energy expenditure (EE), which protects against obesity. I reasoned that the severe hepatic steatosis and hepatomegaly observed in both chow and HFD fed Raptor Adipo-Cre cohorts argues against this scenario. However, the concept was previously proposed in a study that used aP2-Cre to delete Raptor in adipose tissue [61]. This study observed normal food intake but resistance to HFD and improved insulin tolerance in Raptor aP2-Cre mice and this was attributed to increased *Ucp1* mRNA expression in pgWAT and elevated EE; hepatic steatosis and hepatomegaly was not observed in Raptor aP2-Cre mice. Indeed, I find that *Ucp1* mRNA is increased in both the sWAT and pgWAT of Raptor Adipo-Cre mice consuming chow diet (Figure 2.6A). This correlates with elevated *Pgc1a* levels in sWAT, and elevated Cpt1 in both sWAT and pgWAT (Figure 6A). However, in chow fed mice UCP1 protein was barely detectable in either WAT depot (Figure 2.6B). Moreover, I could only detect a slight increase in UCP1 protein in the sWAT of HFD-fed Raptor Adipo-Cre mice after a long exposure (Figure 2.6B). This suggests that total UCP1 protein is only slightly elevated in the sWAT of Raptor Adipo-Cre mice.

To better assess energy balance I contracted out metabolic cage experiments at the UMass Mouse Metabolic Phenotyping Center. I found no

difference in EE between HFD-fed Raptor Adipoq-cre mice and controls when expressing the data “per mouse” as recommend in [[94]] (Figure 2.6C). However, because it is often debated which method of reporting is correct, I provide the raw data in Table S1. I also found that the Respiratory Exchange Ratio (RER) is higher in Raptor Adipoq-cre mice indicating greater utilization of carbo- hydrates for fuel (Figure 2.6D). Raptor Adipoq-cre mice also exhibited normal physical activity (Figure 2.6E) yet interestingly, they are hyperphagic consuming nearly twice as much food as controls (Figure 2.6F). Hyperphagia is likely explained by the fact that HFD-fed Raptor Adipoq-cre mice have greatly reduced circulating leptin (Figure 2.6G). I also examined fecal lipids and found nearly twice the amount of lipid in the feces of Raptor Adipoq-cre mice (Figure 2.6H) indicating a lipid absorption defect. Thus, the mechanism causing resistance to obesity in Raptor Adipoq-Cre mice cannot be explained by decreased food intake or increased EE.

Based on the increased EE reported in aP2-Cre;Raptor mice, it was suggested that adipose mTORC1 could be a potential target for anti- obesity drugs. However, our results indicate several important phenotypic differences compared to Raptor aP2-Cre mice (see detailed comparison in Table S2). These differences likely reflect recent data indicating that the aP2-Cre driver has limited efficiency for adipocytes and targets non-adipocytes such as endothelial cells [62, 88-91]. It would be interesting to identify the exact target cell/mechanism responsible for the beneficial metabolic effects of deleting Raptor with aP2-Cre.

Nevertheless, in light of our characterization of Raptor Adipoq-Cre mice, I would argue against prolonged targeting of mTORC1 in fat as a strategy to reduce obesity, though the effects of temporal or partial mTORC1 loss have not been thoroughly explored.

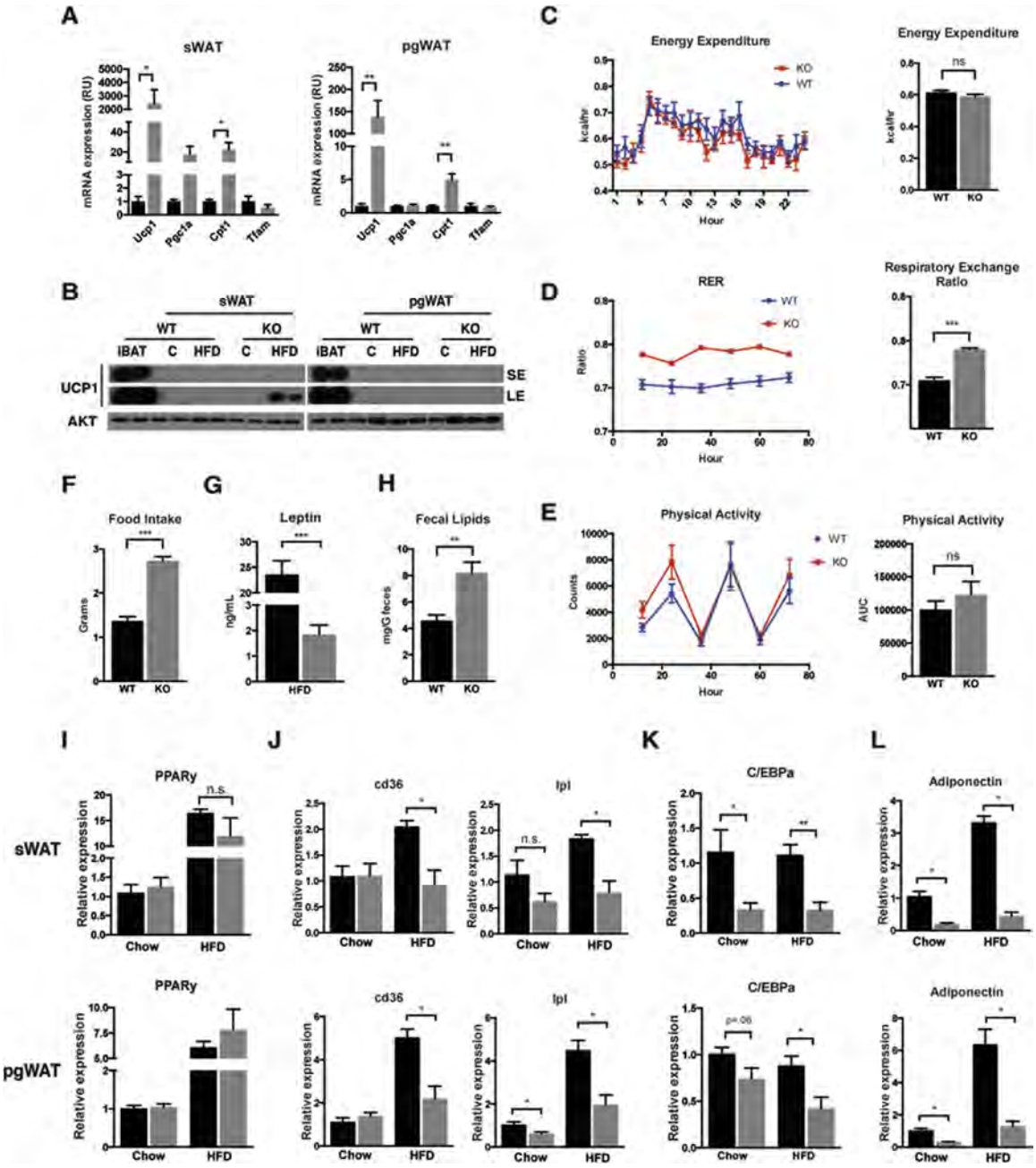

Figure 2.6: 6) Energy utilization and adipocyte transcriptional regulation. (A) mRNA expression levels from whole tissue lysate from Chow fed mice for indicated genes. (n=6) (B) Western blots of whole tissue lysate for indicated proteins from both chow and HFD mice, along with exposure times. SE is short

exposure, LE is long exposure. (C) Mean energy expenditure per mouse over 24 hrs, with AUC. (n=6) (D) Mean respiratory exchange ratio per mouse over 3 days, with AUC. (n=6) (E) Mean activity per mouse over 3 days, with AUC. (F) Daily food intake per mouse after 4 weeks on HFD. (n=6) (G) Serum leptin concentration after HFD. (n=6) (H) Fecal lipid content after 4 weeks HFD. (n=6) (I) PPARy mRNA expression levels in whole tissue lysate for respective mouse models. (n=6) (J) mRNA expression levels of PPARy targets in whole tissue lysate for respective mouse models. (n=6) (K) C/EBPa mRNA expression levels from whole tissue lysate for respective mouse models. (n=6) (L) Adiponectin mRNA expression from whole tissue lysate for respective mouse models. (n=6) (Data were analyzed by Student's t-test. Values expressed as mean ±SEM. *$p < 0.05$; **$p < 0.01$; ***$p < 0.001$).

3.6. Decreased *C/EBPα* activity in Raptor-deficient WAT

We next asked whether adipocytes require mTORC1 to maintain expression of *Ppary*, which encodes the master transcriptional regulator of adipocyte differentiation and function, and is a marker of adipocyte identity. I saw no significant changes in *Ppary* mRNA expression in the sWAT or pgWAT from Raptor Adipoq-Cre mice eating chow or HFD (Figure 2.6I) suggesting Raptor is not required to maintain adipocyte identity per se. I also examined the expression of CD36 and *Lpl*, two *Ppary* targets. In chow fed mice, *Lpl* tended to be lower while CD36 unaffected (Figure 2.6J); in the HFD group, both genes are reduced

(Figure 6J). Thus, *Ppary* activity, particularly during high fat feeding, may be altered in Raptor KO adipocytes.

In contrast to *Ppary*, expression of the *Ppary* co-regulator C/EBPα (the founding member of the CCAAT/enhancer-binding family) is greatly reduced in the sWAT of both chow and HFD-fed mice as well as in pgWAT, though to a lesser extent in this depot (Figure 6K). Interestingly, it was recently reported that C/EBPa in mature adipocytes is dispensable for terminal embryonic adipogenesis and adult adipocyte survival, but required for normal adipose tissue expansion during high fat diet feeding [21, 99]. C/EBPα also promotes adiponectin expression [100-102]. Indeed, adiponectin mRNA expression in WAT (Figure 6L) and circulating Adiponectin levels (Figure 3H) are greatly reduced in Raptor Adipoq-Cre mice. Thus, decreased C/EBPα activity provides a possible mechanism to explain why only older Raptor Adipoq-Cre mice are resistant to adipose tissue expansion.

3.7. Comparison to human lipodystrophy

Raptor Adipoq-Cre mice bear phenotypic resemblance to human patients suffering from congenital generalized lipodystrophy or Berardinelli-Seip lipodystrophy [103]. These patients suffer from adipose tissue loss, and similar to the Raptor Adipoq-Cre model, exhibit insulin resistance, hepatic steatosis, hypertriglyceridemia, and increased RER. Nearly a quarter of the patients develop diabetes mellitus. Other clinical features can include ectopic lipid in muscle and hypertrophic cardiomyopathy. Berardinelli-Seip lipodystrophy is

linked to mutations in AGPAT2 or BSCL2/seipin but the molecular basis of the disease is poorly understood. Interestingly, AGPAT2 and BSCL2 knockout models exhibit several phenotypic similarities to Raptor Adipoq-Cre mice [104-106]. Moreover, the mTORC1 substrate Lipin-1, a phosphatidic acid phosphatase mutated in fatty liver dystrophy (fld) mice, was recently shown to physically interact with Seipin and AGPAT2 [45, 74, 75]. Thus, Raptor Adipoq-Cre mice may be useful in understanding the mechanistic basis of human congenital lipodystrophy.

4. FUTURE DIRECTIONS AND CONCLUSIONS

In this study I investigated the in vivo role of mTORC1 in mature adipocytes by deleting Raptor with Adiponectin-Cre. I conclude that mTORC1 activity in white adipocytes is dispensable for early post-natal WAT growth, but becomes essential for normal adipose tissue expansion with age. Moreover, adipocyte Raptor KO mice consuming a high fat diet are hyperphagic yet resistant to obesity. However, despite increased *Ucp1* mRNA expression in WAT, these mice are not protected from obesity due to increased energy expenditure. Rather, they appear to have a defect in adipose tissue expansion, which redistributes lipids to the liver resulting in severe hepatomegaly and hepatic steatosis, and causes a dietary lipid absorption defect. It does not appear that mTORC1 activity is required in WAT to maintain *Pparg* expression, but it may promote PPARγ activity towards certain targets. I also find that mTORC1 is

required for normal *C/ebpa* and adiponectin expression providing a plausible link to the adipose tissue expansion defect in older mice.

We found no obvious indication that adipocytes were dying in large numbers at least at the time-points examined. One hypothesis is that increased autophagy coupled with defective lipid metabolic pathways, perhaps in part through altered ULK1 and/or Lipin function, could cause defective triglyceride accumulation and/or adipose tissue wasting. Alternatively, mTORC1 in mature adipocytes may promote WAT expansion in older mice by regulating production of a pro-adipogenic paracrine signal. Interestingly, mTORC1 may have a unique function in neo-natal BAT development that requires further examination. Because mTORC1 has several known and putative substrates [47, 48] it will be important to continue delineating the expression and contributions of each downstream pathway in WAT maintenance in vivo using the most updated and precise genetic and metabolic strategies.

We also found that mTORC1 loss did not impair the post-natal BAT-like character of sWAT. Interestingly, it was recently reported that rapamycin blocks the “browning” of WAT in adult mice by inhibiting mTORC1 in mature adipocytes [81, 82] suggesting there may be differential requirements for mTORC1 in post-natal versus adult brite/ beige adipocyte formation. Moreover, another study reported that increased mTORC1 signaling in BAT promotes a brown-to-white phenotypic switch, and in this model, rapamycin reversed the “whitening” of BAT [36, 107]. Thus, the precise role of mTORC1 in BAT/WAT interconversions

remains to be seen. It should be noted that cold-challenge experiments are key in studying BAT, and that was not done in my animals.

Notably, our conclusions are based on chronic (congenital) Raptor loss in adipocytes and thus the primary in vivo defect associated with losing mTORC1 activity cannot be determined by this approach. Future studies utilizing tools that allow us to inhibit mTORC1 in a temporal manner will be key in better understanding primary and secondary responses to mTORC1 loss in adipose tissue. Moreover, it is clearly difficult to obtain the perfect Cre-driver for tissue-specific KO studies, thus future advances may lead to additional refinements in understanding mTORC1 signaling in fat. Nevertheless, Raptor Adipoq-Cre mice exhibit phenotypic similarities to human patients suffering from congenital generalized lipodystrophy suggesting this model may have significant clinical implications. The next chapter will investigate acute vs chronic responses to mTORC1 loss, mechanisms that may contribute to metabolic dysfunction, and a study of upstream regulators involved with mTORC1 activation.

Supplementary Data:

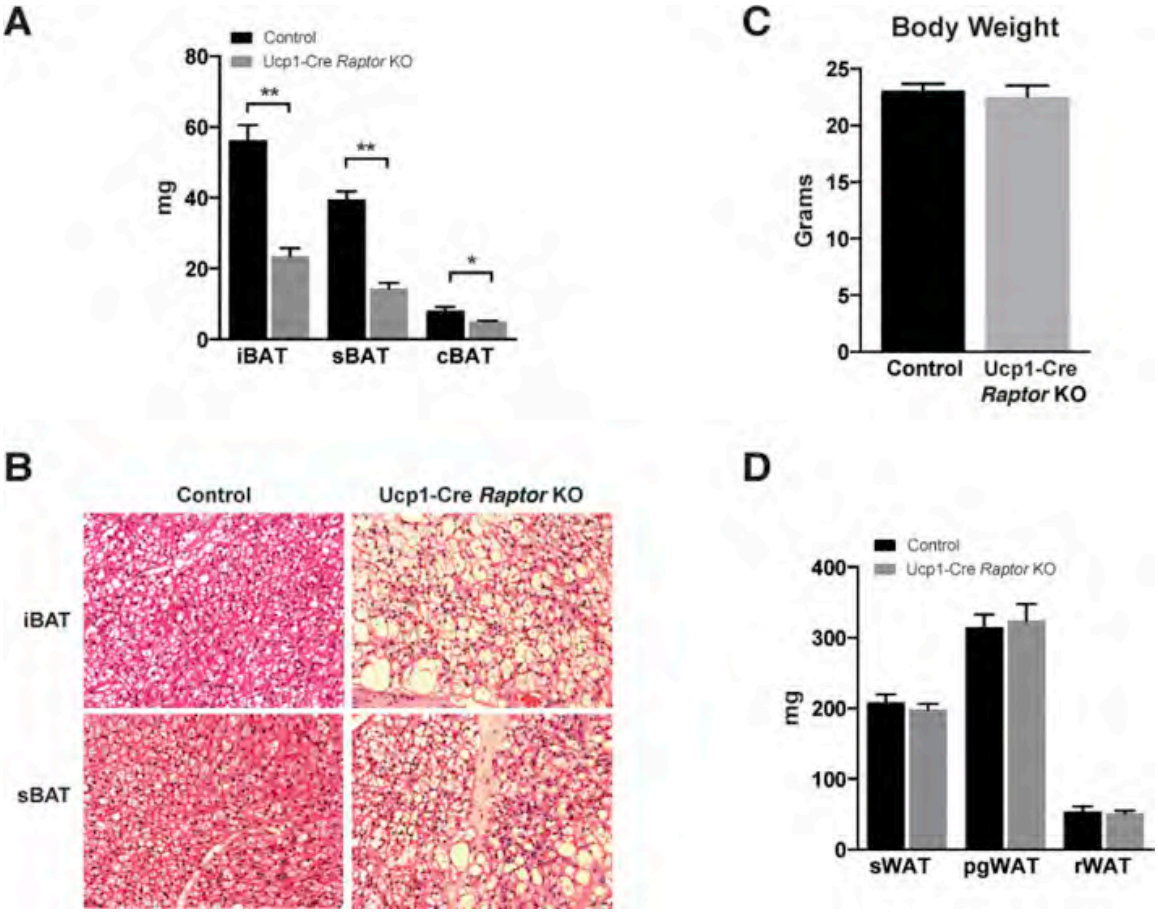

Figure 2.7.) Ucp1-Cre driven *Raptor* KO reveal similar BAT phenotype as Adipoq-Cre driven mice. (A) BAT depot mass in adult Ucp1-Cre *Raptor* L/L KO and WT mice. (n=6) (B) Representative H&E histology of adult WT and KO mice. (n=6) (C) Body weight of adult mice. (n=6) (D) WAT depot mass in adult mice. (n=6)

Body Composition (using 1H-MRS)

Rap L/L mice (n=6)

Mouse #	Fat Mass (g)	Lean Mass (g)	Body Weight (g)
3820	13.87	25.93	40.9
4154	10.11	23.61	35
4292	12.77	28.41	42.6
4692	8.92	23.33	33.5
4693	17	26.27	44.3
4694	13.27	23.93	38.4

Adiponectin -Rap L/L Mice (n=6)

Mouse #	Fat Mass (g)	Lean Mass (g)	Body Weight (g)
3821	2.16	26.22	30.1
3822	1.67	27.42	30.8
4153	1.85	27.52	30.9
4291	2.32	30.67	34.7
4293	1.98	30.71	34.8
4695	3.26	28.55	33.7

Energy Expenditure Rate (24-hr) per Mouse

Rap L/L mice (n=6)

Mouse #	Day 1 (kcal/hr)	Day 2 (kcal/hr)	Day 3 (kcal/hr)	Avg (kcal/hr)
3820	0.6626	0.6230	0.6123	**0.6327**
4154	0.6532	0.6180	0.5988	**0.6233**
4292	0.6566	0.6752	0.6333	**0.6550**
4692	0.5961	0.5669	0.5592	**0.5740**
4693	0.6252	0.6001	0.5589	**0.5947**
4694	0.6231	0.6064	0.6071	**0.6122**
Avg	**0.6361**	**0.6149**	**0.5949**	**0.6153**
SE	**0.0105**	**0.0145**	**0.0123**	**0.0065**

Adiponectin -Rap L/L Mice (n=6)

Mouse #	Day 1 (kcal/hr)	Day 2 (kcal/hr)	Day 3 (kcal/hr)	Avg (kcal/hr)
3821	0.5473	0.5644	0.5362	**0.5493**
3822	0.6411	0.5757	0.5734	**0.5967**
4153	0.5860	0.5657	0.5597	**0.5705**
4291	0.6047	0.6094	0.5812	**0.5984**
4293	0.6514	0.6395	0.6502	**0.6471**
4695	0.5869	0.5683	0.5528	**0.5693**
Avg	**0.6029**	**0.5872**	**0.5756**	**0.5885**
SE	**0.0158**	**0.0125**	**0.0163**	**0.0071**

Figure 2.8: Supplementary Table 1 – Raw Energy Expenditure data

Parameter Examined	**Observed difference relative to control**	
	Raptor Adipo$^{q\text{-}Cre}$	***Raptor$^{aP2\text{-}Cre}$***
Total body mass	**Normal**	**Reduced**
Adipose tissue mass	Reduced	Reduced
Adipocyte Size	**Bimodal distribution**	**Normal**
Liver mass	**Increased**	**Normal**
Hepatic Lipids	**Increased**	**Slightly decreased**
ITT	**Insulin Intolerant**	**n.d.**
GTT	Normal	Normal
Adiponectin	Decreased	Decreased
Fasting Insulin	No difference	Decreased
Leptin	Chow (no difference) HFD (reduced)	Chow (Decreased) HFD (decreased)
Ucp1	Increased (sWAT & pgWAT)	Increased (pgWAT only)
UCP1 (protein)	Very low (sWAT); Undetectable (pgWAT)	n.d.

Response to HFD	**Reduced adipose tissue growth; severe hepatomegaly <u>and hepatic steatosis</u>**	**Reduced adipose tissue growth; no difference in hepatic steatosis**
Energy Expenditure (HFD)	**No change** (normalized per mouse)	**Increased** (normalized to 0.75 power of total body weight)
Food Intake (HFD)	**Increased**	**No difference**
Physical Activity (HFD)	**No difference**	**Decreased**
Fecal Lipids (HFD)	**Increased**	**No difference**
Basal Lipolysis in WAT (ex vivo)	**Slightly Increased (pgWAT)**	**No difference**
Ppary	(mRNA) normal in vivo	(mRNA) normal in vivo
Cebpa	**Decreased**	**No difference**
Chrebb	Increased in sWAT & pgWAT	n.d.
DNL pathway (*Acly, Acc, Fasn*)	mRNA & protein increased	n.d.

BOLD Indicates key differences between models
n.d. Not determined
ITT Insulin tolerance test
GTT Glucose tolerance test
HFD High fat diet
sWAT Subcutaneous white adipose tissue
pgWAT Peri-gonadal white adipose tissue

Figure 2.9: Supplementary Table 2- A comparison between the *Raptor Adipo*$^{q\text{-}Cre}$ mice described in this study and previously described *Raptor*$^{aP2\text{-}Cre}$ mice

CHAPTER III: Adipose mTORC1 Regulates Adipose Tissue Health Independent of Autophagy-mediated Lipoatrophy, and Amino Acid Sensing RagGTPases.

INTRODUCTION:

In the previous chapter, I reported that the mechanistic target of rapamycin complex 1 (mTORC1) plays an important role in maintaining normal adipose tissue growth. mTORC1 is a metabolic node that integrates upstream indicators of energy availability and uses these inputs to act upon downstream targets that regulate anabolic pathways [28]. The specific loss of mTORC1 signaling in mature, differentiated adipocytes of mice leads to the development of lipodystrophy that becomes evident as mice age into adulthood [77]. After several months of age, adipose-mTORC1 deficient mice suffer from numerous metabolic abnormalities such as severe hepatomegaly, insulin resistance, hyperphagy, and defective dietary lipid absorption. The underlying mechanism that lead to the lipodystrophy seen in adipose-Raptor KO mice was unclear. With a constitutive deletion, several factors may contribute to the progression of lipodystrophy, including interference with development, lipid accumulation, adipocyte differentiation, and adipocyte death. To better understand and model the role of adipocyte mTORC1 signaling in mature adipose tissue, I generated chemically inducible genetic models that allow us to specifically inhibit mTORC1 signaling in mature adipocytes, at any point of development. This allows for mice to develop normally to adulthood before inhibiting mTORC1 activity, in a way mimicking signaling changes that may occur in obese patients [108] [109]. Ultimately this may be a useful model in understanding mechanisms that lead to adipose tissue malfunction in adult onset obesity.

I find that loss of mTORC1 signaling in adult mice leads to lipodystrophy over a prolonged period of time, similar to mTORC1 congenital deletion, while there are little to no metabolic changes in the short term. I find that acute loss of mTORC1 may induce pathways that in fact promote adipocyte survival, but chronic ablation leads to wasting of AT and evidence of adipocyte death. In conjunction with this loss of AT mass, I see increases in AT inflammation, hepatic steatosis, and insulin resistance. Interestingly, it appears that autophagic flux leads to wasting of AT and progressive lipoatrophy. I show that, using Atg7/Raptor dKO mice, this phenomenon is reversed when autophagy is inhibited, however, accompanying AT inflammation and steatosis persisted. These results suggest that adipose mTORC1 plays an important role in whole body metabolic homeostasis, independent of adipocyte capacity and AT mass.

2. MATERIALS & METHODS

2.1. Mice

R26R-mTmG (stock 007676) were from Jackson Laboratory. Raptor floxed mice are described in [13] and were backcrossed 10 generations to C57BL/6J background mice from Jackson Laboratory and crossed to C57BL/6J mice expressing the Adiponectin-Cre driver or the Adiponectin-CreER driver (generous gifts of Evan Rosen). Doxycycline inducible KO mice were generated with Tre-Cre Adiponectin-rtTA mice crossed with Raptor L/L. Both Cre control and Floxed Cre-negative mice were bred. Floxed-cre negative mice were used as controls. Male mice were used in experiments. Mice were kept on a daily 12 h light/dark

cycle and fed a normal chow diet (Prolab Isopro RMH 3000) from Lab Diet ad libitum at 22 C. All animal experiments were approved by the University of Massachusetts Medical School animal care and use committee.

2.2. Drug inducible deletion

Tamoxifen-inducible mice were treated with IP injection of 3 mg Tamoxifen per day (i.p.) for 6 constitutive days. Prolonged Tamoxifen treatment involved a single injection on a weekly basis, after initial 6-day treatment. Doxycycline inducible mice were fed a 600mg doxycycline/kg diet (Bioserv S4107), for indicated lengths of time.

2.3. Antibodies and reagents

Antibodies were purchased from Cell Signaling Technologies: ACC (3676), ACLY (4332), AKT (9727), P-AKT-S473 (4058), ATGL (2439), FASN (3180), HSL (4107), P-HSL-S660 (4126), ULK1 (8054), P-ULK1-S757 (6888), 4EBP1 (9644), P-4EBP1- S65 (9456), P-4EBP1-T37/46. UCP1 antibody was from AbCam (ab-10983). Mitochondrial OxPhos antibody was from AbCam (ab110413) All other All other reagents were from Sigma Aldrich.

2.4. Metabolic studies

Serum samples were sent to the MMPC at the University of Cincinnati for analysis of circulating metabolites. For glucose tolerance tests (GTT) mice were fasted overnight (16 h) and then administered 2 g/kg of body weight of glucose or sodium pyruvate by intraperitoneal (i.p.) injection. For insulin tolerance tests (ITT), mice were fasted for 6 h before i.p. administration of 0.75 unit/kg of body

weight of insulin. Blood glucose concentrations were measured using a GE100 blood glucose monitor, using blood vein collection before and after the injection at indicated time points.

2.5. Tissue harvest and histology

Adipose tissue depots were carefully dissected to avoid contamination from surrounding tissue. Samples for RNA or protein were snap frozen in liquid nitrogen and stored at 80°C until analysis. For histology, tissue pieces were fixed in 10% formalin. Embedding, sectioning, and Hematoxylin & Eosin (HE) staining was done by the UMass Medical School Morphology Core. For Oil Red O staining, liver samples were embedded in Optimal Cutting Temperature compound before sectioning and staining. For cell size measurements a minimum of 10 images were taken used per mouse. Image J was used to measure cell size and the distribution of cell size as percentage of total counted cells was analyzed.

2.6. Adipocyte precursor cell (APC) isolation and FACS analysis

Adipose progenitor cells (APC) were isolated as described in [19] : Stromal vascular fraction (SVF) was prepared from each fat pad by collagenase treatment and SVF pellets were resuspended in erythrocyte lysis buffer (0.15 M $ClNH_4$, 0.01 M HCO_3K in water). Cells were then pelleted by centrifugation, resuspended in staining media (HBSS + 2% FBS), and labeled with appropriate antibodies. After staining, cells were filtered through a 35-μm cell-strainer capped tube to ensure single cell suspension and stained with live/dead Blue. Live single

cells were gated according to the expression of surface markers ($CD31^{-}CD45^{-}CD29^{+}CD34^{+}Sca1^{+}$) in a BD LSRII analyzer. Data was analyzed with FlowJo. Markers: Live/dead Blue (Molecular Probes, L23105), CD31-PE-CY7 (eBioscience, 25-0311), CD45-PE-CY7 (eBioscience, 25-0451), CD29-AlexaFluor700 (Biolegend, 102218), CD34-AlexaFluor647 (Biolegend, 119314), Sca1-Pacific Blue (BD Bioscience, 560653), CD45-FITC (eBioscience, 11-0451)

2.7. Adipocyte Labeling

R26R-mTmG L/L (stock 007676) mice were crossed with Adiponectin-Cre Raptor L/L to generate Adiponectin Cre Raptor L/L mTmG L/L mice. Depots were dissected mounted whole and intact. Fragments were mounted with Fluoromount-G (Southern Biotech). Mounted samples were imaged the same day on a LSM 5 Pascal (Zeiss) point scanner confocal system. To acquire the images for quantification, a general survey of the entire tissue was first performed using a 10X objective to determine the uniformity of labeling throughout the tissue. Then, the tissue was subdivided into quadrants and a 40X oil immersion objective was used to obtain random images from each quadrant. Background fluorescence was offset using tissues from animals not carrying the *R26R-mTmG* reporter. tdTomato and eGFP settings were set using fat tissues from mice carrying the *R26R-mTmG* reporter and from *adiponectin-Cre;R26R-mTmG* mice, respectively. eGFP was excited at 488 nm and detected from 515 to 565 nm. tdTomato was excited at 543 nm and detected from 575 to 640 nm.

2.8. Western blots

Tissue samples or cells were lysed in a buffer containing 50 mM Hepes, pH 7.4, 40 mM NaCl, 2 mM EDTA, 1.5 mM NaVO4, 50 mM NaF, 10 mM sodium pyrophosphate, 10 mM sodium β-glycerophosphate and 1% Triton X-100. Tissues were homogenized using a TissueLyser (Qiagen) in the same lysis buffer supplemented with 0.1% SDS, 1% sodium deoxycholate. Equal amounts of total protein were loaded into acrylamide/bis-acrylamide gels and transferred to PVDF membranes for detection with the indicated antibodies. Membranes were incubated with primary antibodies in 5% milk/PBST or 5% BSA/PBST overnight. Membranes were then incubated for 1hr with HRP-conjugated secondary antibodies. Western blots were developed by enhanced chemiluminescence (PerkinElmer) and detected by X-ray films.

2.9. Gene expression analysis

Cells or tissues were lysed with Qiazol (Invitrogen) and total RNA was isolated with the RNeasy kit (Invitrogen). Equal amounts of RNA were retro-transcribed to cDNA using a High capacity cDNA reverse transcription kit (#4368813, Applied Biosystems). Quantitative RT- PCR was performed in 10 mL reactions using a StepOnePlus real- time PCR machine from Applied Biosystems using SYBR Green PCR master mix (#4309156, Applied Biosystems) according to manufacturer instructions. Relative mRNA expression was determined by the DCt method, and Tbp (TATA sequence binding protein) expression was used as

a normalization gene in all conventional RT- PCR experiments. Mouse primers used:

Gene	Forward primer (5'-3')	Reverse primer (5'-3')
Tbp	GAAGCTGCGGTACAATTCCAG	CCCCTTGTACCCTTCACCAAT
Sreb1c	AAGCAAATCACTGAAGGACCTGG	AAAGACAAGCTACTCTGGGAG
Chrebpα	CGACACTCACCCACCTCTTC	TTGTTCAGCCGGATCTTGTC
Chrebpβ	TCTGCAGATCGCGTGGAG	CTTGTCCCGGCATAGCAAC
Acly	CTCACACGGAAGCTCCATAA	ACGCCCTCATAGACACCATC
Acaca	GGAGATGTACGCTGACCGAGAA	ACCCGACGCATGGTTTTCA
Fasn	GCTGCGGAAACTTCAGGAAAT	AGAGACGTGTCACTCCTGGACTT
Scd1	CCCTGCGGATCTTCCTTATC	TGTGTTTCTGAGAACTTGTGGTG
Ppary1	TGAAAGAAGCGGTGAACCACTG	TGGCATCTCGTGTCAACCATG
Ppary2	TGGCATCTCTGTGTCAACCATG	GCATGGTGCCTTCGCTGA
Ucp1	CTGCCAGGACAGTACCCAAG	TCAGCTGTTCAAAGCACACA
Ppargc1a	CCCTGCCATTGTTAAGACC	TGCTGCTGTTCCTGTTTTC
Lpl	GGCCAGATTCATCAACTGGAT	GCTCCAAGGCTGTACCCTAAG
Prdm16	CACCTCTGTATCCGTCAGCA	CACCTCTGTATCCGTCAGCA
Pgc1a	CCCTGCCATTGTTAAGACC	TGCTGCTGTTCCTGTTTTC
Ucp1	CTGCCAGGACAGTACCCAAG	CTGCCAGGACAGTACCCAAG
C/ebpα	CAAGCCCAGCAACGAGTACCG	GTCACTGGTCAACTCCAGCAC
C/ebpβ	TCGGGACTTGATGCAATCC	AAACATCAACAACCCCGC
C/ebpδ	GCTTTGTGGTTGCTGTTGAA	ATCGACTTCAGCGCCTACA
aP2	GATGCCTTTGTGGGAACCT	CTGTCGTCTGCGGTGATTT
Cidea	ATCACAACTGGCCTGGTTACG	TACTACCCGGTGTCCATTTCT
Dpt	CTGCCGCTATAGCAAGAGGT	TGGCTTGGGTACTCTGTTGTC
Srebf2	GGATCCTCCCAAAGAAGGAG	TTCCTCAGAACGCCAGACTT
Tfam	GTCCATAGGCACCGTATTGC	CCCATGCTGGAAAAACACTT
Cpt1b	GGGCACCTCTGGGAGTTTGT	TTGGCTCACCCACACAGTGT

2.10. Statistics

Unless otherwise stated, values given are mean SEM. Two-way ANOVA was performed where indicated. For most experiments, un- paired two-tailed Student's t test was used to determine statistical significance among two groups (*$p < 0.05$; **$p < 0.01$; ***$p < 0.001$).

RESULTS:

Adipose Raptor KO mice do not regain metabolic homeostasis:

It was previously reported that adipose Raptor KO mice experience physiological changes in metabolic function such as reduced fecal lipid uptake

and increased RER, and development of lipodystrophy [77]. To see whether or not these physiological changes were adaptive in order to reestablish metabolic homeostasis and possibly sufficient to overcome Raptor loss, I allowed conditional Raptor KO to reach 1 year of age. I found these mice are unable to compensate for the loss of Raptor in mature adipocytes. These mice suffer from increased severity of lipodystrophy with extremely small adipose tissue depots, including a near absence of visceral WAT (Figure 3.1A-B), along with evidence of adipose tissue necrosis in both brown and white depots (Figure 3.1C). The mice suffer from extreme splenomegaly and hepatomegaly, with masses at least 2-fold greater than control mice (Figure 3.1D). In addition, I see development of tumors in these enlarged livers in 7/9 mice (Figure 3.1F). Despite depletion of adipose tissue depots as a whole, there are still adipocytes that remain and appear to be viable. To understand whether or not these remaining adipocytes were in fact targeted by the Adiponectin-Cre, I crossed in a fluorescent reporter that labels with GFP all cells that express Adiponectin-Cre. Using this tool, I found that in Adiponectin-Cre Raptor L/L mTmG L/L mice, the adipose depots are labeled with near 100% efficiency (Figure 3.1E).

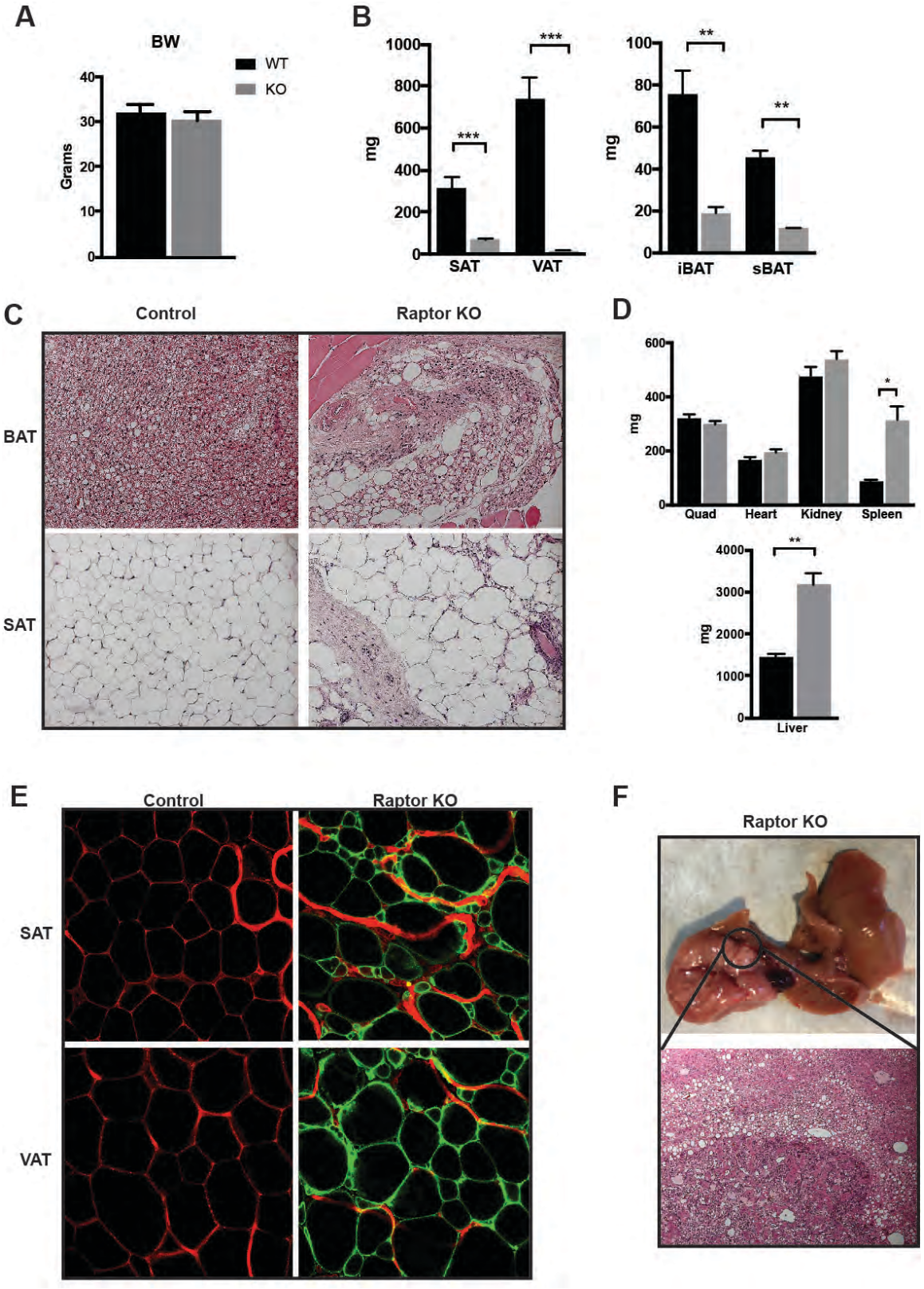
A
BW
WT
KO
Grams
40
30
20
10
0
B
1000
800
600
400
200
0
mg
***
***
SAT
VAT
100
80
60
40
20
0
mg
**
**
iBAT
sBAT
C
Control
Raptor KO
BAT
SAT
D
600
400
200
0
mg
Quad
Heart
Kidney
Spleen
*
4000
3000
2000
1000
0
mg
**
Liver
E
Control
Raptor KO
SAT
VAT
F
Raptor KO

Figure 3.1: 1) Adipose Raptor KO adipocytes are universally targeted, and KO mice are unable to metabolically adapt as they age. A-B) Body weight and tissue weight of control, and Adiponectin-Cre Raptor L/L mice at >1yr of age (n= 9) C) Representative H&E staining of respective tissues (n=9) D) Lean tissue mass (n=9) E) GFP/RFP imaging of mTmG floxed mice, and Adiponectin-Cre Raptor L/L mTmG L/L mice (n=6) F) Example of a diseased liver with tumor from KO mouse (n=9) (Data were analyzed by Student's t-test. Values expressed as mean ±SEM. *$p < 0.05$; **$p < 0.01$; ***$p < 0.001$).

Inducing Raptor deletion in healthy adult mice causes a similar progressive lipodystrophy

To better understand the role of Raptor signaling in fully developed, adult mice, I generated two chemically inducible systems to delete Raptor in mature adipocytes. One commonly used model is a tamoxifen-dependent CreER recombinase, although there are concerns regarding lipotoxicity with tamoxifen [110]. Another model is a tetracycline-dependent Tet-On system, although the use of doxycycline may affect mitochondrial health, gut microbiome, and I find the labeling to be incomplete in adipocytes when paired with Adiponectin-Cre (Figure 3.3C). Nevertheless, both systems offer advantages in the study of Raptor deletion in adult mice. In an acute setting, both tamoxifen and doxycycline treatment had no effect on the mice, in contrast to other models such as a tamoxifen-induced double KO of IR and IGF1 [87]. Over time, however, such as

at 4wks of deletion with tamoxifen, I began to see mild changes in WAT depot size and adipocyte diameter, although there is no apparent metabolic phenotype yet at this point (Figure 3.2A, E). With the CreER system and utilizing mTmG labeling, I find very efficient labeling in the AT depots, with roughly 95% labeling in SAT and 90% in VAT within a week after tamoxifen injection. Over time this labeling remains strong with 90% and 85% respectively at 5 weeks (Figure 3.2B). To better understand a chronic loss of Raptor in adult mice, I used the doxycycline inducible Tet-On mice to avoid issues such as toxicity with tamoxifen, and the chronic stress of exposing mice to long term IP injections of tamoxifen over the course of 10 weeks. Despite incomplete labeling (Figure 3.3C), I see that after 10wks of doxycycline treatment, these mice begin to suffer from lipodystrophy, altered adipocyte size in vivo, with a corresponding hepatomegaly and metabolic defect in insulin sensitivity, similar to what was seen with a constitutive adipose specific deletion of Raptor (Figure 3.2C-E) [77].

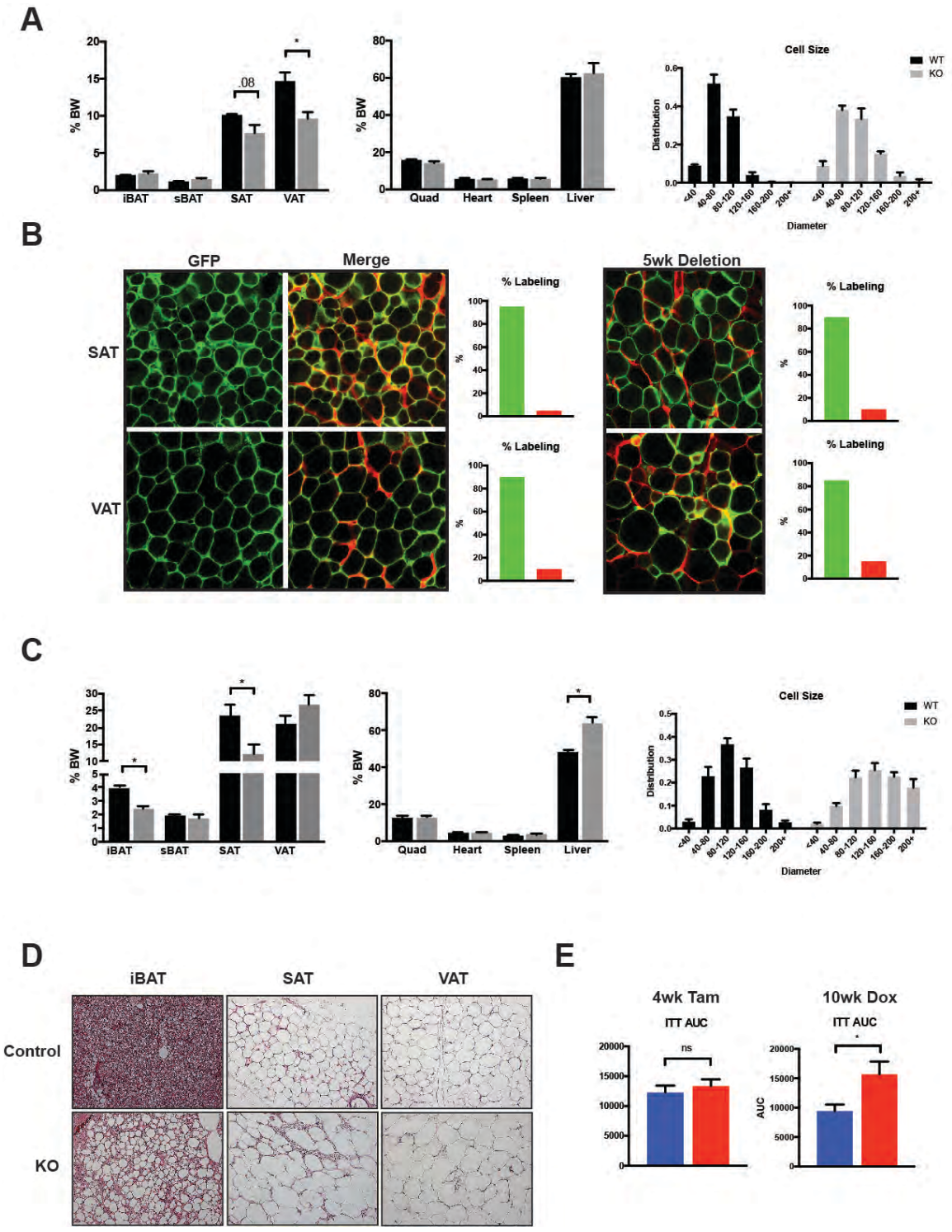

Figure 3.2 2) In vivo, metabolic consequences arise weeks after inducing Raptor deletion. A) Tissue mass and adipocyte size distribution of adult mice treated

with tamoxifen for 5 weeks. (n=6) B) mTmG labeling of control and KO mice treated with tamoxifen for indicated times (n=3) C) Tissue mass and adipocyte size distribution of adult mice treated with doxycycline for 10 weeks (n=6) D) Representative H&E imaging of adipose tissue from KO mice treated with doxycycline for 10 weeks (n=6) E) ITT for indicated mice. (n=6) (Data were analyzed by Student's t-test. Values expressed as mean ±SEM. *p < 0.05; **p < 0.01; ***p < 0.001).

Adipocyte differentiation is preserved in acute Raptor deletion, while chronic deletion leads to adipocyte death

As mentioned earlier, contributing factors to lipodystrophy may include impaired lipid accumulation, disruption of adipocyte differentiation, and increased adipocyte cell death [111]. Using a cell culture model, I am able to delete Raptor after adiponectin expression during adipocyte differentiation, mimicking the adipocyte differentiation process of the KO mice in vivo (Figure 3.3A). In vitro, adipocytes are able to differentiate and accumulate lipids despite Raptor loss (Figure 3.3B). Additionally, sorting for cell surface markers of the stromal vascular fraction from WAT depots show that KO mice do not have a deficiency in adipose precursor cells. Overtime, in the setting of incomplete adipocyte targeting, adipocytes that are not targeted for deletion have a competitive advantage that lead to a recovery of the AT (Figure 3.3C). Utilizing doxycycline inducible Raptor KO animals with the mTmG reporter, I see significant

repopulation with a majority of untargeted, RFP labeled, cells (Figure 3.3C). With this recovery in adipose tissue mass is also a recovery in liver mass, and insulin sensitivity, suggesting that Raptor KO induced lipodystrophy and associated metabolic disfunction may be recovered given the presence of normal adipocytes (Figure 3.3D). In the setting of Raptor KO induced lipodystrophy, however, the adipose tissue depots of these mice develop evidence of adipocyte death as seen by presence of atrophied GFP labeled cells in reporter mice, TUNEL staining, and presence of Crown like structures (CLS) (Figure 3.3C, E, F). Additionally, as has been reported previously, adipocyte specific Raptor deletion results in inflammation and increased macrophage markers within the adipose tissue (Figure 3.3G) [112].

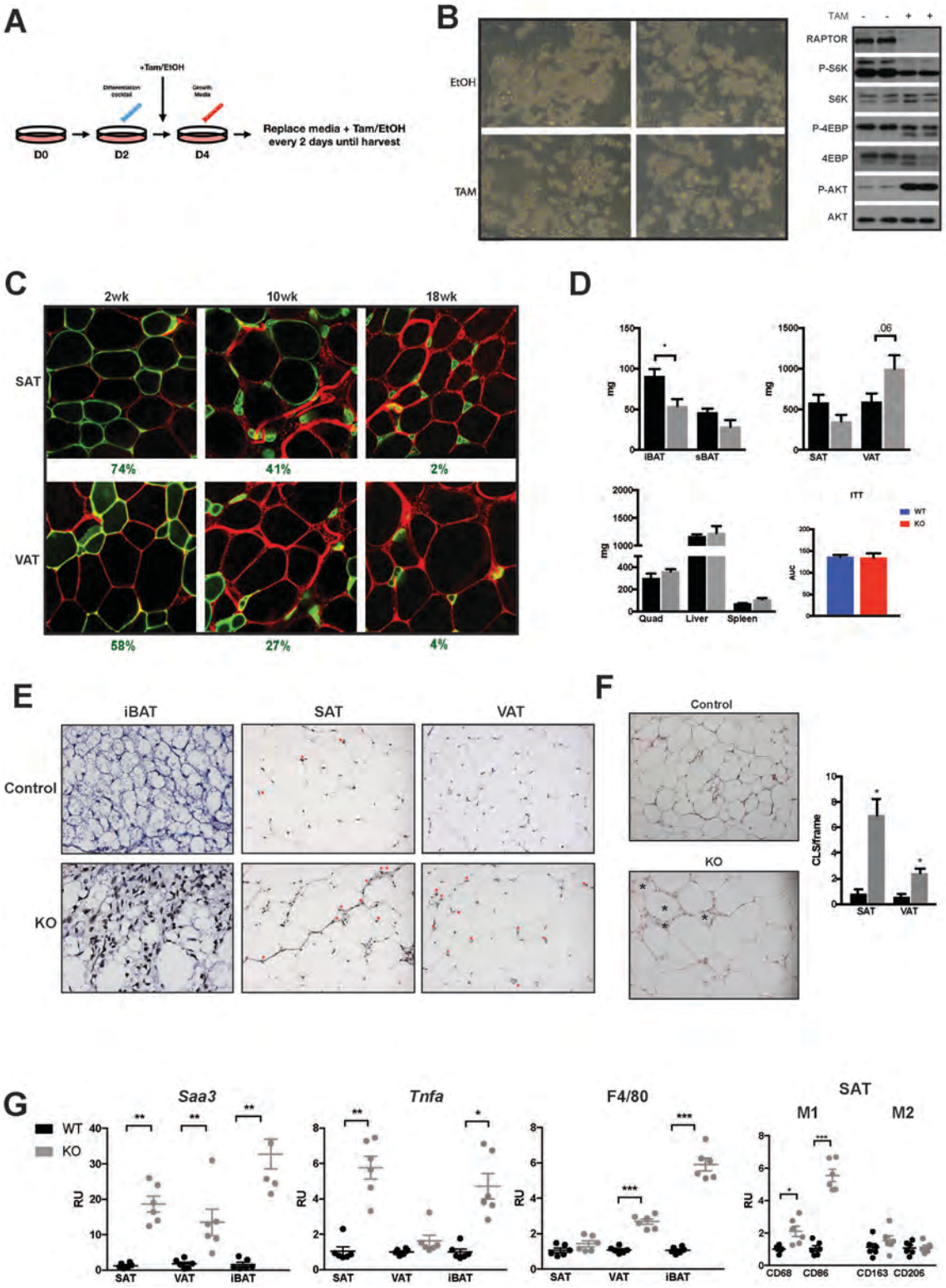
A
+Tam/EtOH
Differentiation cocktail
Growth Media
D0
D2
D4
Replace media + Tam/EtOH every 2 days until harvest
B
EtOH
TAM
TAM - - + +
RAPTOR
P-S6K
S6K
P-4EBP
4EBP
P-AKT
AKT
C
2wk
10wk
18wk
SAT
VAT
74%
41%
2%
58%
27%
4%
D
mg
iBAT
sBAT
SAT
VAT
.06
Quad
Liver
Spleen
ITT
WT
KO
AUC
E
iBAT
SAT
VAT
Control
KO
F
Control
KO
CLS/frame
SAT
VAT
G
Saa3
Tnfa
F4/80
SAT
M1
M2
WT
KO
RU
SAT
VAT
iBAT
CD68
CD86
CD163
CD206

Figure 3.3: 3) Evidence of chronic cell death in Raptor KO adipose tissue depots. A) Mice that were fed doxycycline diet for 18 weeks recover their metabolic phenotype, with a recovery in WAT mass, liver mass, and ITT. (n=6) B) Acutely, the Tet-On system partially labels WAT. Following overtime, nontargeted adipocytes accumulate and comprise the majority of the tissue depot (n=3) C) In adult mice treated with doxycycline for 10 weeks, there is a significantly increased number of crown like structures in both SAT and VAT (n=6) D) Tissue mass and metabolic data of mice fed doxycycline diet for 18 weeks (n=6) E) TUNEL staining of indicated AT depots, showing increased TUNEL positive cells in KO animals (n=6) F) Increased evidence of crown-like structures in KO animals (n=6) G) qPCR for markers of inflammation and macrophage infiltration in sWAT. (Data were analyzed by Student's t-test. Values expressed as mean ±SEM. *$p < 0.05$; **$p < 0.01$; ***$p < 0.001$).

Raptor loss in vivo impairs autophagy inhibition, while also associating with a decrease in mitochondrial mass. Paradoxically, mitochondria are significantly larger in KO tissues

AT depots taken from KO mice show significantly increased LC3II levels, indicating increased autophagic flux (Figure 3.4A). This is consistent with literature indicating the role of mTORC1 signaling in inhibiting autophagy through regulation of ULK1 phosphorylation [113]. In normal mice, I see that autophagy is particularly downregulated after feeding, this downregulation is uninhibited in

knockout animals (Figure 3.4A). I hypothesized that an increase in autophagic flux may play a role in progressive cell death by excessive scavenging of important intracellular organelles. I examined markers of mitochondrial content in the AT of these KO animals. Associated with this increase in autophagy is a decrease in mitochondrial mass. Both western blot for mitochondria associated proteins and qPCR for mtDNA show decreased mitochondrial markers from AT depots of KO mice (Figure 3.4B,C). Interestingly, when visualizing the mitochondria by TEM, the adipocyte mitochondria of KO animals are significantly larger by several fold (Figure 3.4D). I hypothesized this may be due to the role that mTORC1 plays in mitochondrial dynamics, in particular its role in regulation of mitochondrial fission dynamics [114]. I find that indeed a mitochondrial fission protein DRP1 appears to be in its inactive state (p-DRP1 S637), indicating a decrease in mitochondrial fission ability (Figure 3.4E).

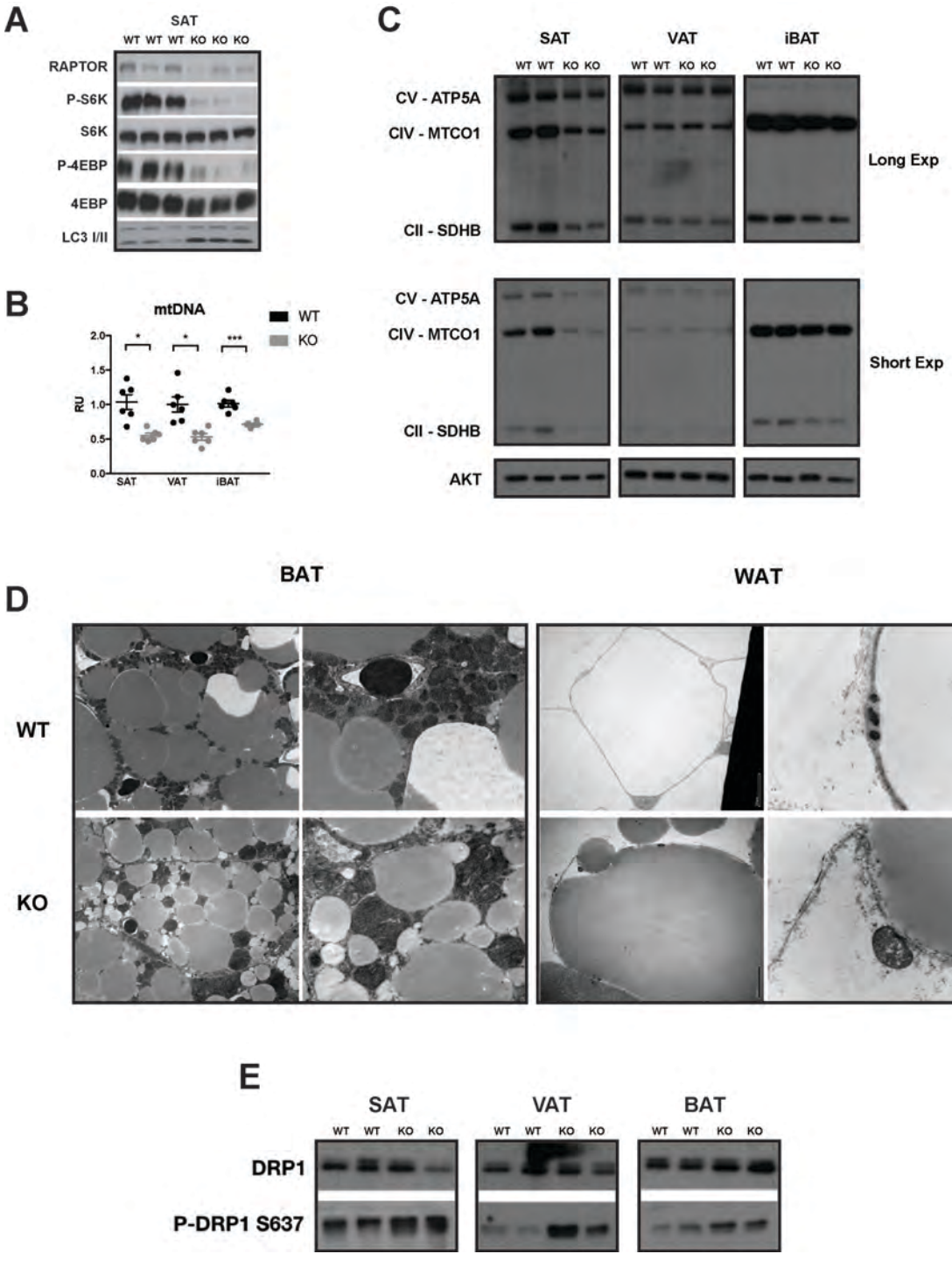

Figure 3.4: 4) mTORC1 exhibits control over mitochondrial size and maintenance in adipose tissue. A) Western blot of control and Raptor KO mice

indicated increased autophagy in KO animals. B-C) Gene and protein markers indicating reduced mitochondrial mass in KO animals (n=6)D) Transmission election microscopy of BAT and SAT showing large individual mitochondria in KO tissues, with evidence of increased autophagic bodies and disorganized mitochondria. (Data were analyzed by Student's t-test. Values expressed as mean ±SEM. *p < 0.05; **p < 0.01; ***p < 0.001).

Acute response to Raptor deletion *in vitro* induces mitochondrial growth, increased autophagic flux, and resistance to classical apoptotic cell death.

In order to better understand the timeline of metabolic responses to deletion of Raptor, I isolated primary preadipocytes from UBC-CreER Raptor L/L mice. This allows us to inducibly delete Raptor (via tamoxifen treatment) in cell culture at specific points in adipocyte differentiation, as previously described (Figure 3.3). While deletion before treating with induction media blocks adipocyte differentiation, lipid accumulation and storage is maintained when Raptor is ablated after initiation of the differentiation process (Figure 3.5A). Contrary to what is seen in vivo after chronic inhibition, I see an acute increase in markers of mitochondrial mass, both by qPCR and western blot (Figure 3.5A). Consistently, however, I find a decrease in DRP1 activity and corresponding increase in mitochondrial size of the KO cells, again suggesting mitochondrial fission is acutely perturbed(Figure 3.5B,C). Additionally, I see evidence of increased

autophagic flux in the KO cells (Figure 3.5B), consistent with findings of increased late autophagic markers (LC3-II levels) in adipose tissue from KO animals. While chronic deletion in vivo leads to evidence of adipocyte death, KO cells in culture do not have accelerated death, and in fact appear to be resistant to apoptotic cell death, with decreased PARP and Caspase-3 cleavage when treated with staurosporine (Figure 3.5D). This phenomenon has been reported, and it has been suggested that increased autophagy may play a role in preventing apoptotic cell death in the short term [115].

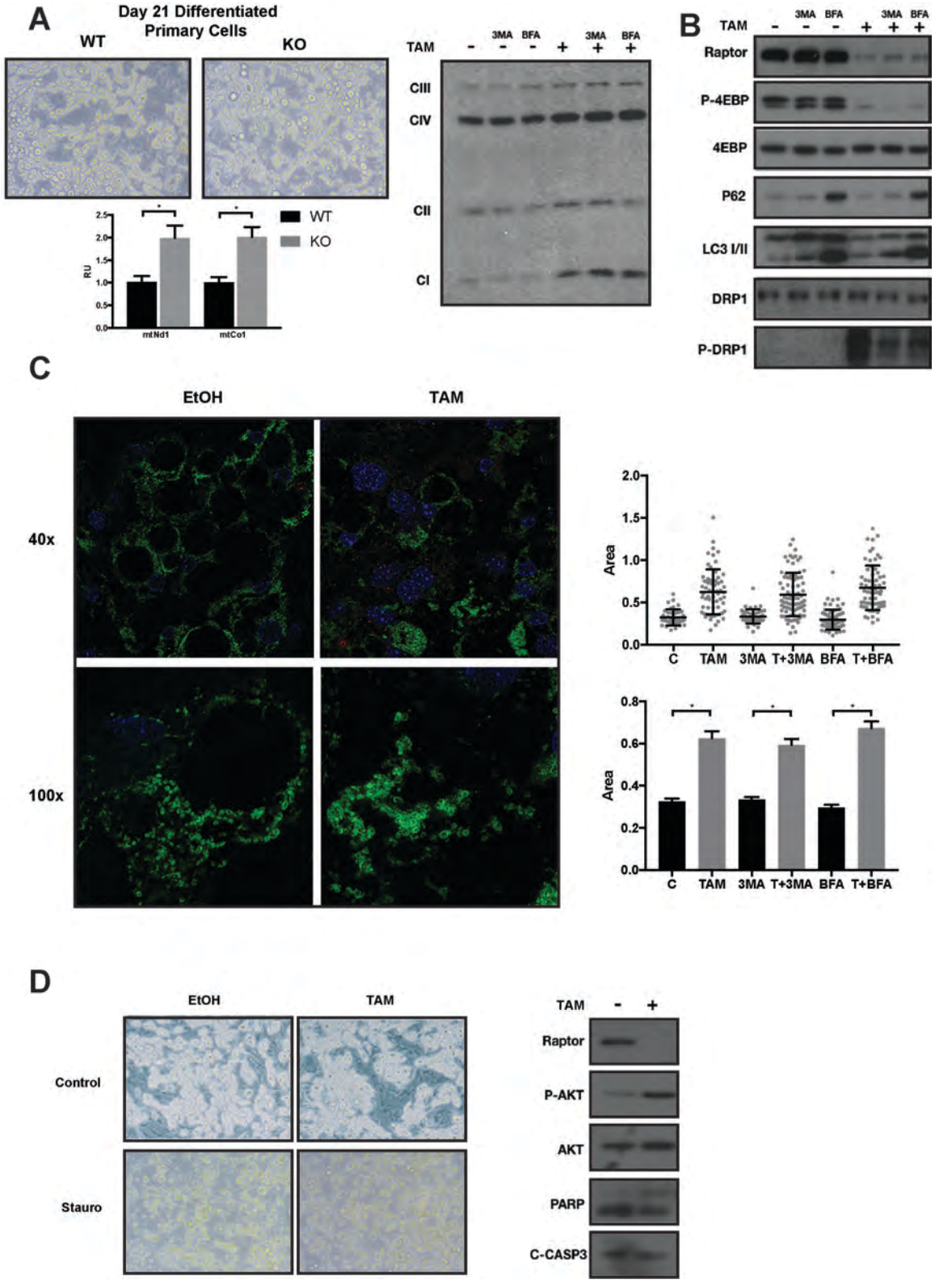
A
Day 21 Differentiated Primary Cells
WT
KO
WT
KO
RU
mtNd1
mtCo1
TAM
3MA
BFA
CIII
CIV
CII
CI
B
Raptor
P-4EBP
4EBP
P62
LC3 I/II
DRP1
P-DRP1
C
EtOH
TAM
40x
100x
Area
C
TAM
3MA
T+3MA
BFA
T+BFA
D
EtOH
TAM
Control
Stauro
Raptor
P-AKT
AKT
PARP
C-CASP3

Figure 3.5: 5) Contrasting changes in mitochondria in response to acute Raptor inhibition in vitro A) Gene and protein markers indicating increased mitochondrial mass after acute deletion of Raptor in vitro. B) Immunofluorescent labeling of mitochondria in vitro indicating increased mitochondrial size after acute Raptor deletion. C) Western blot showing increased phosphorylation at the inhibiting site of mitochondrial fission protein DRP1 D) Representative images and western blots from cell lysates after treatment with apoptotic promoting staurosporine (Data were analyzed by Student's t-test. Values expressed as mean ±SEM. *$p < 0.05$; **$p < 0.01$; ***$p < 0.001$).

Lipoatrophy is rescued by inhibiting autophagy in the setting of Raptor KO mice, however AT inflammation and hepatosteatosis persist.

While Raptor KO cells may be resistant in vitro to acute stimulation of cell death pathways, chronic inhibition leads to adipocyte death in vivo. In both cases, elevated levels of autophagic flux are evident, a mechanism that may be involved in eventual atrophy of the AT. To test this I generated Adiponectin-Cre driven double KO mice Raptor and ATG7, a key autophagic protein. I find that blocking the upregulated autophagic flux due to Raptor loss helps restore overall adipose tissue mass in these animals [Figure 3.6A]. WAT depots return to normal size, and surprisingly iBAT depots become significantly larger than even in control animals [Figure 3.6A]. Despite this recovery in AT capacity, livers from

double KO mice still appear to suffer from steatosis as seen by Oil Red O staining, and liver TG analysis [Figure 3.6B]. Consistent with Raptor KO mice, the glucose sensitive ChREBP – DNL pathway appears to be upregulated [Figure 3.6C]. Additionally, restoration of AT mass and capacity in this case does not appear to alleviate adipose tissue inflammation seen as a result of adipose *Raptor* deletion, as indicated by increased qPCR markers of inflammation and macrophage infiltration [Figure 3.6D].

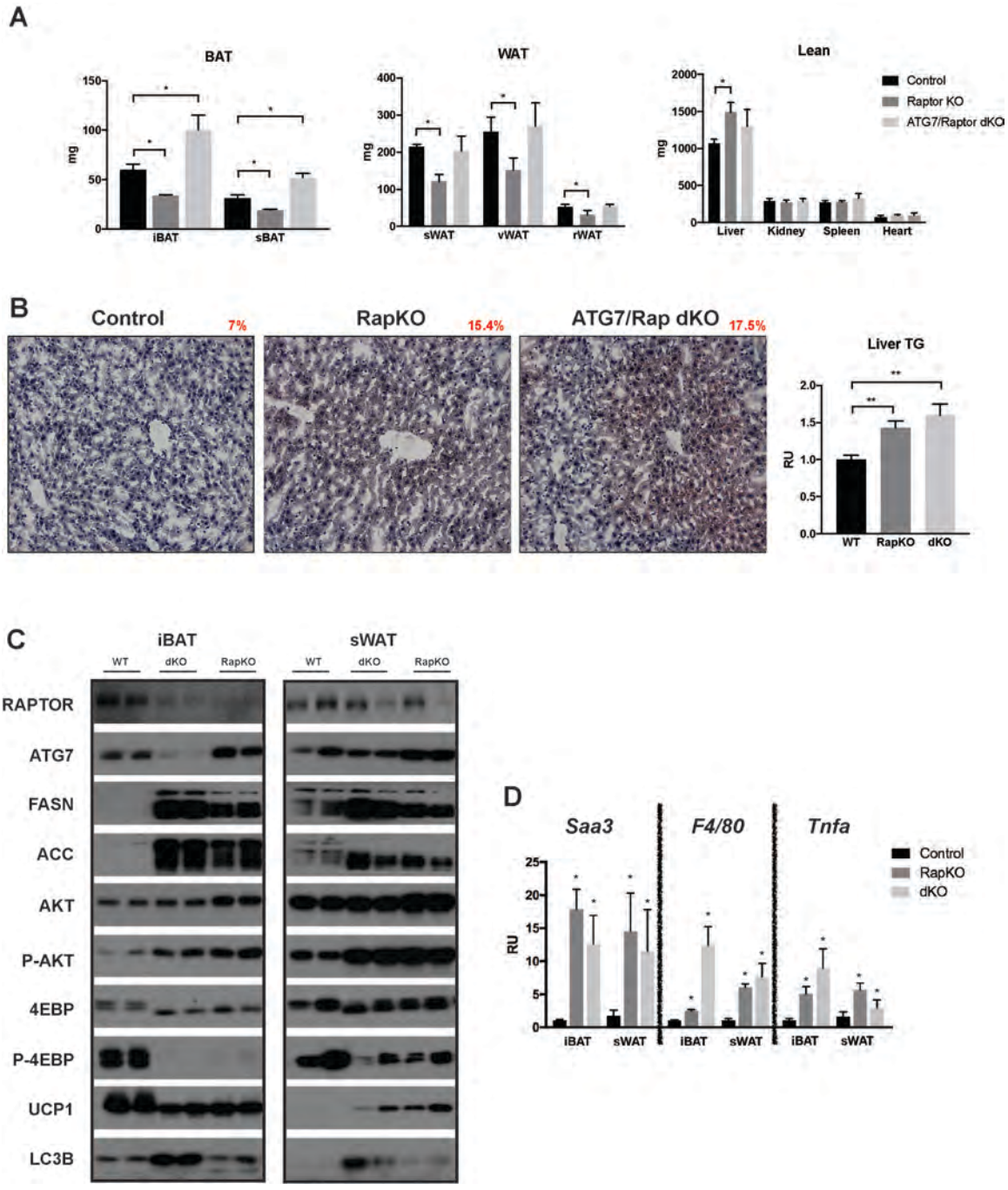

Figure 3.6: 6) Inhibition of autophagy in Raptor KO rescues adipose tissue mass, but not hepatic steatosis of AT inflammation. (n=4) A) Tissue mass of

Control, Adiponectin-Cre driven Raptor KO, ATG7/Raptor dKO, and ATG7 KO mice. (n=4) B) Oil Red O staining of livers from indicated mouse strains and liver TG content with quantification of ORO signal (n=4) C) Western blots from iBAT and sWAT of WT and KO animals for proteins indicated. (n=4) D) qPCR markers for genes indicated from iBAT and sWAT of WT and KO animals. (n=4) (Data were analyzed by Student's t-test. Values expressed as mean ±SEM. *$p < 0.05$; **$p < 0.01$; ***$p < 0.001$).

DISCUSSION:

Loss of Raptor in all mature adipocytes has been shown to induce a progressive lipodystrophy apparent in adult, but not young, mice [77]. It has also been shown that Raptor is essential for brown adipose tissue expansion and adaptation to cold environment [76]. Previously, it was noted that lipodystrophic mice in the setting of Adiponectin-Cre driven Raptor deletion experienced physiological changes such as increased fecal lipid excretion, and increased RER, indicating a possible metabolic shift towards carbohydrate utilization [77]. I hypothesized that such metabolic changes may be an adaptive response to the lipodystrophy to reestablish a metabolic homeostasis, however, it is now clear that these adaptations are insufficient to restore a metabolic homeostasis in the setting of chronic adipocyte Raptor inhibition. mTORC1 signaling in mature adipocytes is critical for the maintenance of metabolic health throughout the lifespan of an adult mouse.

Chronic nutrient excess begets extreme adipose tissue growth (obesity), which then leads to metabolic complications including common diseases such as insulin resistance, hepatosteatosis, and coronary heart disease [1, 11]. At the same time, an inability of adipose tissue to expand, lipodystrophy, also leads to very similar metabolic consequences [111, 116, 117]. The normal development and maintenance of adipose tissue is necessary for the appropriate storage of lipids in order to prevent energy stress on other organs in the body. Interestingly, in both settings, mTORC1 signaling has shown to play a role. In obese humans, there is evidence of impaired mTORC1 activity [108, 109]. Concurrently, in lipodystrophic humans, there is evidence of mutations that may also be related to mTORC1 [72, 73]. In the setting of Raptor-ablation induced lipodystrophy, I show that acute deletion of mTORC1 is generally benign, both in vitro and in vivo. In vitro, KO mature adipocytes retain their ability to accumulate and store lipids in the setting of up to 14 days. In fact, these KO cells appear to be resistant to classical, Caspase-3 driven apoptosis. This may be related to an upregulation in autophagic flux, as it is understood that autophagy is regarded as a mechanism that promotes cell survival, and may inhibit caspase mediated apoptosis [118] [119]. In vivo, acute inhibition of mTORC1 in adult mice similarly has little effect on adipose tissue mass and adipocyte morphology. In concordance, these mice do not appear to suffer from metabolic disturbances such as insulin resistance or hepatic steatosis.

When deletion is induced for a longer period of time, however, I see that the adipose tissue begins to experience dysfunction, and metabolic consequences arise. Again, it's evident that inhibition of mTORC1 signaling plays a critical role in the long-term maintenance of adipocytes, however it is largely dispensable in the short term. In the setting of a chronic, 10wk induced deletion, I show the development of lipoatrophy in conjunction with metabolic changes seen in the lipodystrophic congenital KO model. Also contrasting the acute deletion, chronic inhibition of mTORC1 leads to evidence of adipocyte death in vivo, including evidence of crown-like structures, increased signal upon TUNEL staining, adipose tissue inflammation, and atrophy of GFP positive cells using the mTmG reporter. Furthermore, given an abundant population of normal adipocytes, mice are able to recover from a transient state of metabolic function as the adipose tissue is able to regenerate. I present this in the doxycycline inducible model, where inefficient deletion allows for the adipose tissue depots to repopulate overtime with untargeted cells, reestablishing their ability to store lipids and maintain metabolic homeostasis.

Given the understanding of mTORC1's role in inhibiting autophagy, and our data indicating increased autophagic flux in KO adipocytes, I hypothesized that the progressive lipoatrophy and adipocyte death may be related to chronic and unregulated increases in autophagy. Here I present that deleting a key autophagic protein ATG7 in the setting of Raptor KO does restore overall adipose tissue mass in adult mice. However, this restoration in AT capacity does

not appear to alleviate other metabolic changes such as hepatic steatosis and AT inflammation. These results suggest that while AT capacity to store lipids may be critical for metabolic homeostasis in many models, mTORC1 signaling in adipocytes may play key roles in regulating whole body metabolism that remain independent of lipid storage capacity. I would argue that lipid sequestration is only one of multiple key roles that adipose tissue plays in metabolic regulation.

In conclusion, I present that acute inhibition of mature adipocyte mTORC1 activity by chemically inducible genetic ablation of Raptor has little to no metabolic consequence in the short term. Cultured adipocytes accumulate and maintain lipid droplets after ablation, as do adipose tissue depots of inducible KO animals. Over time, on the order of weeks, adipose tissue depots begin to atrophy, and KO animals present with evidence of adipocyte cell death. Associated with this change in adipose is an increase in liver size, and metabolic dysfunction as reported by insulin tolerance tests. Like the congenital model previously reported, it appears there is a redistribution of lipid storage from adipose to other organs, namely the liver. The chronic progression of lipoatrophy death seen in Raptor KO animals is likely related to the upregulation of autophagic flux, due to the loss of mTORC1 inhibition of autophagy. Inhibition of autophagy, through genetic ablation of adipose Atg in conjunction with Raptor rescues AT mass maintenance, but not corresponding metabolic changes such as hepatic steatosis and AT inflammation. Rather, these mice share some similar

changes in adipocyte morphology, however, they do not suffer from lipodystrophy or metabolic dysfunction.

Overall, it is clear that mTORC1's regulation of autophagic flux is critical for maintenance of adipose tissue in adult mice. Maintenance of AT mass by this pathway, however, is not sufficient to restore all metabolic anomalies seen in Raptor KO mice. It is possible that mTORC1 affects other pathways within adipocytes that are important in signaling to peripheral metabolic organs, such as regulation of adipose tissue inflammation, or production of circulating adipokines. Given the evidence of aberrant mTOR signaling in human obese patients, further studies on the changes that occur with adipocyte mTORC1 signaling in the context of obesity may play a critical role in understanding the development of metabolic syndrome.

CHAPTER IV: RagGTPases are dispensable for mTORC1 in adipose tissue. RagA and RagB have an mTORC1 independent role in regulating Ucp1 activity in WAT

INTRODUCTION:

One of the goals set at the beginning of this project was to better understand how amino acid sensing through the RagGTPases control adipose tissue health and function. Based on the literature, it is believed that RagGTPase activity is a required step in the activation of mTORC1 [120-122]. Multiple in vitro studies have shown that eliminating the RagGTPases is sufficient to inhibit downstream mTORC1 signaling even in the presence of other stimulating factors [30, 34, 46, 121-123]. As mentioned earlier, the model is that for downstream activity, mTORC1 must be localized at the lysosomal membrane. Here it is directly activated by Rheb, whose activity is controlled by the TSC complex, a GAP regulated by the insulin/AKT signaling pathway. While the majority of signaling studies have been conducted in cancer cell models, there is scant data on the implications of tissue specific loss of RagGTPase activity in vivo [121].

Based on my findings of mTORC1 loss in adipose tissue, I hypothesized that RagGTPase activity in adipose tissue is critical for adipocyte health, and that loss of adipocyte Rags would lead to lipodystrophy and metabolic dysfunction. I expected that, using Adiponectin-Cre to delete Rag, I would find these mice to phenocopy mice with mTORC1 loss. To test this, I first generated Adiponectin-Cre RagA L/L mice. Despite there being two different functional RagGTPase pairs (RagA/C, and RagB/D), it is believed that RagA is the most abundant, and most important for mTORC1 activity [121]. In fact, it was shown that RagB was not essential for embryonic development in mice.

Surprisingly, I found that Adiponectin-Cre RagA L/L mice were phenotypically normal, with no defects in adipose tissue mass, or metabolic function. Additionally, mTORC1 signaling in the adipose tissue appeared to be intact. Absence of metabolic dysfunction or impaired mTORC1 signaling was maintained even when these mice were put through environmental stressors, such as high-fat diet, and thermoneutrality. These results suggested that either mTORC1 in adipocytes in fact does not require RagGTPase activity, or perhaps RagB/D alone are sufficient to sustain mTORC1 signaling under normal conditions. To address the possibility of RagB compensation, I then generated Adiponectin-Cre RagA RagB dKO mice. While these mice do not suffer from metabolic deficiency or lipodystrophy, they do exhibit stronger inhibition of downstream mTORC1 signaling accompanied by phenotypic changes in the adipose tissue, particularly in BAT.

Overall, these findings were surprising given the model that RagGTPases are required for mTORC1 activity. My results suggest that in vivo, adipocyte mTORC1 activity may be maintained absent RagA and RagB. Furthermore, there may be mTORC1 independent roles for the RagGTPases, particularly in relationship with *Ucp1* expression in white adipocytes.

MATERIALS & METHODS

2.1. Mice

RagA floxed and Rag B floxed mice (generously donated by Alejo Efeyan) were backcrossed 10 generations to C57BL/6J stock mice from Jackson Laboratory and crossed to C57BL/6J mice expressing the Adiponectin-Cre driver. Male mice were used for experiments. Mice were kept on a daily 12 h light/dark cycle and fed a normal chow diet (Prolab Isopro RMH 3000) from Lab Diet ad libitum at 22 C. All animal experiments were approved by the University of Massachusetts Medical School animal care and use committee.

2.2. Antibodies and reagents

Antibodies were purchased from Cell Signaling Technologies: ACC (3676), ACLY (4332), AKT (9727), P-AKT- S473 (4058), ATGL (2439), FASN (3180), HSL (4107), P-HSL-S660 (4126), ULK1 (8054), P-ULK1-S757 (6888), 4EBP1 (9644), P-4EBP1- S65 (9456), P-4EBP1-T37/46 (2855), RAGA (4357), RAPTOR (24C12). All other reagents were from Sigma Aldrich.

2.3. Tissue harvest and histology

Adipose tissue depots were carefully dissected to avoid contamination from surrounding tissue. Samples for RNA or protein were snap frozen in liquid nitrogen and stored at 80° C until analysis. For histology, tissue pieces were fixed in 10% formalin. Embedding, sectioning, and Hematoxylin & Eosin (HE) staining was done by the UMass Medical School Morphology Core. For Oil Red O staining, liver samples were embedded in Optimal Cutting Temperature

compound and frozen before sectioning and staining. For cell size measurements a minimum of 10 images were taken used per mouse. Image J was used to measure cell size and the distribution of cell size as percentage of total counted cells was analyzed.

2.4. Western blots

Tissue samples or cells were lysed in a buffer containing 50 mM Hepes, pH 7.4, 40 mM NaCl, 2 mM EDTA, 1.5 mM NaVO4, 50 mM NaF, 10 mM sodium pyrophosphate, 10 mM sodium b-glycerophosphate and 1% Triton X-100. Tissues were homogenized using a TissueLyser (Qiagen) in the same lysis buffer supplemented with 0.1% SDS, 1% sodium deoxycholate. Equal amounts of total protein were loaded into acrylamide/bis-acrylamide gels and transferred to PVDF membranes for detection with the indicated antibodies. Membranes were incubated with primary antibodies in 5% milk/PBST or 5% BSA/PBST overnight. Membranes were then incubated for 1hr with HRP-conjugated secondary antibodies. Western blots were developed by enhanced chemiluminescence (PerkinElmer) and detected by X-ray films.

2.5. Diet & metabolic studies

At 10-12 weeks of age, male mice were placed on a 60% high fat diet (HFD) (D12492 Harlan Laboratories) for 8 weeks. Body weight was recorded weekly. Serum samples were sent to the MMPC at the University of Cincinnati for analysis of circulating metabolites. For glucose tolerance tests (GTT) mice were fasted overnight (16 h) and then administered 2 g/kg of body weight of glucose or

sodium pyruvate by intraperitoneal (i.p.) injection. For insulin tolerance tests (ITT), mice were fasted for 6 h before i.p. administration of 0.75 unit/kg of body weight of insulin. Blood glucose concentrations were measured using a GE100 Blood Glucose monitor. Blood was from tail vein collection before and after the injection at indicated time points.

2.6. Gene expression analysis

Cells or tissues were lysed with Qiazol (Invitrogen) and total RNA was isolated with the RNeasy kit (Invitrogen). Equal amounts of RNA were retro-transcribed to cDNA using a High capacity cDNA reverse transcription kit (#4368813, Applied Biosystems). Quantitative RT- PCR was performed in 10 mL reactions using a StepOnePlus real- time PCR machine from Applied Biosystems using SYBR Green PCR master mix (#4309156, Applied Biosystems) according to manufacturer instructions. Relative mRNA expression was determined by the ΔCt method, and Tbp (TATA sequence binding protein) expression was used as a normalization gene in all conventional RT- PCR experiments. Mouse primers used:

Gene	Forward primer (5'-3')	Reverse primer (5'-3')
Tbp	GAAGCTGCGGTACAATTCCAG	CCCCTTGTACCCTTCACCAAT
Ucp1	CTGCCAGGACAGTACCCAAG	TCAGCTGTTCAAAGCACACA

2.7. Statistics

Unless otherwise stated, values given are mean SEM. Two-way ANOVA was performed where indicated. For most experiments, unpaired two-tailed Student's t test was used to determine statistical significance among two groups (*$p < 0.05$; **$p < 0.01$; ***$p < 0.001$).

RESULTS

Adipose specific RagA KO mice are phenotypically normal, with evidence of increased Ucp1 expression in WAT

Primary adipocyte precursor cells were isolated from inguinal adipose tissue depots of wildtype C57BL/J mice. The cells were plated and differentiated into mature adipocytes in culture. After differentiation, cells were deprived of nutrients for 2 hours, then stimulated with either insulin alone, or insulin and amino acids. Phosphorylation of downstream mTORC1 target S6K appears to be dependent on amino acids, while 4EBP appears to be partially dependent. Phosphorylation of insulin signaling dependent AKT is unchanged in AA deprived or supplemented conditions [Figure 4.1A]. Adiponectin-Cre RagA L/L mice were generated, and allowed to grow to 10 weeks of age under chow diet, at standard (22°C) housing conditions. Adipocyte RagA knockout mice did not appear to have any changes in BAT or WAT depot size, or lean tissue mass [Figure 4.1B]. Adipocytes in both BAT and WAT depots appeared to be morphologically normal [Figure 4.1D]. Despite efficient RagA deletion, downstream mTORC1 phosphorylation targets do not appear to be changed. Phosphorylation of AKT, commonly seen to be elevated in Raptor KO mice, was also unchanged [Figure 4.1C]. Notably, there was a persistent increase in Ucp1 expression, both in protein and mRNA, in the sWAT depot [Figure 4.1E]. Overall, adipocyte RagA deletion did not adversely affect metabolic function [Figure 4.1F].

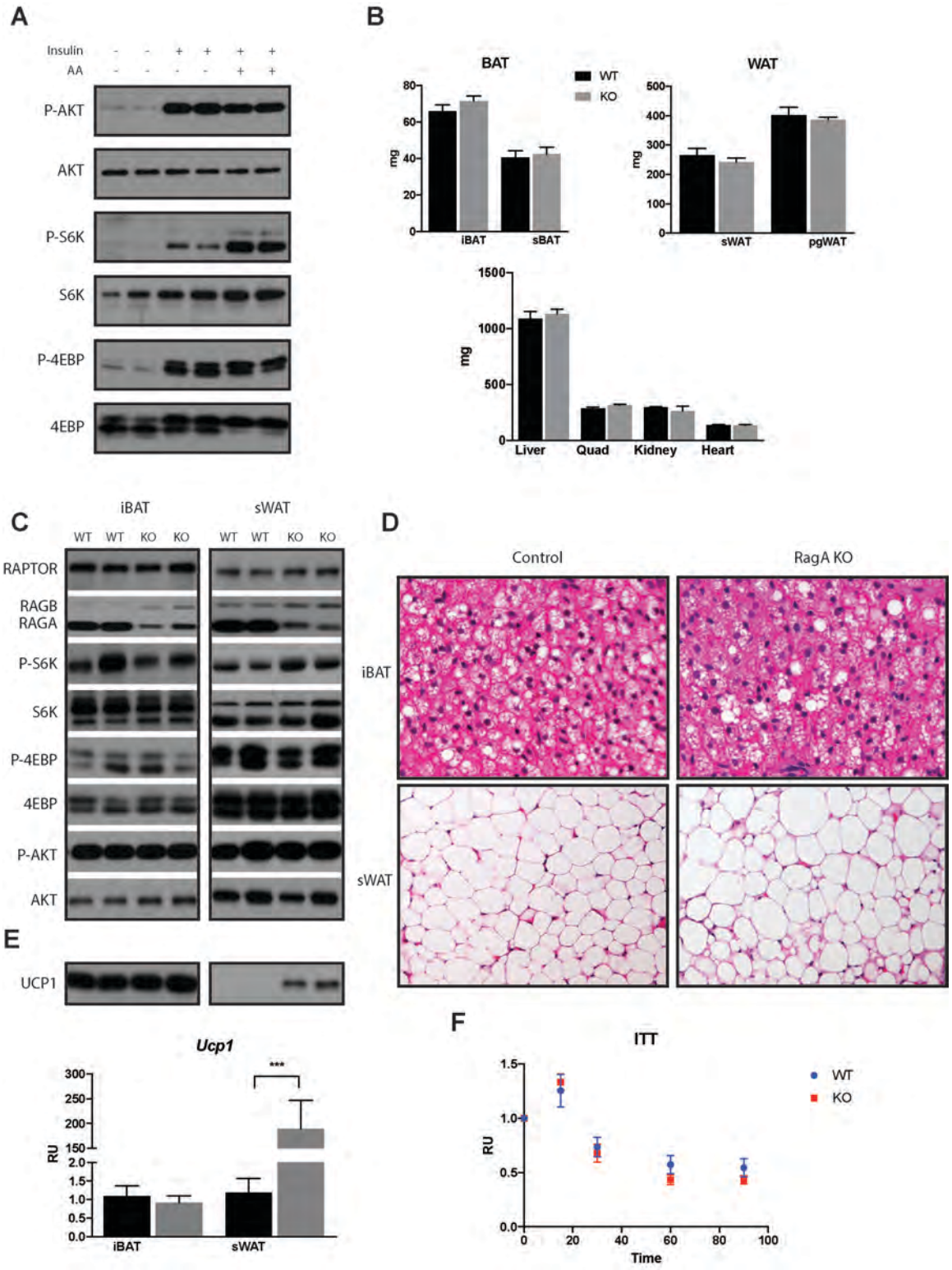
A
Insulin
AA
P-AKT
AKT
P-S6K
S6K
P-4EBP
4EBP
B
BAT
WT
KO
mg
iBAT
sBAT
WAT
sWAT
pgWAT
Liver
Quad
Kidney
Heart
C
iBAT
sWAT
WT WT KO KO WT WT KO KO
RAPTOR
RAGB
RAGA
P-S6K
S6K
P-4EBP
4EBP
P-AKT
AKT
D
Control
RagA KO
iBAT
sWAT
E
UCP1
Ucp1
RU
***
F
ITT
WT
KO
RU
Time

Figure 4.1: Adipose specific RagA KO mice are phenotypically normal, with evidence of increased Ucp1 expression in WAT A) Western blots of primary adipocytes differentiated in culture, stimulated with insulin alone, or insulin with amino acids. B) Tissue mass of Adiponectin-Cre RagA L/L and corresponding controls. (n=6) C) Western blots for indicated proteins of WT and RagA KO mice. D) Histology representative of BAT and WAT depots from WT and KO mice. (n=6) E) Protein and mRNA levels of Ucp1 F) Insulin tolerance test for WT and KO mice on chow diet at 22C housing conditions. (n=6) (Data were analyzed by Student's t-test. Values expressed as mean ±SEM. *$p < 0.05$; **$p < 0.01$; ***$p < 0.001$).

RagA KO mice are not resistant to HFD induced obesity.

Adiponectin-Cre Rag A mice were challenged with a 60% kcal high-fat diet, under normal (22C) housing temperatures. Adult mice at ~10 weeks of age were fed HFD for a total of 8 weeks. Despite higher Ucp1 expression seen in the chow diet cohort, HFD fed KO mice gained similar amounts of body weight when compared to controls [Figure 4.2A]. Fat mass, brown and white, were again similar between KO and control mice, along with lean tissues including liver. Again, RagA KO did not appear to produce any type of lipodystrophy similar to what was seen in Raptor KO [Figure 4.2B]. RagA deletion did not appear to impair mTORC1 signaling in adipose tissue of these mice [Figure 4.2C]. Histological analysis also did not reveal major changes in adipocyte morphology

or size due to RagA deletion [Figure 4.2D]. Lastly, insulin sensitivity remained comparable to control HFD fed mice [Figure 4.2E].

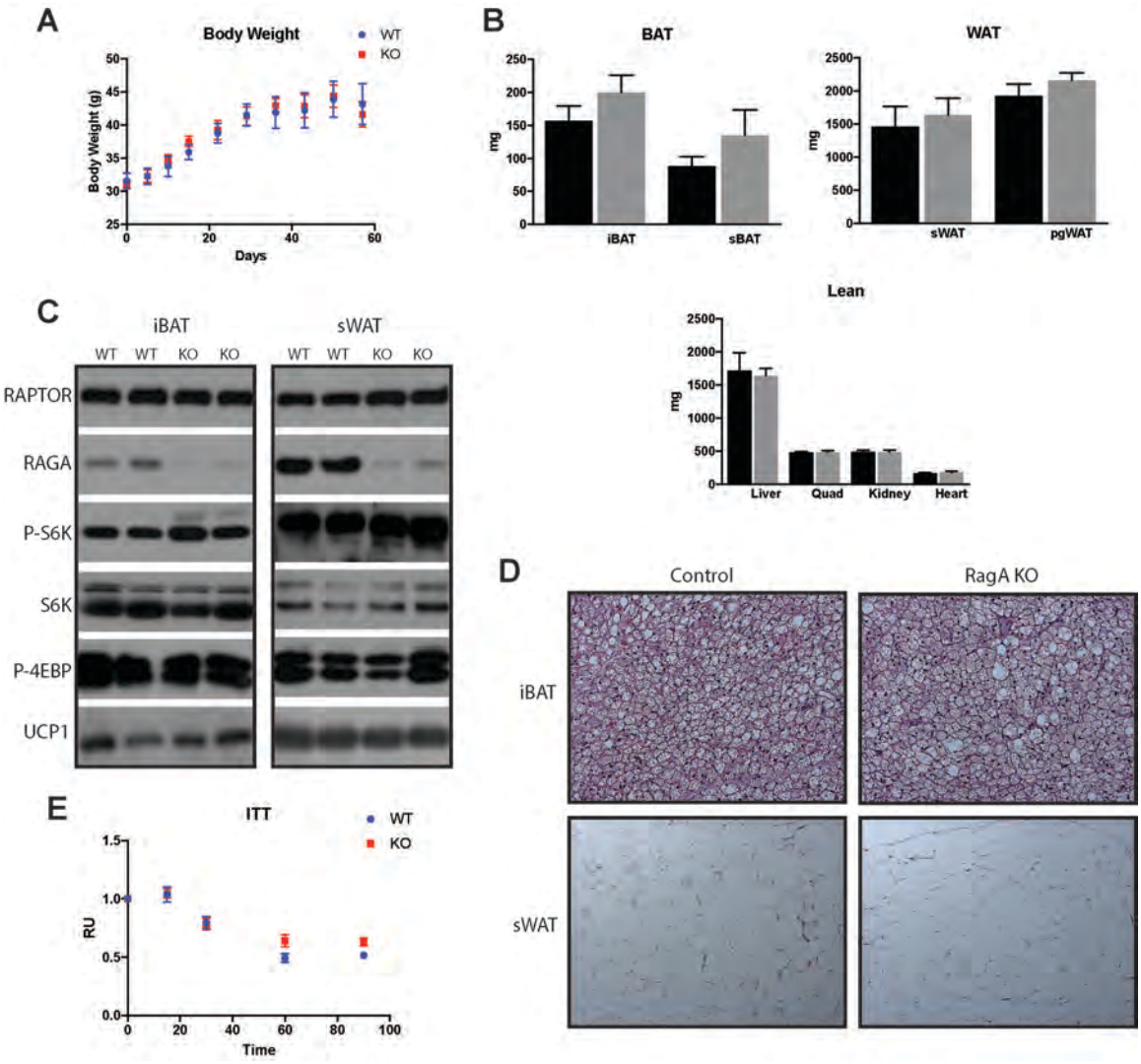

Figure 4.2: RagA KO mice are not resistant to HFD induced obesity. A) Body weight gain in response to HFD feeding. (n=6) B) Tissue mass comparison between WT and KO mice. (n=6) C) Western plots of indicated proteins from iBAT and sWAT of WT and KO mice. D) Representative histology of BAT and WAT. E) Insulin tolerance test of animals after 7 weeks of HFD feeding at 22C

housing conditions. (n=6) (Data were analyzed by Student's t-test. Values expressed as mean ±SEM. *p < 0.05; **p < 0.01; ***p < 0.001).

Increased UCP1 expression persists at thermoneutrality, but does not alter energy balance

Further environmental factors were selected in an attempt to reduce noise and magnify any metabolic effects of RagA that may be present. Adiponectin-Cre RagA breeding colonies were housed at thermoneutral temperatures (30°C) in order to generate KO mice that develop in an absence of BAT and Ucp1 stimulating cold stress. Like the previous experiments, RagA appeared to be dispensable for overall adipose tissue function. Despite persistent increased expression of Ucp1 [Figure 4.3D], KO mice did not have lower body weight or AT tissue weights [Figure 4.3A, B]. Morphologically, the BAT of both control and KO mice appeared to take on a "white" type appearance, but Ucp1 expression was equivalent between the cohorts [Figure 4.3C].

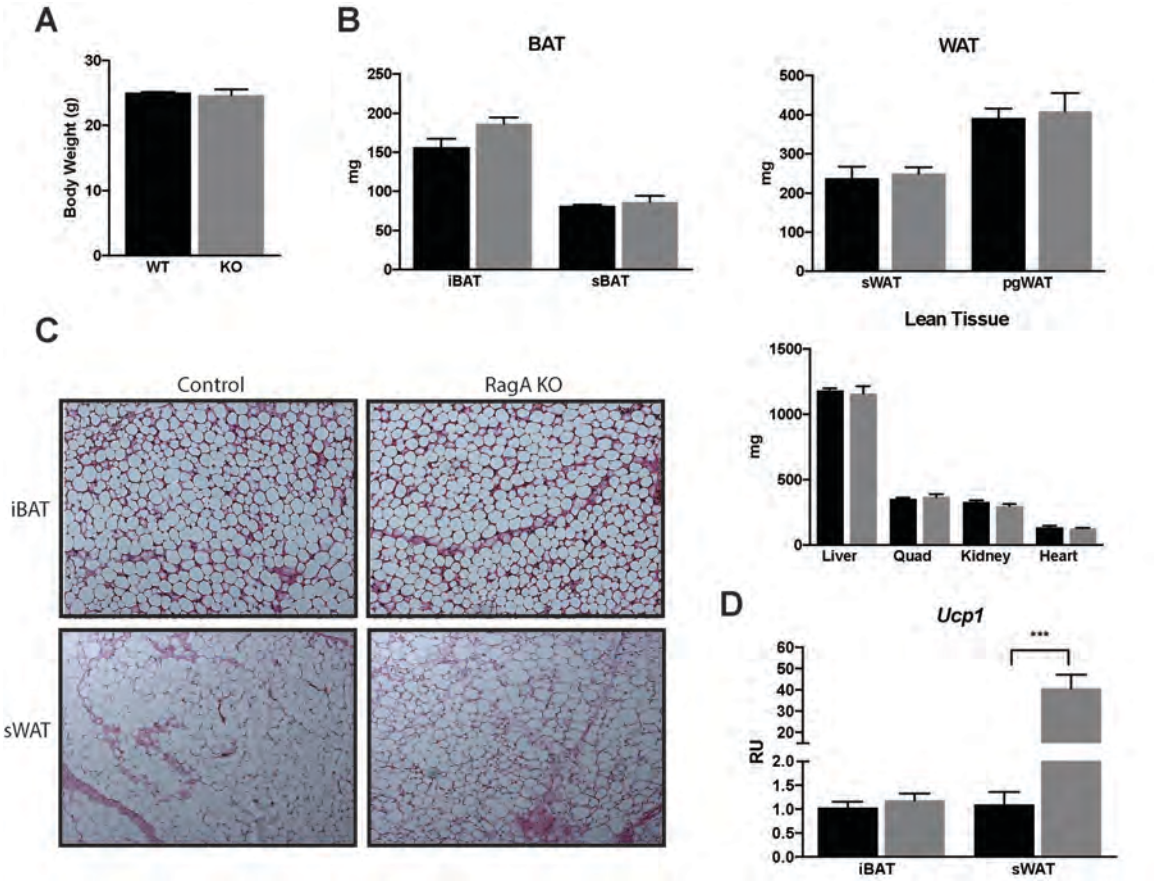

Figure 4.3: Increased UCP1 expression persists at thermoneutrality, but does not alter energy balance A-B) Body weight and tissue mass for adult WT and KO mice raised at thermoneutrality. (n=6) C) Histology of WAT and BAT for WT and KO mice at thermoneutrality. D) mRNA expression of *Ucp1* (n=6) (Data were analyzed by Student's t-test. Values expressed as mean ±SEM. *p < 0.05; **p < 0.01; ***p < 0.001).

Adiponectin-Cre RagA RagB dKO mice do not phenocopy Adiponectin-Cre Raptor KO mice. Adipose deletion of RagGTPases is dispensable for overall metabolic health in mice.

To examine the possibility that RagB may be compensating for the loss of RagA, and contributing to the maintenance of mTORC1 activity, I generated mice that lacked RagA and RagB in mature adipocytes (Adiponectin-Cre RagA L/L Rag B L/-). When ablating RagA and RagB specifically in mature adipocytes, I find that loss of the amino acid sensing GTPases again does not phenocopy Raptor ablation [Figure 4.4A]. Despite efficient deletion in AT depots, I see that generally downstream targets of mTORC1 remain active [Figure 4.4B]. Despite this, brown adipose tissue in fact expands in mass, with significant lipid accumulation [Figure 4.4B, D]. These mice do not suffer from lipodystrophy or insulin resistance as would be expected if RagAB dKO were to inhibit mTORC1 signaling. When challenged with a high fat diet, RagAB dKO mice retain ability to expand their AT depots greatly, unlike Raptor KO mice [Figure 4.4C]. RagAB dKO animals appear to have slightly smaller sWAT depots, and smaller livers as well. This slight, but statistically significant, change in SAT and liver mass does not appear to improve insulin sensitivity in these mice [Figure 4.4C]. It is prudent to note that the BAT depots of RagAB dKO mice appear to accumulate larger lipid both at chow fed and HFD conditions when housed at 22C [Figure 4.4D, E]. Also notable is that UCP1 expression increases in the WAT, a phenomenon previously associated with Rag GTPase signaling [124] [Figure 4.4B]. This UCP1

expression is also increased in a RagA single KO model, where mTORC1 signaling is not perturbed, suggesting the RagGTPases may play a role in UCP1 regulation in WAT, though this does not appear to have a whole body metabolic effect.

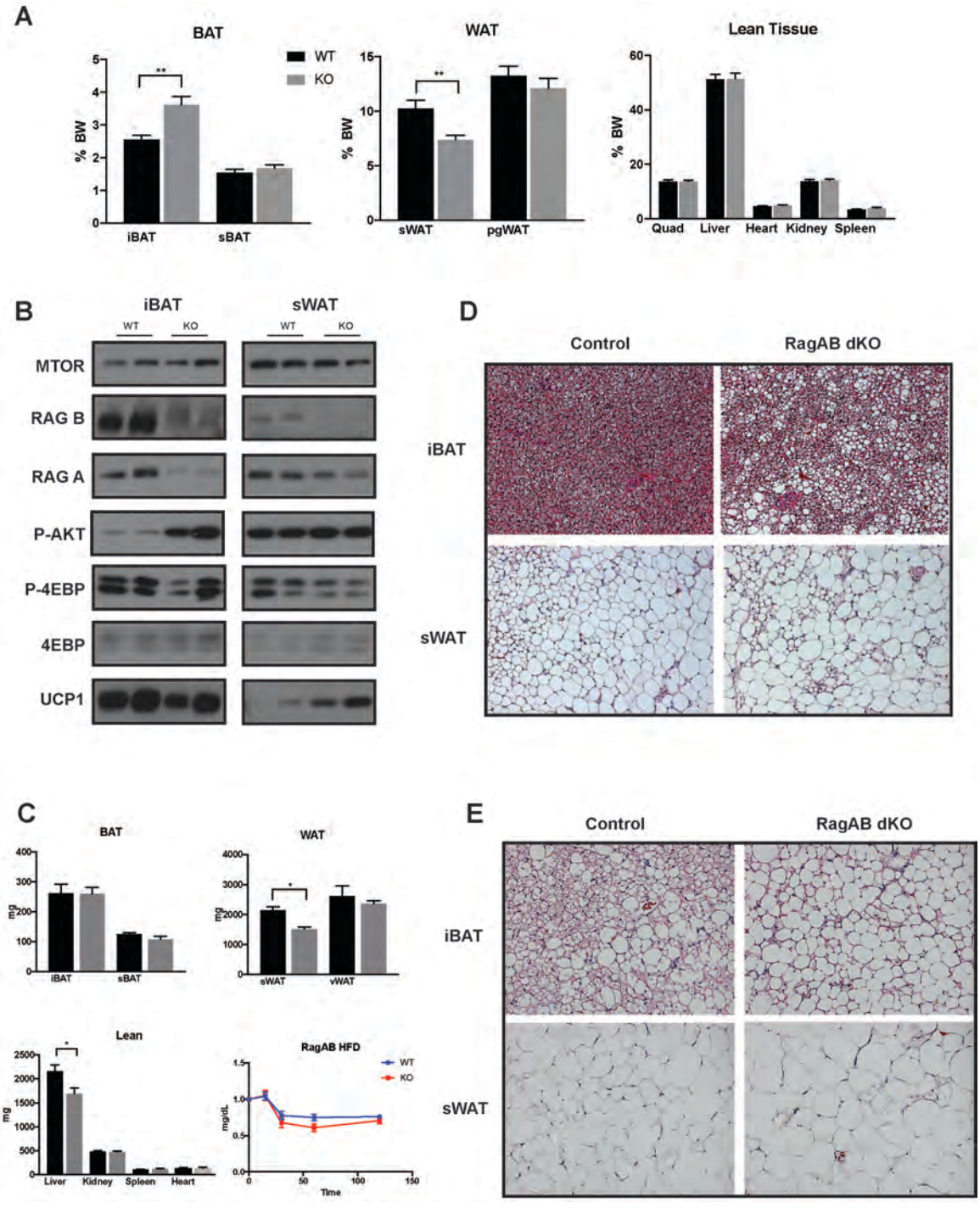
A
BAT
WT
KO
% BW
iBAT
sBAT
WAT
sWAT
pgWAT
Lean Tissue
Quad
Liver
Heart
Kidney
Spleen
B
iBAT
sWAT
MTOR
RAG B
RAG A
P-AKT
P-4EBP
4EBP
UCP1
D
Control
RagAB dKO
iBAT
sWAT
C
BAT
WAT
vWAT
Lean
RagAB HFD
Time
E
Control
RagAB dKO
iBAT
sWAT

Figure 4.4: Adipose tissue RagGTPase deletion does not phenocopy Raptor KO mice. Adipocyte RagGTPases appear to be dispensable for overall metabolic stability. A) Tissue mass of Control, and Adiponectin-Cre RagA/RagB double KO mice. Adult mice at 10 weeks of age on chow diet at 22°C. B) Western blots from iBAT and sWAT of WT and KO animals for indicated proteins. C) Tissue weight and ITT from WT and KO animals at 18 weeks of age after 8 weeks of 60% HFD feeding. (n=6) D) Representative H&E staining of iBAT and sWAT depots from WT and KO animals on chow diet (n=6) E) Representative H&E staining of iBAT and sWAT depots from WT and KO animals on HFD. (n=6) (Data were analyzed by Student's t-test. Values expressed as mean ±SEM. *$p < 0.05$; **$p < 0.01$; ***$p < 0.001$).

Discussion:

In this chapter I demonstrate that the RagGTPases may have a less significant role in the regulation of mTORC1 activity in vivo than they appear to have in vitro. Initially, I expected adipocyte Rag ablated to phenocopy *Raptor* KO given the current literature indicating that RagGTPase activity is required for mTORC1 localization, and downstream activation. While mTORC1 signaling in cultured primary adipocytes appeared to be amino acid sensitive, this was not recapitulated in various mouse KO models.

My first mouse model was generated only to delete RagA with the understanding that it is the dominant Rag, and that RagB appeared to be

dispensable for mTORC1 activity [121]. Initial results were surprising in that RagA deletion had no effect on mTORC1 signaling in adipose tissue, and KO mice were phenotypically normal, although they did express higher Ucp1 levels in sWAT depots. In light of this, I thought it was possible that the increased Ucp1 expression may have a metabolic effect on these mice if they were put under certain conditions such as high-fat diet (to test weight gain), and thermoneutrality (to test energy balance absent environmental stress). Putting the RagA mice separately on HFD, or at thermoneutrality, however did not reveal any metabolic abnormalities or changes in weight gain and adipose tissue accumulation. Together these data indicate that, while RagA may be inducing some type of *Ucp1* expression in WAT, this increase does not alter the energy balance of KO mice.

The second question to understand from the RagA mice is why is mTORC1 signaling not perturbed? One possibility is that RagA ablation alone is not sufficient to eliminate RagGTPase activity, and that Rag B, of the RagB/D complex, is able to compensate and maintain mTORC1 localization. There is evidence to support this in that I saw increased RagB protein levels in the RagA single KO mice [Figure 4.4C]. To address this possibility, I generated Rag A/B dKO mice. The dKO mice did appear to result in a more severe decrease in canonical mTORC1 signaling, particularly in the BAT, however they still did not phenocopy adipose *Raptor* KO. These results suggest that the RagGTPases may be involved in fully activating mTORC1 in adipocytes, however, mTORC1 is

still able to phosphorylate common targets in the absence of Rag activity. Interestingly, *Ucp1* is persistently elevated in RagAB dKO, supporting the idea that Rags alone have an mTORC1 independent role in regulation of Ucp1 expression in WAT [124].

Conclusion:

The results from this chapter were generally surprising. First, they support the idea that RagGTPases may play in role in an mTORC1-independent pathway regulating Ucp1 expression in WAT. This idea is supported in the literature by a study examining RagC and D and their involvement in the role of "browning" [124]. Specifically, it's been shown that increased *Ucp1* by PGC-1β is regulated by RagC/D dependent localization of TFE3. Mechanistically, it has been proposed that FLCN interaction with mTORC1 is RagC/D dependent. Lack of this interaction leads to activity of TFE3 and PGC-1β to induce a non-canonical activation of *Ucp1* and "beiging" of WAT. However, I find the increased Ucp1 expression appears to have little impact on energy balance, even in conditions that should be sensitive to increased energy expenditure such as at thermoneutrality or on high-fat diet.

Secondly, my data argue against the model that Rag activity is necessary for mTORC1 activation. Significant differences that may be found between *in vitro* and *in vivo* conditions. While few in vivo studies involving Rag have been published, there is some evidence that tissues genetically ablated for Rags may

still maintain some level of mTORC1 signaling. Further work will need to be done to understand how mTORC1 may be signaling in absence of RagGTPases. Two possibilities include: 1 - mTORC1 is still able to respond to amino acids and localize to the lysosomal membrane through alternative pathways, or 2 – mTORC1 can be activated and phosphorylate its downstream targets in areas of the cell other than at the lysosomal membrane. Further thoughts on this are discussed in the next chapter.

CHAPTER 5: DISCUSSION AND FUTURE DIRECTIONS

Adipose mTORC1

Initially, based on current knowledge in the field, I aimed to study the role of mTORC1 signaling in regulating adipocyte metabolism. At the time, significant work had been done to elucidate mTORC1 dependent signaling pathways. While much of this work was done *in vitro*, mTORC1 was well understood to be a major metabolic node. These studies had involved mTORC1 with many downstream anabolic pathways, including protein synthesis, nucleotide synthesis, lipogenesis, and autophagy inhibition [28]. Additionally, in vivo work had been done to show the importance of mTORC1 signaling in maintaining muscle development and mass [125]. Less understood was the role of mTORC1 in mature adipocytes. The current model had used the aP2-Cre to delete *Raptor*, however as discussed previously, the aP2-Cre had fallen out of favor in adipose tissue models [62, 89]. First, criticisms of the aP2-Cre included evidence that in addition to adipocytes, it also targeted the brain, endothelial cells, macrophages, and embryonic tissues. These multiple off-target tissues may have significant contributions to the phenotype of the mice, especially considering the many known roles of mTORC1. To address this, I generated Adiponectin-Cre driven *Raptor* KO mice and found that, surprisingly, these mice had a vastly different metabolic outcome than the current model. Contrasting the metabolic efficiency seen in the aP2-Cre mice, these mice were metabolically unfit, and suffered from progressive lipodystrophy and associated metabolic disease.

Adiponectin-Cre Raptor Caveats

It is important to note that, despite higher specificity and efficacy with the Adiponectin-Cre, there remain multiple caveats with my model. While a vast improvement over aP2-Cre, Adiponectin-Cre may also have off-target expression that contributes to some of the phenotypes observed. Additionally, using a constitutive Cre means that expression of the Cre, and thus recombination, will occur in this case immediately after differentiation of the adipocyte. This may significantly interfere with animal development as mouse adipose tissue depots form as early on as *in utero* [126]. While this may be helpful to study the role of adipose mTORC1 in development, it makes it more difficult when trying to compare the model to adult-onset metabolic dysfunction. On a related note, because of this congenital deletion, I am also only able to see the long-term effects of adipocyte *Raptor* ablation in these mice. Without having the ability to control the timing of deletion, I am unable to differentiate acute responses to mTORC1 ablation versus chronic, secondary adaptations. Lastly, it was mentioned earlier that there was a need to understand the effects of kinase inhibitors on normal tissue. Unlike these kinase inhibitors, a Cre driven genetic ablation of *Raptor* will likely not affect translated proteins or already assembled mTOR complexes. As a result, mTORC1 inhibition in my model relies on the turnover of already made protein, after recombination occurs. This differs from the relatively immediate effects on signaling when using kinase inhibitors.

Several of the aforementioned caveats have been or can be addressed, while others may prove to be more difficult. On the complications with a constitutive, congenitally expressed Cre, I was able to address this by developing inducible genetic models again linked to an Adiponectin promoter. In subsequent studies, I was able to use these alternative tools to then interfere with mTORC1 at specific time points of development. This allowed me to bypass any possible developmental effects of early mTORC1 inhibition, and also allowed me to study acute versus chronic responses to *Raptor* deletion. Off-target expression of Cre promoters is an unfortunate concern for all models. While Adiponectin-Cre appears to be a very promising tool to target mature adipocytes, there may be more specific and effective promoters yet to be discovered. On the topic of kinase inhibitors, unfortunately the genetic models will be limited and dependent on protein turnover. *In vitro*, this can be addressed by studying primary adipocytes in culture, and using said inhibitors, however adipocytes in culture are not exposed to the complexity of a complete adipose depot. Of interest is the development of 3D scaffolds to better mimic adipose tissue structure in culture. Some materials used include plasma, alginate, fibrin, and collagen [127]. While an improvement over 2D dish surfaces, still lacking is are the complex intra-organ signaling factors that are constantly in flux in an animal system.

Dissecting WAT vs BAT roles in Whole Body Metabolism

One interesting question to pursue is what is the contribution of white adipose tissue dysfunction to the metabolic dysfunction seen in Adiponectin-Cre *Raptor* KO mice? While it's been discussed that mTORC1 signaling appears to be critical for brown fat development, function, and maintenance, these brown fat specific KO mice (Ucp1-Cre driven) do not appear to have severe metabolic disorders [76]. This suggests that the white adipose tissue may be a main driver towards the insulin resistance and liver steatosis seen in adipose *Raptor* KO animals. Furthermore, it is understood that adult humans generally have very little brown fat, particularly those who are obese, and those who have access to adequate shelter. In fact, it has been suggested that mice housed at thermoneutrality, consuming a high-fat diet, most closely mimics a modern human metabolic state [128]. For this reason, I believe it would be beneficial to further study the role of mTORC1 signaling specifically in white adipose tissue. Unfortunately, at this time there are no known Cre promoters that specifically target mature white adipocytes, however with growing interest in understanding the origins of adipocytes, some may be developed in the near future.

By developing drug inducible deletion models, I was able to better differentiate acute and chronic responses to mTORC1 inhibition in vivo. In vitro, I was also able to inhibit *Raptor* in primary differentiated adipocytes, and saw that adipocyte maintenance and lipid accumulation were in tact acutely. Again, these genetic models are not perfect, and may be confounded by off-target effects, and

delayed downstream signaling inhibition due to existing complexes at time of recombination. Additionally, there are concerns that the drugs used for deletion have negative effects on adipose tissue themselves. Tamoxifen has been shown to have lipotoxic properties, while doxycycline is a mitochondrial toxin that may also perturb the microbiome. With this in mind, however, the phenotypes seen in inducible mouse models compared very closely with that of constitutive models, suggesting minor, if any, deleterious metabolic consequences of the drug treatment. With these inducible mice, I was able to show several signaling responses occur well before the onset of lipoatrophy and metabolic dysfunction. Additionally, cell death and lipoatrophy are dependent on unhinged autophagic flux during *Raptor* ablation, however, adipose tissue inflammation and ectopic lipid deposition still occurred even when overall adipose tissue mass was recovered by autophagy inhibition.

Further Work for Adipose ATG7/Raptor dKO

In the immediate future, there are several experiments I believe are worthwhile to conduct to further understand the role of autophagy in *Raptor* KO mice. First, I would better characterize the metabolic status of *Atg7 Raptor* dKO animals. Analysis of insulin tolerance tests and glucose tolerance tests are key, along with possible utilization of a metabolic cage study, although I would not expect to have a difference in energy consumption given that they do not vary from control animals with respect to overall body mass. I mentioned that

signaling changes in adipose tissue precede the development of lipoatrophy and disease in the *Raptor* KO mice. One prominent change is an increase in expression of de novo lipogenesis proteins, and expression of Chrebp, a gene closely linked with glucose uptake. While expression increases, it is not known how the actual nutrient flux is affected under these conditions. It may be worthwhile to analyze glucose and lipid uptake in adipose tissue of KO mice, both in single *Raptor* KO and *Atg7/Raptor* double KO. Because this expression phenomena persists in the double KO model, it may be a significant contributor to overall metabolic dysfunction.

Regarding metabolic dysfunction, it is evident that restoring adipose tissue mass through inhibition of autophagy is not sufficient to prevent ectopic lipid accumulation and adipose tissue inflammation. These results indicate that mTORC1 separately regulates autophagy, and other signaling pathways in adipose tissue that globally affect metabolism. While adipose tissue mass is important for the proper storage of excess nutrients, my results suggest that mTORC1 signaling mediates adipose tissue inflammation and whole-body metabolism independent of lipid accumulation. Possible mechanisms might include mediation of AT inflammation and macrophage recruitment, adipokine production, and lipid turnover/release. It would be interesting to examine the adipocyte secretome in the setting of *Raptor* KO. Further metabolomic studies of these animals may uncover interesting and novel aspects of whole body

metabolic regulation that are dependent specifically on adipocyte mTORC1 activity.

In a longer timeframe, I would cross into the double KO animals the mTmG reporter. In our *Raptor* KO mice, the mTmG reporter proved to be a valuable tool to track deleted adipocytes, showing that overtime these cells shrank in size, and the depot was repopulated with unlabeled cells. Importantly, the double KO mice with the mTmG reporter should be driven by inducible Cre promoters, as this will give the ability to pulse and trace adipocyte fate in an adult mouse. Issues would arise if using a constitutive Adiponectin-Cre both due to developmental concerns, and an inability to differentiate between new and old cells. While blocking autophagy does not appear to block adipose tissue inflammation, it would be interesting to see if in fact elevated autophagic flux was the sole cause for the apparent shrinkage of these KO adipocytes. Further, I've mentioned the relevance of thermoneutrality conditions to normal human life. It can be argued that any study attempting to use mice to model human metabolism should be conducted at the very least under thermoneutral conditions, if not also paired with high-fat diet feeding. It is apparent that perturbed mTORC1 signaling in adipocytes may contribute to metabolic dysfunction, even when adipose tissue mass is maintained. To best emulate and compare these findings with human metabolic disease, I believe there will be a benefit to studying these mice under humanized conditions.

Can Adipocyte mTORC1 Localize to Lysosomes Absent RagGTPases?

On the topic of amino acids, my *in vivo* findings greatly contrast the well-established model of the amino acid sensing complex in cancer cells. Strong evidence indicates that mTORC1 localization to the lysosomal membrane, by the amino acid sensing RagGTPase complex, is a required step in the process of mTORC1 activation. While I confirm that adipocytes are amino acid sensitive in culture, I also find that the RagGTPases may be dispensable for adipose tissue *in vivo*. At this point, I believe it is imperative to see if mTORC1 is in fact able to localize to the lysosome in absence of the RagGTPases. This would most easily be conducted in culture, and could be carried out using primary adipocytes isolated from RagA/B dKO mice. Similar to the model used for the *Raptor* model, I would develop a drug-inducible system to genetically delete the RagGTPases in primary isolated cells. Alternatively one could use CRISPR to efficiently delete the RagGTPases in an adipocyte cell line, as this may be faster than generating the mice needed for primary cells. The caveat again being that in vitro studies poorly mimic *in vivo* conditions, and that often many differences arise between the two models, especially if desired readouts are dependent on nutrient flux and microenvironmental conditions. In vivo tracking of mTORC1 localization would be ideal. One approach could be the use of fluorescence electron microscopy. By fluorescently labeling a component of mTORC1, fluorescence electron microscopy may provide high enough resolution to show if mTORC1 is colocalizing with lysosomes in the setting of RagGTPase deletion. Lastly, it

should be noted that there was a persistent increase in *Ucp1* expression in the WAT of Rag KO animals. While this did not appear to have any gross metabolic effect, it may still be an interesting phenomenon to study further. It has been reported before that RagC/D may be linked to Ucp1 expression [124]. More specifically, it is reported that RagC/D dependent activity of mTORC1 regulates a noncanonical TFE3-PGC1β-UCP1 pathway, which is responsible for mTORC1 dependent suppression of UCP1 activity by FLCN. Interestingly, it was shown that RagD activity could regulated TFE3 sequestration but not RagB activity. This model suggests a role of the Rags in Ucp1 activity, however does not necessarily explain the phenomenon I see in that both RagA, and RagA/B deletion promote *Ucp1* expression in WAT. It is possible that the presence of RagA or B is required for stability of C/D, and that the TFE3 axis may still be responsible for the increased *Ucp1* that I find in my animal models. For curiosity's sake, it would be interesting to further understand the Rag specific control of Ucp1 expression in WAT, even though it may not be of any major metabolic consequence.

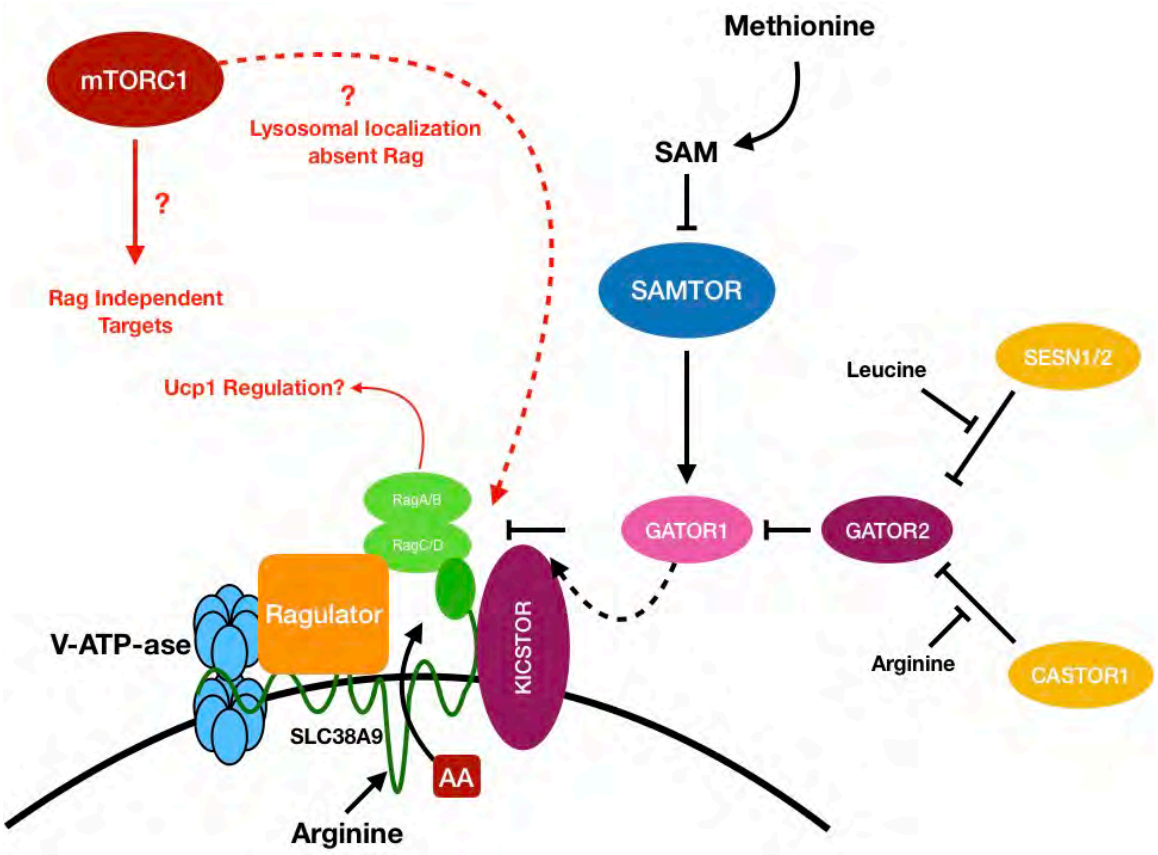

Figure 5.1: Diagram of known carriers for amino acid sensing. Speculative pathways highlighted in red.

Adipocyte Mitochondrial Dynamics in Relationship With mTORC1

In my study of *Raptor* KO adipocytes, I saw a significant change in overall mitochondrial mass, and morphology. mTORC1 has been associated with both mitochondrial dynamics, and biogenesis, through various mechanisms. While my studies were limited to observing the general morphology, it may be worthwhile to better understand the functional capacity of these “mutant” mitochondria. While they undoubtedly grow massively in size, is it possible that they are less

efficient metabolically than normal mitochondria? In the setting of over active autophagy, or blocked autophagy, do these mitochondria accumulate excessive damage? I would start with studying the respiratory capacity of *Raptor* KO cells by utilizing the Seahorse metabolic analyzer. I would also utilize mitochondrial damage and stress kits to analyze mitochondrial health in these cells. Overall, the relationships that have been made between mTORC1 and mitochondrial dynamics are intriguing, and my findings add to the current evidence that mTORC1 is critical in mitochondrial maintenance. Further work to understand the importance of mitochondria in adipocytes is warranted.

mTORC1, Adipose Tissue Health, and Tumor Environments

From my work, I have developed a particular interest in the association between obesity and cancer. Obesity has been clearly linked with increased risk of developing several types of cancer, including breast, colon, endometrial, esophageal, kidney, and pancreatic cancers [129]. Many theories have been proposed to link obesity with these cancers, including altered immune function, inflammation, elevated growth factor circulation, epigenetic modifications, and more [130-132]. In particular, women who are obese have been shown to have a 20%-40% high risk of developing breast cancer, and a 5-point increase in BMI has been associated with a 12% increase of developing breast cancer [133]. This is highly interesting to me given the localization of breast cancer, as it develops within an adipose tissue environment. One theory suggests that simply the

excessive nutrient availability of large adipose stores “feed” local cancer cells leading to tumor growth [134]. While possible, I wonder if it may be more complicated, and that perhaps the “health” of surrounding adipose tissue may be important in tumor development. If health, more than gross mass, is important, I believe that tumor growth may be promoted in a lipodystrophic model as much as it would in an obese model. If inflammation is a contributory factor, it is possible that adipose tissue inflammation, seen both in obese and in lipodystrophic settings, is providing a tumorigenic environment within the breast tissue. To study this, I would utilize the Adiponectin-Cre *Raptor* model of lipodystrophy and xenograft a breast tumor line within the mammary adipose tissue depot. Initially, tumor development can be compared between control, KO, and possibly control mice on high-fat diet to mimic obesity. It would be prudent to conduct these experiments under humanized conditions as well. If particularly ambitious, one could also utilize the *Atg7/Raptor* double KO mice as they also suffer from inflammation, despite preserving adipose tissue mass. I believe the *Raptor* KO model can be an extremely useful tool in studying the development of cancer within the setting of adipose tissue dysfunction. While straying away from the original goals of this project, it would be an interesting avenue to connect adipose tissue function with development of related serious diseases.

Conclusion:

The results of this dissertation have provided novel insight into the role of mTORC1 and nutrient signaling in regulating mature adipocyte function. I have argued against the model that adipocyte mTORC1 loss may be metabolically beneficial, and have shown that mTORC1 is in fact critical in adipose tissue growth and maintenance. In animal models, loss of mTORC1 signaling in mature adipocytes leads to a progressive loss of adipose tissue mass, and development of severe metabolic dysfunction including insulin resistance, hepatosteatosis, and hepatic tumors. I also show that, while mTORC1 dependent inhibition of autophagy is critical for adipose tissue mass, restoring mass alone is not sufficient to prevent whole body metabolic disturbances such as adipose tissue inflammation, and ectopic lipid accumulation in the liver. These findings suggest that metabolic homeostasis is dependent not only on the ability of adipose tissue to store lipids, but also on how the adipocytes function internally, with respect to nutrient and growth factor signaling. mTORC1 appears to regulate important adipocyte signaling pathways that have a global effect on metabolism. While some questions are answered, many more now arise. Continued work in understanding metabolic signaling in adipose tissue will undoubtedly lead to beneficial discoveries in human health and disease.

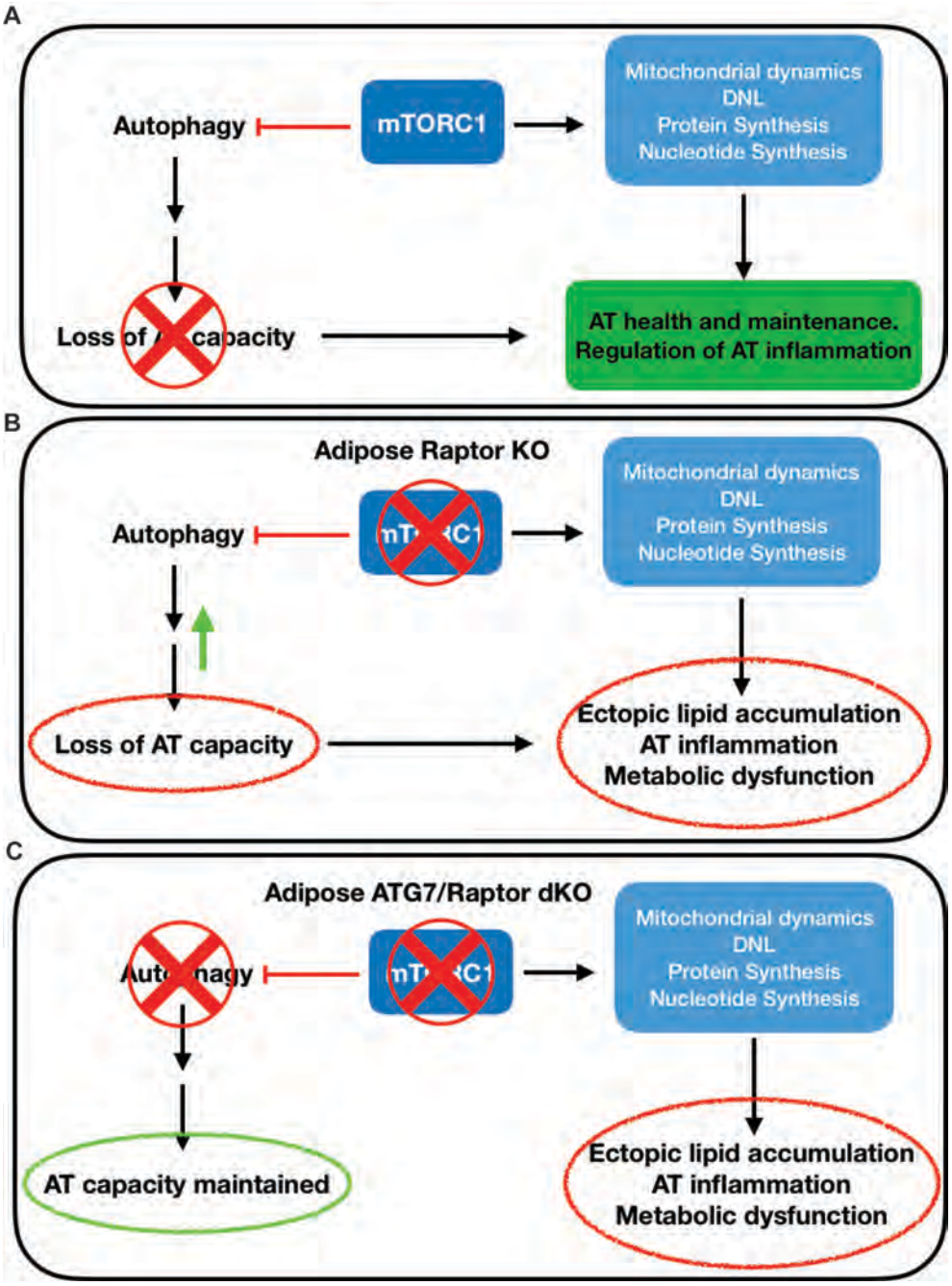

Figure 5.2: Model of mTORC1 pathways and their influence on adipose tissue metabolism in wildtype (A), adipose Raptor KO (B), and adipose ATG7/Raptor KO (C) mice.

References

1. *State of Obesity*. 2017; Available from: https://stateofobesity.org/adult-obesity/.
2. Hales, C.M., et al., *Prevalence of Obesity Among Adults and Youth: United States, 2015-2016.* NCHS Data Brief, 2017(288): p. 1-8.
3. Ghisdal, L., et al., *New-Onset Diabetes After Renal Transplantation.* Diabetes Care, 2011. **35**(1): p. 181.
4. Ruderman, N.B., S.H. Schneider, and P. Berchtold, *The "metabolically-obese," normal-weight individual.* Am J Clin Nutr, 1981. **34**(8): p. 1617-21.
5. Conus, F., R. Rabasa-Lhoret, and F. Peronnet, *Characteristics of metabolically obese normal-weight (MONW) subjects.* Appl Physiol Nutr Metab, 2007. **32**(1): p. 4-12.
6. Jung, C.H., *Metabolically healthy obesity: a friend or foe?* 2017. **32**(4): p. 611-21.
7. Samocha-Bonet, D., et al., *Metabolically healthy and unhealthy obese--the 2013 Stock Conference report.* Obes Rev, 2014. **15**(9): p. 697-708.
8. Stefan, N., et al., *Metabolically healthy obesity: epidemiology, mechanisms, and clinical implications.* Lancet Diabetes Endocrinol, 2013. **1**(2): p. 152-62.
9. Hsu, W.C., et al., *BMI Cut Points to Identify At-Risk Asian Americans for Type 2 Diabetes Screening.* Diabetes Care, 2015. **38**(1): p. 150.
10. Waltermann, M. and A. Steinbuchel, *Neutral lipid bodies in prokaryotes: recent insights into structure, formation, and relationship to eukaryotic lipid depots.* J Bacteriol, 2005. **187**(11): p. 3607-19.
11. Engin, A.B., *What Is Lipotoxicity?* Adv Exp Med Biol, 2017. **960**: p. 197-220.
12. Guebre-Egziabher, F., et al., *Ectopic lipid accumulation: A potential cause for metabolic disturbances and a contributor to the alteration of kidney function.* Biochimie, 2013. **95**(11): p. 1971-9.
13. Boden, G., *Free fatty acids, insulin resistance, and type 2 diabetes mellitus.* Proc Assoc Am Physicians, 1999. **111**(3): p. 241-8.
14. Daniele, G., et al., *Chronic reduction of plasma free fatty acid improves mitochondrial function and whole-body insulin sensitivity in obese and type 2 diabetic individuals.* Diabetes, 2014. **63**(8): p. 2812-20.
15. Porter, S.A., et al., *Abdominal Subcutaneous Adipose Tissue: A Protective Fat Depot?* Diabetes Care, 2009. **32**(6): p. 1068-75.
16. Birsoy, K., W.T. Festuccia, and M. Laplante, *A comparative perspective on lipid storage in animals.* Journal of Cell Science, 2013. **126**(7): p. 1541.
17. Sanchez-Gurmaches, J. and D.A. Guertin, *Adipocytes arise from multiple lineages that are heterogeneously and dynamically distributed.* Nat Commun, 2014. **5**: p. 4099.

18. Sanchez-Gurmaches, J., W.Y. Hsiao, and D.A. Guertin, *Highly selective in vivo labeling of subcutaneous white adipocyte precursors with Prx1-Cre.* Stem Cell Reports, 2015. **4**(4): p. 541-50.
19. Berry, R. and M.S. Rodeheffer, *Characterization of the adipocyte cellular lineage in vivo.* Nat Cell Biol, 2013. **15**(3): p. 302-8.
20. Hamdy, O., S. Porramatikul, and E. Al-Ozairi, *Metabolic obesity: the paradox between visceral and subcutaneous fat.* Curr Diabetes Rev, 2006. **2**(4): p. 367-73.
21. Jacobsson, A., et al., *Mitochondrial uncoupling protein from mouse brown fat. Molecular cloning, genetic mapping, and mRNA expression.* Journal of Biological Chemistry, 1985. **260**(30): p. 16250-16254.
22. Cannon, B. and J. Nedergaard, *Brown adipose tissue: function and physiological significance.* Physiol Rev, 2004. **84**(1): p. 277-359.
23. Seale, P. and M.A. Lazar, *Brown Fat in Humans: Turning up the Heat on Obesity.* Diabetes, 2009. **58**(7): p. 1482.
24. Harms, M. and P. Seale, *Brown and beige fat: development, function and therapeutic potential.* Nature Medicine, 2013. **19**: p. 1252.
25. Wu, J., P. Cohen, and B.M. Spiegelman, *Adaptive thermogenesis in adipocytes: Is beige the new brown?* Genes Dev, 2013. **27**(3): p. 234-50.
26. Zuriaga, M.A., et al., *Humans and Mice Display Opposing Patterns of "Browning" Gene Expression in Visceral and Subcutaneous White Adipose Tissue Depots.* Front Cardiovasc Med, 2017. **4**.
27. Shimizu, I. and K. Walsh, *The Whitening of Brown Fat and Its Implications for Weight Management in Obesity.* Curr Obes Rep, 2015. **4**(2): p. 224-9.
28. Laplante, M. and David M. Sabatini, *mTOR Signaling in Growth Control and Disease.* Cell, 2012. **149**(2): p. 274-293.
29. Wullschleger, S., R. Loewith, and M.N. Hall, *TOR Signaling in Growth and Metabolism.* Cell, 2006. **124**(3): p. 471-484.
30. Chantranupong, L., et al., *The CASTOR proteins are arginine sensors for the mTORC1 pathway.* Cell, 2016. **165**(1): p. 153-164.
31. Ben-Sahra, I., et al., *mTORC1 induces purine synthesis through control of the mitochondrial tetrahydrofolate cycle.* Science, 2016. **351**(6274): p. 728-33.
32. Liu, P., et al., *Sin1 phosphorylation impairs mTORC2 complex integrity and inhibits downstream Akt signalling to suppress tumorigenesis.* Nat Cell Biol, 2013. **15**(11): p. 1340-50.
33. Sarbassov, D.D., et al., *Phosphorylation and regulation of Akt/PKB by the rictor-mTOR complex.* Science, 2005. **307**(5712): p. 1098-101.
34. Bar-Peled, L. and D.M. Sabatini, *Regulation of mTORC1 by amino acids.* Trends Cell Biol, 2014. **24**(7): p. 400-6.
35. Duran, R.V., et al., *Glutaminolysis activates Rag-mTORC1 signaling.* Mol Cell, 2012. **47**(3): p. 349-58.
36. Wang, S., et al., *Lysosomal amino acid transporter SLC38A9 signals arginine sufficiency to mTORC1.* Science, 2015. **347**(6218): p. 188.

37. Rebsamen, M., et al., *SLC38A9 is a component of the lysosomal amino acid sensing machinery that controls mTORC1.* Nature, 2015. **519**(7544): p. 477-481.
38. Inoki, K., et al., *Rheb GTPase is a direct target of TSC2 GAP activity and regulates mTOR signaling.* Genes Dev, 2003. **17**(15): p. 1829-34.
39. Tee, A.R., et al., *Tuberous sclerosis complex gene products, Tuberin and Hamartin, control mTOR signaling by acting as a GTPase-activating protein complex toward Rheb.* Curr Biol, 2003. **13**(15): p. 1259-68.
40. Sancak, Y., et al., *PRAS40 is an insulin-regulated inhibitor of the mTORC1 protein kinase.* Mol Cell, 2007. **25**(6): p. 903-15.
41. Jung, J., H.M. Genau, and C. Behrends, *Amino Acid-Dependent mTORC1 Regulation by the Lysosomal Membrane Protein SLC38A9.* Molecular and Cellular Biology, 2015. **35**(14): p. 2479-2494.
42. Groenewoud, M.J. and F.J. Zwartkruis, *Rheb and Rags come together at the lysosome to activate mTORC1.* Biochem Soc Trans, 2013. **41**(4): p. 951-5.
43. Kim, J., et al., *AMPK and mTOR regulate autophagy through direct phosphorylation of Ulk1.* Nat Cell Biol, 2011. **13**(2): p. 132-141.
44. Roczniak-Ferguson, A., et al., *The transcription factor TFEB links mTORC1 signaling to transcriptional control of lysosome homeostasis.* Sci Signal, 2012. **5**(228): p. ra42.
45. Huffman, T.A., I. Mothe-Satney, and J.C. Lawrence, Jr., *Insulin-stimulated phosphorylation of lipin mediated by the mammalian target of rapamycin.* Proc Natl Acad Sci U S A, 2002. **99**(2): p. 1047-52.
46. Peterson, T.R., et al., *mTOR complex 1 regulates lipin 1 localization to control the SREBP pathway.* Cell, 2011. **146**(3): p. 408-20.
47. Hsu, P.P., et al., *The mTOR-regulated phosphoproteome reveals a mechanism of mTORC1-mediated inhibition of growth factor signaling.* Science, 2011. **332**(6035): p. 1317-22.
48. Yu, Y., et al., *Phosphoproteomic analysis identifies Grb10 as an mTORC1 substrate that negatively regulates insulin signaling.* Science, 2011. **332**(6035): p. 1322-6.
49. Liu, M., et al., *Grb10 Promotes Lipolysis and Thermogenesis by Phosphorylation-dependent Feedback Inhibition of mTORC1.* Cell metabolism, 2014. **19**(6): p. 967-980.
50. O'Reilly, K.E., et al., *mTOR Inhibition Induces Upstream Receptor Tyrosine Kinase Signaling and Activates Akt.* Cancer research, 2006. **66**(3): p. 1500-1508.
51. Palepu, S. and G.V. Prasad, *New-onset diabetes mellitus after kidney transplantation: Current status and future directions.* World J Diabetes, 2015. **6**(3): p. 445-55.
52. Johnston, O., et al., *Sirolimus Is Associated with New-Onset Diabetes in Kidney Transplant Recipients.* Journal of the American Society of Nephrology : JASN, 2008. **19**(7): p. 1411-1418.

53. Yilmaz, V.T., et al., *New-Onset Diabetes Mellitus Associated with Sirolimus Use in Renal Transplant Recipients.* The Eurasian Journal of Medicine, 2015. **47**(3): p. 213-215.
54. Sarbassov, D.D., et al., *Prolonged rapamycin treatment inhibits mTORC2 assembly and Akt/PKB.* Mol Cell, 2006. **22**(2): p. 159-68.
55. Lamming, D.W., et al., *Rapamycin-induced insulin resistance is mediated by mTORC2 loss and uncoupled from longevity.* Science, 2012. **335**(6076): p. 1638-43.
56. Foster, D.A. and A. Toschi, *Targeting mTOR with rapamycin: One dose does not fit all.* Cell cycle (Georgetown, Tex.), 2009. **8**(7): p. 1026-1029.
57. Xie, J., X. Wang, and C.G. Proud, *mTOR inhibitors in cancer therapy.* F1000Research, 2016. **5**: p. F1000 Faculty Rev-2078.
58. Zaytseva, Y.Y., et al., *mTOR inhibitors in cancer therapy.* Cancer Letters, 2012. **319**(1): p. 1-7.
59. Forbes, S.A., et al., *COSMIC: mining complete cancer genomes in the Catalogue of Somatic Mutations in Cancer.* Nucleic Acids Res, 2011. **39**(Database issue): p. D945-50.
60. Rodrik-Outmezguine, V.S., et al., *Overcoming mTOR resistance mutations with a new-generation mTOR inhibitor.* Nature, 2016. **534**(7606): p. 272-276.
61. Polak, P., et al., *Adipose-Specific Knockout of raptor Results in Lean Mice with Enhanced Mitochondrial Respiration.* Cell Metabolism, 2008. **8**(5): p. 399-410.
62. Jeffery, E., et al., *Characterization of Cre recombinase models for the study of adipose tissue.* Adipocyte, 2014. **3**(3): p. 206-11.
63. Wang, F., et al., *Lipoatrophy and severe metabolic disturbance in mice with fat-specific deletion of PPARgamma.* Proc Natl Acad Sci U S A, 2013. **110**(46): p. 18656-61.
64. Lee, M.J., Y. Wu, and S.K. Fried, *Adipose tissue heterogeneity: implication of depot differences in adipose tissue for obesity complications.* Mol Aspects Med, 2013. **34**(1): p. 1-11.
65. Softic, S., et al., *Lipodystrophy Due to Adipose Tissue–Specific Insulin Receptor Knockout Results in Progressive NAFLD.* Diabetes, 2016. **65**(8): p. 2187.
66. Shearin, A.L., et al., *Lack of AKT in adipocytes causes severe lipodystrophy.* Mol Metab, 2016. **5**(7): p. 472-9.
67. Laplante, M., et al., *DEPTOR cell-autonomously promotes adipogenesis, and its expression is associated with obesity.* Cell Metab, 2012. **16**(2): p. 202-12.
68. Yoon, M.S., et al., *Mechanistic target of rapamycin controls homeostasis of adipogenesis.* J Lipid Res, 2013. **54**(8): p. 2166-73.
69. Shan, T., et al., *Adipocyte-specific deletion of mTOR inhibits adipose tissue development and causes insulin resistance in mice.* Diabetologia, 2016. **59**(9): p. 1995-2004.

70. Carnevalli, L.S., et al., *S6K1 Plays a Critical Role in Early Adipocyte Differentiation.* Developmental cell, 2010. **18**(5): p. 763-774.
71. Singh, M., et al., *4E-BPs control fat storage by regulating the expression of Egr1 and ATGL.* Journal of Biological Chemistry, 2015.
72. Agarwal, A.K., et al., *AGPAT2 is mutated in congenital generalized lipodystrophy linked to chromosome 9q34.* Nat Genet, 2002. **31**(1): p. 21-3.
73. Miranda, D.M., et al., *Novel mutations of the BSCL2 and AGPAT2 genes in 10 families with Berardinelli-Seip congenital generalized lipodystrophy syndrome.* Clin Endocrinol (Oxf), 2009. **71**(4): p. 512-7.
74. Talukder, M.M.U., et al., *Seipin oligomers can interact directly with AGPAT2 and lipin 1, physically scaffolding critical regulators of adipogenesis.* Molecular Metabolism, 2015. **4**(3): p. 199-209.
75. Peterfy, M., et al., *Lipodystrophy in the fld mouse results from mutation of a new gene encoding a nuclear protein, lipin.* Nat Genet, 2001. **27**(1): p. 121-4.
76. Labbé, S.M., et al., *mTORC1 is Required for Brown Adipose Tissue Recruitment and Metabolic Adaptation to Cold.* Scientific Reports, 2016. **6**: p. 37223.
77. Lee, P.L., et al., *Raptor/mTORC1 loss in adipocytes causes progressive lipodystrophy and fatty liver disease.* Mol Metab, 2016. **5**(6): p. 422-432.
78. Nicholls, D.G. and R.M. Locke, *Thermogenic mechanisms in brown fat.* Physiol Rev, 1984. **64**(1): p. 1-64.
79. Lo, Kinyui A. and L. Sun, *Turning WAT into BAT: a review on regulators controlling the browning of white adipocytes.* Bioscience Reports, 2013. **33**(5): p. e00065.
80. Harms, M. and P. Seale, *Brown and beige fat: development, function and therapeutic potential.* Nat Med, 2013. **19**(10): p. 1252-1263.
81. Tran, C.M., et al., *Rapamycin Blocks Induction of the Thermogenic Program in White Adipose Tissue.* Diabetes, 2016. **65**(4): p. 927-41.
82. Liu, D., et al., *Activation of mTORC1 is essential for beta-adrenergic stimulation of adipose browning.* J Clin Invest, 2016. **126**(5): p. 1704-16.
83. Li, J., S.G. Kim, and J. Blenis, *Rapamycin: one drug, many effects.* Cell Metab, 2014. **19**(3): p. 373-9.
84. Thoreen, C.C. and D.M. Sabatini, *Rapamycin inhibits mTORC1, but not completely.* Autophagy, 2009. **5**(5): p. 725-6.
85. Magdalon, J., et al., *Constitutive adipocyte mTORC1 activation enhances mitochondrial activity and reduces visceral adiposity in mice.* Biochim Biophys Acta, 2016. **1861**(5): p. 430-8.
86. Albert, V., et al., *mTORC2 sustains thermogenesis via Akt-induced glucose uptake and glycolysis in brown adipose tissue.* EMBO Mol Med, 2016. **8**(3): p. 232-46.

87. Sakaguchi, M., et al., *Adipocyte Dynamics and Reversible Metabolic Syndrome in Mice with an Inducible Adipocyte-Specific Deletion of the Insulin Receptor.* Cell Metab, 2017. **25**(2): p. 448-462.
88. Eguchi, J., et al., *Transcriptional control of adipose lipid handling by IRF4.* Cell Metab, 2011. **13**(3): p. 249-59.
89. Lee, K.Y., et al., *Lessons on Conditional Gene Targeting in Mouse Adipose Tissue.* Diabetes, 2013. **62**(3): p. 864-74.
90. Wang, F., et al., *Lipoatrophy and severe metabolic disturbance in mice with fat-specific deletion of PPARγ.* Proceedings of the National Academy of Sciences, 2013. **110**(46): p. 18656.
91. Mullican, S.E., et al., *A Novel Adipose-Specific Gene Deletion Model Demonstrates Potential Pitfalls of Existing Methods.* Molecular Endocrinology, 2013. **27**(1): p. 127-134.
92. Xue, B., et al., *Genetic variability affects the development of brown adipocytes in white fat but not in interscapular brown fat.* J Lipid Res, 2007. **48**(1): p. 41-51.
93. Sanchez-Gurmaches, J., et al., *PTEN loss in the Myf5 lineage redistributes body fat and reveals subsets of white adipocytes that arise from Myf5 precursors.* Cell metabolism, 2012. **16**(3): p. 348-362.
94. Sanchez-Gurmaches, J., C.M. Hung, and D.A. Guertin, *Emerging Complexities in Adipocyte Origins and Identity.* Trends Cell Biol, 2016. **26**(5): p. 313-326.
95. Chakrabarti, P., et al., *Mammalian target of rapamycin complex 1 suppresses lipolysis, stimulates lipogenesis, and promotes fat storage.* Diabetes, 2010. **59**(4): p. 775-81.
96. Soliman, G.A., H.A. Acosta-Jaquez, and D.C. Fingar, *mTORC1 Inhibition via Rapamycin Promotes Triacylglycerol Lipolysis and Release of Free Fatty Acids in 3T3-L1 Adipocytes.* Lipids, 2010. **45**(12): p. 1089-100.
97. Herman, M.A., et al., *A novel ChREBP isoform in adipose tissue regulates systemic glucose metabolism.* Nature, 2012. **484**(7394): p. 333-8.
98. Ro, S.H., et al., *Distinct functions of Ulk1 and Ulk2 in the regulation of lipid metabolism in adipocytes.* Autophagy, 2013. **9**(12): p. 2103-14.
99. Wang, Q.A., et al., *Distinct regulatory mechanisms governing embryonic versus adult adipocyte maturation.* Nat Cell Biol, 2015. **17**(9): p. 1099-111.
100. Park, S.K., et al., *CCAAT/enhancer binding protein and nuclear factor-Y regulate adiponectin gene expression in adipose tissue.* Diabetes, 2004. **53**(11): p. 2757-66.
101. Qiao, L., et al., *C/EBPalpha regulates human adiponectin gene transcription through an intronic enhancer.* Diabetes, 2005. **54**(6): p. 1744-54.
102. Qiao, L., J. Schaack, and J. Shao, *Suppression of adiponectin gene expression by histone deacetylase inhibitor valproic acid.* Endocrinology, 2006. **147**(2): p. 865-74.

103. Patni, N. and A. Garg, *Congenital generalized lipodystrophies--new insights into metabolic dysfunction.* Nat Rev Endocrinol, 2015. **11**(9): p. 522-34.
104. Zhou, H., et al., *Berardinelli-Seip congenital lipodystrophy 2 regulates adipocyte lipolysis, browning, and energy balance in adult animals.* J Lipid Res, 2015. **56**(10): p. 1912-25.
105. Liu, L., et al., *Adipose-specific knockout of SEIPIN/BSCL2 results in progressive lipodystrophy.* Diabetes, 2014. **63**(7): p. 2320-31.
106. Cortes, V.A., et al., *Molecular mechanisms of hepatic steatosis and insulin resistance in the AGPAT2-deficient mouse model of congenital generalized lipodystrophy.* Cell Metab, 2009. **9**(2): p. 165-76.
107. Xiang, X., et al., *Tuberous sclerosis complex 1-mechanistic target of rapamycin complex 1 signaling determines brown-to-white adipocyte phenotypic switch.* Diabetes, 2015. **64**(2): p. 519-28.
108. Kosacka, J., et al., *Autophagy in adipose tissue of patients with obesity and type 2 diabetes.* Mol Cell Endocrinol, 2015. **409**: p. 21-32.
109. Ost, A., et al., *Attenuated mTOR signaling and enhanced autophagy in adipocytes from obese patients with type 2 diabetes.* Mol Med, 2010. **16**(7-8): p. 235-46.
110. Ye, R., et al., *Impact of tamoxifen on adipocyte lineage tracing: Inducer of adipogenesis and prolonged nuclear translocation of Cre recombinase.* Mol Metab, 2015. **4**(11): p. 771-8.
111. Cortes, V.A. and M. Fernandez-Galilea, *Lipodystrophies: adipose tissue disorders with severe metabolic implications.* J Physiol Biochem, 2015. **71**(3): p. 471-8.
112. Chimin, P., et al., *Adipocyte mTORC1 deficiency promotes adipose tissue inflammation and NLRP3 inflammasome activation via oxidative stress and de novo ceramide synthesis.* J Lipid Res, 2017. **58**(9): p. 1797-1807.
113. Hosokawa, N., et al., *Nutrient-dependent mTORC1 association with the ULK1-Atg13-FIP200 complex required for autophagy.* Mol Biol Cell, 2009. **20**(7): p. 1981-91.
114. Morita, M., et al., *mTOR Controls Mitochondrial Dynamics and Cell Survival via MTFP1.* Mol Cell, 2017. **67**(6): p. 922-935.e5.
115. Liang, J., et al., *The energy sensing LKB1-AMPK pathway regulates p27(kip1) phosphorylation mediating the decision to enter autophagy or apoptosis.* Nat Cell Biol, 2007. **9**(2): p. 218-24.
116. Garg, A., *Lipodystrophies.* Am J Med, 2000. **108**(2): p. 143-52.
117. Huang-Doran, I., et al., *Lipodystrophy: metabolic insights from a rare disorder.* J Endocrinol, 2010. **207**(3): p. 245-55.
118. Hou, W., et al., *Autophagic degradation of active caspase-8: a crosstalk mechanism between autophagy and apoptosis.* Autophagy, 2010. **6**(7): p. 891-900.

119. Amir, M., et al., *Inhibition of hepatocyte autophagy increases tumor necrosis factor-dependent liver injury by promoting caspase-8 activation.* Cell Death Differ, 2013. **20**(7): p. 878-87.
120. Efeyan, A. and D.M. Sabatini, *Nutrients versus growth factors in mTORC1 activation.* Biochem Soc Trans, 2013. **41**(4).
121. Efeyan, A., et al., *RagA, but not RagB, is essential for embryonic development and adult mice.* Dev Cell, 2014. **29**(3): p. 321-9.
122. Efeyan, A., et al., *Regulation of mTORC1 by the Rag GTPases is necessary for neonatal autophagy and survival.* Nature, 2013. **493**(7434): p. 679-83.
123. Sancak, Y., et al., *The Rag GTPases bind raptor and mediate amino acid signaling to mTORC1.* Science, 2008. **320**(5882): p. 1496-501.
124. Wada, S., et al., *The tumor suppressor FLCN mediates an alternate mTOR pathway to regulate browning of adipose tissue.* Genes Dev, 2016. **30**(22): p. 2551-64.
125. Risson, V., et al., *Muscle inactivation of mTOR causes metabolic and dystrophin defects leading to severe myopathy.* J Cell Biol, 2009. **187**(6): p. 859-74.
126. Han, J., et al., *The spatiotemporal development of adipose tissue.* Development, 2011. **138**(22): p. 5027-37.
127. Girandon, L., et al., *In vitro models for adipose tissue engineering with adipose-derived stem cells using different scaffolds of natural origin.* Folia Biol (Praha), 2011. **57**(2): p. 47-56.
128. Fischer, A.W., B. Cannon, and J. Nedergaard, *Optimal housing temperatures for mice to mimic the thermal environment of humans: An experimental study.* Mol Metab, 2018. **7**: p. 161-170.
129. Gallagher, E.J. and D. LeRoith, *Obesity and Diabetes: The Increased Risk of Cancer and Cancer-Related Mortality.* Physiol Rev, 2015. **95**(3): p. 727-48.
130. Mendonca, F. and R. Soares, *Obesity and cancer phenotype: Is angiogenesis a missed link?* Life Sci, 2015. **139**: p. 16-23.
131. Kolb, R., F.S. Sutterwala, and W. Zhang, *Obesity and cancer: inflammation bridges the two.* Curr Opin Pharmacol, 2016. **29**: p. 77-89.
132. Cohen, D.H. and D. LeRoith, *Obesity, type 2 diabetes, and cancer: the insulin and IGF connection.* Endocr Relat Cancer, 2012. **19**(5): p. F27-45.
133. Neuhouser, M.L., et al., *Overweight, Obesity, and Postmenopausal Invasive Breast Cancer Risk: A Secondary Analysis of the Women's Health Initiative Randomized Clinical Trials.* JAMA Oncol, 2015. **1**(5): p. 611-21.
134. Pascual, G., et al., *Targeting metastasis-initiating cells through the fatty acid receptor CD36.* Nature, 2016. **541**: p. 41.